BUCKLING OF IMPERFECT CIRCULAR CYLINDRICAL SHELLS

Thesis by

Prem Bhatia

In Partial Fulfillment of the Requirements

For the Degree of

Doctor of Philosophy

California Institute of Technology

Pasadena, California

1973

(Submitted October 17, 1972)

ACKNOWLEDGMENTS

I am indebted to Professor C. D. Babcock, Jr. for his continuous guidance, advice and discussions during the course of this work. Many suggestions from Professor E. E. Sechler are gratefully acknowledged.

Thanks are due to Dr. J. Arbocz for his continued interest and to Dr. M. S. El Raheb for some very timely help he extended me. Thanks are also accredited to Mrs. Elizabeth Fox for the excellent typing of the manuscript and to Mrs. Betty Wood for drawing the figures. The financial assistance of the California Institute of Technology is very much appreciated and is acknowledged.

This thesis is gratefully dedicated to my brothers, Shri Pritam Nath Bhatia and Shri Pran Nath Bhatia.

ABSTRACT

In this project, the buckling of imperfect circular cylindrical shells under uniform axial compression has been investigated. The imperfection considered is prismatic and is in the form of flat spots along the complete length of the shell. The problem is solved by considering it as an interaction problem between curved and flat panels. Shell equations are satisfied in the curved portions of the shell while flat plate equations are used in the flat spot regions. At the common edge between two adjacent panels, forces and displacements are matched to arrive at the eigenvalue problem for the critical load of the shell.

Two flat spot configurations have been studied. In the first case, a single flat spot along the complete length of the shell is considered. Curved and flat panels join to form sharp corners at their common edges. Numerical results are presented to show the effect of the width of the flat spot, thickness ratio and length to radius ratio of the shell, on the buckling load of the shell.

In the second case, the imperfection is in the form of two or more identical flat spots distributed uniformly along the circumference of the shell. Between two consecutive flat spots is a uniform radius cylindrical panel joining smoothly to the flat panels. This analysis is valid for any integral number of identical flat spots. Numerical results are presented for 2, 3, 4, 8-flat spots. The effect of width of flat spots, radius of curved panels, thickness ratio of the shell has been investigated.

The results, presented in this paper, clearly demonstrate a very significant reduction in the buckling load of the shell below its classical value. This is true even in the presence of relatively small flat spots. This reduction becomes more severe with a decrease in the thickness of the shell or an increase in the width of the flat spot.

NOMENCLATURE

a_i, b_i - Components of vectors $\{\underline{a}\}$ and $\{\underline{b}\}$ respectively

$\{\underline{a}_i\}$ - Vector of unknown coefficients for the ith panel

$2b$ - Width of flat panels (unless otherwise specified)

$[C], [C_A], [C_B]$ - (8 x 8) real matrices relating forces and displacements across sharp corners

D - Bending rigidity = $\dfrac{Eh^3}{12(1-\nu^2)}$

E - Young's modulus of the material of the shell

F - Non-dimensional Airy stress function, non-dimensionalized w.r.t.* $\dfrac{Eh^3}{\sqrt{12(1-\nu^2)}}$

F', f - Non-dimensional prebuckling and perturbation parts of F respectively

g - Determinant of the final matrices of the shell. $g = 0$ determines the critical load of the shell

h_p, h_s - Thickness of the flat panels and the curved panels respectively

$h' = h_p/h_s$, $\bar{h}_p = \dfrac{h_p/L}{\sqrt{12(1-\nu^2)}}$, $\bar{h}_s = \dfrac{h_s/L}{\sqrt{12(1-\nu^2)}}$

$[H], [H_1]$ - (8 x 8) real matrices relating forces and displacements of two panels with different thicknesses (Eqns. (96) and (117))

$k = m\pi$

L - Length of the cylindrical shell

m - Number of half waves in axial direction

M_y - Bending moment on y = constant edge

N - Number of panels of each kind in multiple flat spot shells (unless otherwise specified)

N_{xy}, N_{yy} - In-plane shear and y-direction normal stress resultants respectively

$[P], [Q]$ - Final matrices of the shell

Q_y - Out-of-plane shear on y = constant edge

r - Inscribed radius of the multi-spot shell

R - Radius of the curved panels. Also the radius of the single flat spot shell

$\{\underline{S}_i\}$ - State vector of the ith panel

2T - Width of the curved panel

U - Non-dimensional displacement in axial direction, non-dimensionalized w. r. t. thickness of the panel

V - Non-dimensional displacement in the circumferential direction, non-dimensionalized w. r. t. thickness of the panel

W - Non-dimensional out-of-plane displacement, non-dimensionalized w. r. t. thickness of the shell

W', w - Prebuckling and perturbation parts of W

x, y, z - Non-dimensional coordinates. Non-dimensionalized w. r. t. the length L of the shell (unless otherwise specified)

$$Z_s = \left(\frac{L}{R}\right)^2 \left(\frac{R}{h_s}\right) \sqrt{12(1-\nu^2)}$$

$$Z_p = \left(\frac{h_s}{h_p}\right)^2 Z_s$$

Subscript s - for the curved panels

Subscript p - for the flat panels

α - Nth root of unity (Eqn. (179))

$2\beta_1, 2\beta_2$ - Angle subtended by the flat panel at the center of the shell or inscribed circle and the angle subtended by the curved panel at the center of the circle describing it respectively

$\theta, \gamma, \xi_1, \xi_2, \eta_1, \eta_2, \ell_1, \ell_2, \varphi, \psi$ - See Eqns. (32) through (39)

ζ_1, ζ_2 - See Eqn. (57)

(ϕ_y) - Rotations (see Appendix I)

$\lambda = \cos\theta = \sigma/\sigma_{CL}$, $\lambda_s = \sigma/\sigma_{CL}(R, h_s)$

σ - Uniformly applied axial compressive stress

$$\sigma_{CL}(R, h_s) = \frac{Eh_s/R}{\sqrt{3(1-\nu^2)}}, \quad \sigma_{CL}(r, h) = \frac{Eh/r}{\sqrt{3(1-\nu^2)}}$$

$$\nabla^4 = \nabla^2 \nabla^2 = \left(\frac{\partial^2}{\partial x^2} + \frac{\partial^2}{\partial y^2}\right)^2 = \text{Biharmonic operator}$$

* w. r. t. - with respect to

TABLE OF CONTENTS

TABLE OF CONTENTS (Continued)

LIST OF TABLES

LIST OF FIGURES

LIST OF FIGURES (Continued)

I. BUCKLING OF IMPERFECT CIRCULAR CYLINDRICAL SHELL UNDER AXIAL COMPRESSION: SHELL WITH SINGLE FLAT SPOT

1. INTRODUCTION

Since the beginning of the twentieth century the buckling of circular cylindrical shells has been investigated theoretically and experimentally. Ever since the first experiments on the buckling of thin shells under axial compression, it has been common knowledge that theory and experiments differ substantially. While the classical theory, based on the small deflection shell theory, predicted the critical stress for axial compression as $\frac{Eh/R}{\sqrt{3(1-\nu^2)}}$, experimentally obtained values were as low as 10% of this value. Moreover, there has usually been considerable scatter in the experimental results. Much effort has gone into trying to explain this large discrepancy.

Various possible causes have been investigated to account for the deviations. Among them are

(i) presence of geometric imperfections in the assumed perfect shell,

(ii) residual stresses in the shells due to manufacturing methods,

(iii) difference between theoretical and experimental boundary conditions,

(iv) possible non-isotropic behavior of the materials of shells,

(v) accidental or unintended loads on the shells, etc.

Using improved theories, various investigators, among them Donnell,[5] Karman and Tsien,[14] Koiter,[10] Donnell and Wan,[6] Hutchinson,[8] and many others, have, over the years, established

the initial imperfections in the assumed perfect shell as the prime cause of the difference between the classical values and experimental values of the buckling stress of such shells. In addition, various experimental investigations, e.g., Babcock and Sechler,[4] Tennyson,[12] Horton and Durham[7] and Almroth, Holmes and Brush,[1] have indicated that the experimental buckling stress of the shells can be improved considerably by manufacturing the shells very carefully so that imperfections are reduced to the minimum. In fact, Tennyson[12] obtained an experimental critical stress which was over 90% of the classical value for shells spun cast from a photoelastic plastic.

The solution of the problem of circular cylindrical shells with general imperfections is very difficult to obtain. To make the problem amenable to a solution, various investigators have used special types of imperfections. Koiter[10, 11] considered the effect of a single axisymmetric imperfection mode (with trigonometric distribution along the axial direction). His solution indicated a marked reduction in the buckling load even with deviation amplitudes equal to a small fraction of the shell thickness. However, he pointed out the fact that the axisymmetric imperfection was not very general and was used primarily because it simplified the solution. This fact has been further emphasized by Arbocz[2] in his surveys of experimental shells. His results indicate that the amplitudes of the axisymmetric components of the initial imperfection are generally very very small, except when the shell is specifically designed to have axisymmetric imperfections built into it.

More general imperfections (axisymmetric and asymmetric)

have been considered by Hutchinson[8] and Arbocz,[2] and their effect on the buckling load evaluated. However, not much effort has been directed towards studying the effect of purely prismatic imperfections in thin shells. They are more likely to occur in large circular cylindrical shells, especially if the shell is made by rolling flat sheets to a cylindrical shape and welding the free edges together to form a closed shell. With this in view, in this chapter and the next, we present the results of a study of a special type of prismatic imperfection in basically circular cylindrical thin shells.

The imperfection considered is in the form of constant width flat spots along the complete length of the shell. The reason for considering flat spots may become obvious from the following well-known observations:

Under uniform axial compression, (i) theoretical critical stress for a circular cylindrical shell is given by $\frac{Eh/R}{\sqrt{3(1-\nu^2)}}$, but the shell is highly imperfection sensitive; (ii) the critical stress for a flat plate is given by $\frac{kE}{\sqrt{12(1-\nu^2)}}\left(\frac{h}{b}\right)^2$ where b is a typical dimension of middle surface, but plate under axial compression is not imperfection sensitive and theoretical and experimental results are in fair agreement. These observations lead one to conjecture that it may be possible to explain the low buckling load of shells on the basis of the presence of flat spots.

The constant width flat spots will satisfy the requirements of prismatic initial imperfections while, at the same time, give an indication of the possible effect of general flat spots. In the analysis to follow, it will be assumed that the critical load is not affected by

the stress concentrations associated with the sharp corners at the common edges.

2. DEFINITION OF THE PROBLEM

Let us consider a circular cylindrical shell of length L, radius R, thickness h_s. The shell is assumed to be geometrically perfect except that, along a part of its circumference (for the complete length of the shell), the curvature is zero, i.e., it is like a flat plate in this portion. Let this flat part subtend an angle $2\beta_1$ at the center of the circle. The thickness in the flat plate region is h_p. A schematic representation of the shell is given in Fig. 1. If this shell is subjected to a uniform axial compressive stress σ, we shall attempt to find the effect of the flat spot on the stress at which the shell becomes unstable.

3. GOVERNING EQUATIONS

The problem can be solved by considering the flat spot as an imperfection on an otherwise perfect circular cylindrical shell. The value of imperfection can be shown (Fig. 2) to be:

$$\left.\begin{aligned} W_o &= R\left(1 - \frac{\cos\beta_1}{\cos\beta}\right) \quad -\beta_1 \leq \beta \leq \beta_1 \\ &= 0 \qquad\qquad |\beta| > \beta_1 \end{aligned}\right\} \tag{1}$$

Using appropriate shell equations, in principle, the problem can be solved. However, because of the discontinuous nature of the imperfection defined above, the actual solution may be very difficult to obtain. To overcome this difficulty, the problem is considered as an interaction problem between a curved panel of uniform radius R

and a flat panel of central angle $2\beta_1$. Donnell's shallow shell equations (in terms of out-of-plane displacement and stress function) will be used in the curved panel. In the flat panel, von Kármán's plate equations are used. At the common edges between the panels, forces and displacements from the two sides are matched to maintain equilibrium of forces and continuity of displacements across the interface.

The coordinate system used in the problem is shown in Fig. 1. A typical shell element with appropriate forces and displacements is shown in Fig. 3.

As derived in Appendix I, the governing equations and matching conditions in terms of non-dimensional variables become:

(a) In the curved panel

$$\nabla^4 F_s - Z_s W_{s,xx} + \sqrt{12(1-\nu^2)}\,(W_{s,xx}W_{s,yy} - W_{s,xy}^2) = 0 \tag{2}$$

$$\nabla^4 W_s + Z_s F_{s,xx} - \sqrt{12(1-\nu^2)}\,(F_{s,xx}W_{s,yy} - 2F_{s,xy}W_{s,xy} + F_{s,yy}W_{s,xx}) = 0 \tag{3}$$

(b) In the flat panel

$$\nabla^4 F_p + \sqrt{12(1-\nu^2)}\,(W_{p,xx}W_{p,yy} - W_{p,xy}^2) = 0 \tag{4}$$

$$\nabla^4 W_p - \sqrt{12(1-\nu^2)}\,(F_{p,xx}W_{p,yy} - 2F_{p,xy}W_{p,xy} + F_{p,yy}W_{p,xx}) = 0 \tag{5}$$

(c) At the common edges (see Figs. 1 and 4)

$$\begin{aligned} &\text{Edge A:}\quad y_s = -\frac{R}{L}(\pi-\beta_1),\quad y_p = \frac{R}{L}\sin\beta_1 \\ &\text{Edge B:}\quad y_s = \frac{R}{L}(\pi-\beta_1),\quad y_p = -\frac{R}{L}\sin\beta_1 \end{aligned} \tag{6}$$

At Edge A

At Edge B

Kinematic Conditions

$$W_s = h'(W_p \cos\beta_1 + V_p \sin\beta_1) \qquad W_s = h'(W_p \cos\beta_1 - V_p \sin\beta_1) \tag{7}$$

$$V_s = h'(V_p \cos\beta_1 - W_p \sin\beta_1) \qquad V_s = h'(V_p \cos\beta_1 + W_p \sin\beta_1) \tag{8}$$

$$U_s = h' U_p \qquad U_s = h' U_p \tag{9}$$

$$\frac{\partial W_s}{\partial y} = h' \frac{\partial W_p}{\partial y} \qquad \frac{\partial W_s}{\partial y} = h' \frac{\partial W_p}{\partial y} \tag{10}$$

Force Conditions

$$\left(\frac{\partial^2 W_s}{\partial y^2} + \nu \frac{\partial^2 W_s}{\partial x^2}\right) = h'^4 \left(\frac{\partial^2 W_p}{\partial y^2} + \nu \frac{\partial^2 W_p}{\partial x^2}\right) \qquad \left(\frac{\partial^2 W_s}{\partial y^2} + \nu \frac{\partial^2 W_s}{\partial x^2}\right) = h'^4 \left(\frac{\partial^2 W_p}{\partial y^2} + \nu \frac{\partial^2 W_p}{\partial x^2}\right) \tag{11}$$

$$\frac{\partial^2 F_s}{\partial x \partial y} = h'^3 \frac{\partial^2 F_p}{\partial x \partial y} \qquad \frac{\partial^2 F_s}{\partial x \partial y} = h'^3 \frac{\partial^2 F_p}{\partial x \partial y} \tag{12}$$

At Edge A

$$\frac{\partial^2 F_s}{\partial x^2} = h'^3 \left[\frac{\partial^2 F_p}{\partial x^2} \cos\beta_1 + \frac{h_p/L}{\sqrt{12(1-\nu^2)}} \left\{ \frac{\partial^3 W_p}{\partial y^3} + (2-\nu) \frac{\partial^3 W_p}{\partial y \partial x^2} \right\} \sin\beta_1 \right]$$

$$\frac{h_s/L}{\sqrt{12(1-\nu^2)}} \left\{ \frac{\partial^3 W_s}{\partial y^3} + (2-\nu) \frac{\partial^3 W_s}{\partial y \partial x^2} \right\}$$

$$= h'^3 \left[\frac{h_p/L}{\sqrt{12(1-\nu^2)}} \left\{ \frac{\partial^3 W_p}{\partial y^3} + (2-\nu) \frac{\partial^3 W_p}{\partial y \partial x^2} \right\} \cos\beta_1 - \frac{\partial^2 F_p}{\partial x^2} \sin\beta_1 \right]$$

At Edge B

$$\frac{\partial^2 F_s}{\partial x^2} = h'^3 \left[\frac{\partial^2 F_p}{\partial x^2} \cos\beta_1 - \frac{h_p/L}{\sqrt{12(1-\nu^2)}} \left\{ \frac{\partial^3 W_p}{\partial y^3} + (2-\nu) \frac{\partial^3 W_p}{\partial y \partial x^2} \right\} \sin\beta_1 \right] \qquad (13)$$

$$\frac{h_s/L}{\sqrt{12(1-\nu^2)}} \left\{ \frac{\partial^3 W_s}{\partial y^3} + (2-\nu) \frac{\partial^3 W_s}{\partial y \partial x^2} \right\}$$

$$= h'^3 \left[\frac{h_p/L}{\sqrt{12(1-\nu^2)}} \left\{ \frac{\partial^3 W_p}{\partial y^3} + (2-\nu) \frac{\partial^3 W_p}{\partial y \partial x^2} \right\} \cos\beta_1 + \frac{\partial^2 F_p}{\partial x^2} \sin\beta_1 \right] \qquad (14)$$

(d) Boundary conditions

In what follows, it shall be assumed always that the boundary conditions at x = 0, 1 are to be applied only during the buckling process, i.e., the shell is free to expand during the loading process from the unloaded state to the critical load. During the buckling process, the following simply-supported boundary conditions will be applied:

At x = 0, x = 1, for all y.

$$w_s = w_{s,xx} = f_{s,yy} = v_s = 0 \tag{15}$$

$$w_p = w_{p,xx} = f_{p,yy} = v_p = 0 \tag{16}$$

4. PREBUCKLING SOLUTION

It can be easily verified that, for a uniform axial compressive stress σ, the solution of Eqns. (2) through (14) is:

$$F'_s = -\frac{\sigma h_s L^2 \sqrt{12(1-\nu^2)}}{2Eh_s^3}\, y^2, \qquad W'_s = \frac{\nu\sigma R}{Eh_s} = \text{const.} \tag{17}$$

$$F'_p = -\frac{\sigma h_p L^2 \sqrt{12(1-\nu^2)}}{2Eh_p^3}\, h^2, \qquad W'_p = \frac{h_s W'_s}{h_p}\cos\beta_1 = \text{const.} \tag{18}$$

which solution leads to a bending free deformation. In (18) W'_p is not determined by any force-displacement relations. $h_p W'_p$ is the rigid body motion of the flat panel normal to its plane from the unstressed state to the stressed state (see Fig. 1a).

5. ANALYSIS OF THE BUCKLED STATE

To determine the critical value of σ at which the shell becomes unstable let us consider

$$\left.\begin{aligned} F_s &= F'_s + f_s, \qquad W_s = W'_s + w_s \\ F_p &= F'_p + f_p, \qquad W_p = W'_p + w_p \end{aligned}\right\} \tag{19}$$

where f_s, w_s, f_p, w_p are infinitesimal perturbations on the solution in (17)-(18). Now we must find that σ for which F_s, W_s, F_p, W_p in the form (19), when substituted in the governing equations, lead to non-trivial values for f_s, w_s, f_p, w_p.

Substituting (19) in (2) through (5) and linearizing with respect to small perturbations we get:

In the curved panel:

$$\nabla^4 f_s - Z_s w_{s,xx} = 0 \tag{20}$$

$$\nabla^4 w_s + Z_s f_{s,xx} + 2\lambda Z_s w_{s,xx} = 0 \tag{21}$$

In the flat panel:

$$\nabla^4 f_p = 0 \tag{22}$$

$$\nabla^4 w_p + 2\lambda Z_p w_{p,xx} = 0 \tag{23}$$

where

$$Z_s = \left(\frac{L}{R}\right)^2 \left(\frac{R}{h_s}\right) \sqrt{12(1-\nu^2)} \tag{24}$$

$$Z_p = \left(\frac{h_s}{h_p}\right)^2 Z_s \tag{25}$$

$$\lambda = \sigma/\sigma_{CL}(R,h_s) \qquad \sigma_{CL}(R,h_s) = \frac{Eh_s/R}{\sqrt{3(1-\nu^2)}} \tag{26}$$

5a. Buckled State (Curved Panel)

From (20), (21)

$$\nabla^4 f_s - Z_s w_{s,xx} = 0 \tag{20}$$

$$\nabla^4 w_s + Z_s f_{s,xx} + 2\lambda Z_s w_{s,xx} = 0 \tag{21}$$

Let

$$f_s = p_1(y)\sin kx, \quad w_s = p_2(y)\sin(kx), \quad k = m\pi \tag{27}$$

$$0 \leq x \leq 1$$

where $p_1(y)$, $p_2(y)$ are functions of the circumferential coordinate y only and m is a positive integer denoting the number of half waves in the axial direction.

(20), (21), (27) $\Longrightarrow$

$$(k^2 - \frac{d^2}{dy^2})^2 p_1(y) + Z_s k^2 p_2(y) = 0 \tag{28}$$

$$-Z_s k^2 p_1(y) + \left[(k^2 - \frac{d^2}{dy^2})^2 - 2\lambda Z_s k^2\right] p_2(y) = 0 \tag{29}$$

This is a set of two ordinary differential equations in dependent variables $p_1(y)$ and $p_2(y)$. Substitute $p_1(y) = Ae^{\gamma y}$ and $p_2(y) = Be^{\gamma y}$ in (28), (29) and solve for γ, A, B and hence, $p_1(y)$ and $p_2(y)$. Using (27), the final solution can be put in the form:

$$f_s = \left[e^{\xi_1 y} \left\{ A_1 \cos\eta_1 y + A_2 \sin\eta_1 y \right\} + e^{-\xi_1 y} \left\{ A_3 \cos\eta_1 y + A_4 \sin\eta_1 y \right\} + \right.$$
$$\left. + e^{\xi_2 y} \left\{ A_5 \cos\eta_2 y + A_6 \sin\eta_2 y \right\} + e^{-\xi_2 y} \left\{ A_7 \cos\eta_2 y + A_8 \sin\eta_2 y \right\} \right] \sin kx \quad (30)$$

$$w_s = -\left[e^{\xi_1 y} \left\{ A_1 \cos(\eta_1 y+\theta) + A_2 \sin(\eta_1 y+\theta) \right\} + e^{-\xi_1 y} \left\{ A_3 \cos(\eta_1 y-\theta) + \right.\right.$$
$$\left. + A_4 \sin(\eta_1 y-\theta) \right\} + e^{\xi_2 y} \left\{ A_5 \cos(\eta_2 y-\theta) + A_6 \sin(\eta_2 y-\theta) \right\}$$
$$\left. + e^{-\xi_2 y} \left\{ A_7 \cos(\eta_2 y+\theta) + A_8 \sin(\eta_2 y+\theta) \right\} \right] \sin kx \quad (31)$$

where

$$\lambda = \cos\theta \qquad 0 \leq \lambda \leq 1 \quad (32)$$

$$\left(1 - \frac{\gamma^2}{k^2}\right)^2 = \frac{Z_s}{k^2} \left[\lambda \pm \sqrt{\lambda^2 - 1} \right] \quad (33)$$

$$\gamma_1 = \xi_1 + i\eta_1, \quad \gamma_2 = \xi_2 - i\eta_2, \quad \gamma_3 = \xi_1 - i\eta_1, \quad \gamma_4 = \xi_2 + i\eta_2 \quad (33a)$$

$$\xi_1 = \sqrt{\ell_1} \cos\frac{\varphi}{2}, \quad \eta_1 = \sqrt{\ell_1} \sin\frac{\varphi}{2}, \quad \xi_2 = \sqrt{\ell_2} \cos\frac{\psi}{2}, \quad \eta_2 = \sqrt{\ell_2} \sin\frac{\psi}{2} \quad (34)$$

$$\ell_1 = k^2 \sqrt{1 + 2\sqrt{\frac{Z_s}{k^2}} \cos\frac{\theta}{2} + \frac{Z_s}{k^2}} \quad (35)$$

$$\mathrm{Tan}\varphi = \frac{\sqrt{\frac{Z_s}{k^2}} \sin\frac{\theta}{2}}{1 + \sqrt{\frac{Z_s}{k^2}} \cos\frac{\theta}{2}} \quad (36)$$

$$\ell_2 = k^2 \sqrt{1 - 2\sqrt{\frac{Z_s}{k^2}} \cos\frac{\theta}{2} + \frac{Z_s}{k^2}} \quad (37)$$

$$\text{Tan}\psi = \frac{\sqrt{\frac{Z_s}{k^2}}\ \sin\frac{\theta}{2}}{1 - \sqrt{\frac{Z_s}{k^2}}\cos\frac{\theta}{2}} \tag{38}$$

The expressions given below will be useful in the derivation of various formulae used in what is to follow:

$$\xi_1^2 + \eta_1^2 = \ell_1\ ,\quad \xi_1^2 - \eta_1^2 = \ell_1\cos\varphi\ ,\quad 2\xi_1\eta_1 = \ell_1\sin\varphi$$

$$\xi_2^2 + \eta_2^2 = \ell_2\ ,\quad \xi_2^2 - \eta_2^2 = \ell_2\cos\psi\ ,\quad 2\xi_2\eta_2 = \ell_2\sin\psi \tag{39}$$

Strain in axial direction =

$$\epsilon_x = \frac{h_s}{L}\frac{\partial U_s}{\partial x} = \frac{h_s^2/L^2}{\sqrt{12(1-\nu^2)}}\left[F_{s,yy} - \nu F_{s,xx}\right]$$

or

$$\frac{\partial U_s}{\partial x} = \frac{h_s/L}{\sqrt{12(1-\nu^2)}}\left[F_{s,yy} - \nu F_{s,xx}\right] \tag{40}$$

Strain in circumferential direction =

$$\epsilon_y = \frac{h_s}{L}\frac{\partial V_s}{\partial y} + \frac{h_s}{R}W_s = \frac{h_s^2/L^2}{\sqrt{12(1-\nu^2)}}\left[F_{s,xx} - \nu F_{s,yy}\right]$$

or

$$\frac{\partial V_s}{\partial y} = \frac{h_s/L}{\sqrt{12(1-\nu^2)}}\left[F_{s,xx} - \nu F_{s,yy}\right] - \frac{L}{R}W_s \tag{41}$$

Here

$$\left.\begin{aligned} F_s &= F_s' + f_s = -\frac{\sigma h_s L^2\sqrt{12(1-\nu^2)}}{2\,Eh_s^3}\,y^2 + f_s \\ W_s &= \frac{\nu\sigma R}{Eh_s} + w_s \end{aligned}\right\} \tag{42}$$

Using (30), (31), (40), (41), (42) we arrive at the following expressions to be used in the matching conditions:

$$W_s = \frac{\nu\sigma R}{Eh_s} - [e^{\xi_1 y}\cos(\eta_1 y+\theta)A_1 + e^{\xi_1 y}\sin(\eta_1 y+\theta)A_2 + e^{-\xi_1 y}\cos(\eta_1 y-\theta)A_3$$

$$+e^{-\xi_1 y}\sin(\eta_1 y-\theta)A_4 + e^{\xi_2 y}\cos(\eta_2 y-\theta)A_5$$

$$+ e^{\xi_2 y}\cos\ (\eta_2 y-\theta)A_6 + e^{-\xi_2 y}\cos(\eta_2 y+\theta)A_7$$

$$+e^{-\xi_2 y}\sin(\eta_2 y+\theta)A_8]\ \sin(kx) \qquad (43)$$

$$V_s = + \frac{kh_s/L}{12(1-\nu^2)}\left[\sqrt{\frac{\ell_1}{k^2}}\, e^{\xi_1 y}\left\{\frac{\ell_1}{k^2}\cos(\eta_1 y+\frac{3\varphi}{2})-(2+\nu)\cos(\eta_1 y+\frac{\varphi}{2})\right\}A_1\right.$$

$$+\sqrt{\frac{\ell_1}{k^2}}\, e^{\xi_1 y}\left\{\frac{\ell_1}{k^2}\sin(\eta_1 y+\frac{3\varphi}{2})-(2+\nu)\sin(\eta_1 y+\frac{\varphi}{2})\right\}A_2$$

$$-\sqrt{\frac{\ell_1}{k^2}}\, e^{-\xi_1 y}\left\{\frac{\ell_1}{k^2}\cos(\eta_1 y-\frac{3\varphi}{2})-(2+\nu)\cos(\eta_1 y-\frac{\varphi}{2})\right\}A_3$$

$$-\sqrt{\frac{\ell_1}{k^2}}\, e^{-\xi_1 y}\left\{\frac{\ell_1}{k^2}\sin(\eta_1 y-\frac{3\varphi}{2})-(2+\nu)\sin(\eta_1 y-\frac{\varphi}{2})\right\}A_4$$

$$+\sqrt{\frac{\ell_2}{k^2}}\, e^{\xi_2 y}\left\{\frac{\ell_2}{k^2}\cos(\eta_2 y+\frac{3\psi}{2})-(2+\nu)\cos(\eta_2 y+\frac{\psi}{2})\right\}A_5$$

$$+\sqrt{\frac{\ell_2}{k^2}}\, e^{\xi_2 y}\left\{\frac{\ell_2}{k^2}\sin(\eta_2 y+\frac{3\psi}{2})-(2+\nu)\sin(\eta_2 y+\frac{\psi}{2})\right\}A_6$$

$$-\sqrt{\frac{\ell_2}{k^2}}\, e^{-\xi_2 y}\left\{\frac{\ell_2}{k^2}\cos(\eta_2 y-\frac{3\psi}{2})-(2+\nu)\cos(\eta_2 y-\frac{\psi}{2})\right\}A_7$$

$$-\sqrt{\frac{\ell_2}{k^2}}\, e^{-\xi_2 y}\left\{\frac{\ell_2}{k^2}\sin(\eta_2 y-\frac{3\psi}{2})-(2+\nu)\sin(\eta_2 y-\frac{\psi}{2})\right\}A_8\Bigg]\sin(kx) \quad (44)$$

$$U_s = -\frac{\sigma Lx}{Eh_s} - \frac{kh_s/L}{\sqrt{12(1-\nu^2)}}\Bigg[e^{\xi_1 y}\left\{\frac{\ell_1}{k^2}\cos(\eta_1 y+\varphi)+\nu\cos(\eta_1 y)\right\}A_1$$

$$+ e^{\xi_1 y}\left\{\frac{\ell_1}{k^2}\sin(\eta_1 y+\varphi)+\nu\sin(\eta_1 y)\right\}A_2 + e^{-\xi_1 y}\left\{\frac{\ell_1}{k^2}\cos(\eta_1 y-\varphi)\right.$$

$$\left.+\nu\cos(\eta_1 y)\right\}A_3$$

$$+e^{-\xi_1 y}\left\{\frac{\ell_1}{k^2}\sin(\eta_1 y-\varphi)+\nu\sin(\eta_1 y)\right\}A_4 + e^{\xi_2 y}\left\{\frac{\ell_2}{k^2}\cos(\eta_2 y+\psi)\right.$$

$$\left.+\ \nu\cos(\eta_2 y)\right\}A_5$$

$$+e^{\xi_2 y}\left\{\frac{\ell_2}{k^2}\sin(\eta_2 y+\psi)+\nu\sin(\eta_2 y)\right\}A_6 + e^{-\xi_2 y}\left\{\frac{\ell_2}{k^2}\cos(\eta_2 y-\psi)\right.$$

$$\left.+\ \nu\cos(\eta_2 y)\right\}A_7$$

$$+e^{-\xi_2 y}\left\{\frac{\ell_2}{k^2}\sin(\eta_2 y-\psi)+\nu\sin(\eta_2 y)\right\}A_8\Bigg]\cos(kx) \quad (45)$$

$$\frac{\partial W_s}{\partial y} = -k\left[\sqrt{\frac{\ell_1}{k^2}}\, e^{\xi_1 y}\cos(\eta_1 y+\theta+\tfrac{\varphi}{2})A_1+\sqrt{\frac{\ell_1}{k^2}}\, e^{\xi_1 y}\sin(\eta_1 y+\theta+\tfrac{\varphi}{2})\, A_2\right.$$

$$-\sqrt{\frac{\ell_1}{k^2}}\, e^{-\xi_1 y}\cos(\eta_1 y-\theta-\tfrac{\varphi}{2})A_3 -\sqrt{\frac{\ell_1}{k^2}}\, e^{-\xi_1 y}\sin(\eta_1 y-\theta-\tfrac{\varphi}{2})\, A_4$$

$$+\sqrt{\frac{\ell_2}{k^2}}\, e^{\xi_2 y}\cos(\eta_2 y-\theta+\tfrac{\psi}{2})A_5 +\sqrt{\frac{\ell_2}{k^2}}\, e^{\xi_2 y}\sin(\eta_2 y-\theta+\tfrac{\psi}{2})\, A_6$$

$$\left.-\sqrt{\frac{\ell_2}{k^2}}\, e^{-\xi_2 y}\cos(\eta_2 y+\theta-\tfrac{\psi}{2})A_7 -\sqrt{\frac{\ell_2}{k^2}}\, e^{-\xi_2 y}\sin(\eta_2 y+\theta-\tfrac{\psi}{2})\, A_8\right]\sin(kx)$$

(46)

$$\left(\frac{\partial^2 W_s}{\partial y^2}+\nu\,\frac{\partial^2 W_s}{\partial x^2}\right) = -k^2\left[e^{\xi_1 y}\left\{\frac{\ell_1}{k^2}\cos(\eta_1 y+\theta+\varphi)-\nu\cos(\eta_1 y+\theta)\right\}A_1\right.$$

$$+\, e^{\xi_1 y}\left\{\frac{\ell_1}{k^2}\sin(\eta_1 y+\theta+\varphi)-\nu\,\sin(\eta_1 y+\theta)\right\}A_2+e^{-\xi_1 y}\left\{\frac{\ell_1}{k^2}\cos(\eta_1 y-\theta-\varphi)\right.$$

$$\left.-\,\nu\cos(\eta_1 y-\theta)\right\}A_3$$

$$+e^{-\xi_1 y}\left\{\frac{\ell_1}{k^2}\sin(\eta_1 y-\theta-\varphi)-\,\nu\sin(\eta_1 y-\theta)\right\}A_4$$

$$+e^{\xi_2 y}\left\{\frac{\ell_2}{k^2}\cos(\eta_2 y-\theta+\psi)-\nu\cos(\eta_2 y-\theta)\right\}A_5$$

$$+e^{\xi_2 y}\left\{\frac{\ell_2}{k^2}\sin(\eta_2 y-\theta+\psi)-\nu\sin(\eta_2 y-\theta)\right\}A_6$$

$$+e^{-\xi_2 y}\left\{\frac{\ell_2}{k^2}\cos(\eta_2 y+\theta-\psi)\nu\cos(\eta_2 y+\theta)\right\}A_7$$

$$\left.+e^{-\xi_2 y}\left\{\frac{\ell_2}{k^2}\sin(\eta_2 y+\theta-\psi)-\nu\,\sin(\eta_2 y+\theta)\right\}A_8\right]\sin(kx) \qquad (47)$$

$$F_{s,xy} = k^2\left[\sqrt{\frac{\ell_1}{k^2}}\, e^{\xi_1 y}\cos(\eta_1 y+\tfrac{\varphi}{2})A_1+\sqrt{\frac{\ell_1}{k^2}}\, e^{\xi_1 y}\sin(\eta_1 y+\tfrac{\varphi}{2})A_2\right.$$

$$-\sqrt{\frac{\ell_1}{k^2}}\, e^{-\xi_1 y}\cos(\eta_1 y-\tfrac{\varphi}{2})A_3-\sqrt{\frac{\ell_1}{k^2}}\, e^{-\xi_1 y}\sin(\eta_1 y-\tfrac{\varphi}{2})A_4$$

$$+\sqrt{\frac{\ell_2}{k^2}}\, e^{\xi_2 y}\cos(\eta_2 y+\tfrac{\psi}{2})A_5+\sqrt{\frac{\ell_2}{k^2}}\, e^{\xi_2 y}\sin(\eta_2 y+\tfrac{\psi}{2})A_6$$

$$\left.-\sqrt{\frac{\ell_2}{k^2}}\, e^{-\xi_2 y}\cos(\eta_2 y-\tfrac{\psi}{2})A_7-\sqrt{\frac{\ell_2}{k^2}}\, e^{-\xi_2 y}\sin(\eta_2 y-\tfrac{\psi}{2})A_8\right]\cos(kx) \tag{48}$$

$$F_{s,xx} = -k^2\left[e^{\xi_1 y}\cos(\eta_1 y)A_1+e^{\xi_1 y}\sin(\eta_1 y)A_2+e^{-\xi_1 y}\cos(\eta_1 y)A_3\right.$$

$$+e^{-\xi_1 y}\sin(\eta_1 y)A_4+e^{\xi_2 y}\cos(\eta_2 y)A_5+e^{\xi_2 y}\sin(\eta_2 y)A_6$$

$$\left.+e^{-\xi_2 y}\cos(\eta_2 y)A_7+e^{-\xi_2 y}\sin(\eta_2 y)A_8\right]\sin(kx) \tag{49}$$

$$\left(\frac{\partial^3 W_s}{\partial y^3}+(2-\nu)\frac{\partial^3 W_s}{\partial y\,\partial x^2}\right) = -k^3\left[\sqrt{\frac{\ell_1}{k^2}}\, e^{\xi_1 y}\left\{\frac{\ell_1}{k^2}\cos(\eta_1 y+\theta+\tfrac{3\varphi}{2})\right.\right.$$

$$\left.-(2-\nu)\cos(\eta_1 y+\theta+\tfrac{\varphi}{2})\right\}A_1$$

$$+\sqrt{\frac{\ell_1}{k^2}}\, e^{\xi_1 y}\left\{\frac{\ell_1}{k^2}\sin(\eta_1 y+\theta+\tfrac{3\varphi}{2})-(2-\nu)\sin(\eta_1 y+\theta+\tfrac{\varphi}{2})\right\}A_2$$

$$-\sqrt{\frac{\ell_1}{k^2}}\, e^{-\xi_1 y}\left\{\frac{\ell_1}{k^2}\cos(\eta_1 y-\theta-\tfrac{3\varphi}{2})-(2-\nu)\cos(\eta_1 y-\theta-\tfrac{\varphi}{2})\right\}A_3$$

$$-\sqrt{\frac{\ell_1}{k^2}}\, e^{-\xi_1 y}\left\{\frac{\ell_1}{k^2}\sin(\eta_1 y-\theta-\tfrac{3\varphi}{2})-(2-\nu)\sin(\eta_1 y-\theta-\tfrac{\varphi}{2})\right\}A_4$$

$$+\sqrt{\frac{\ell_2}{k^2}}\, e^{\xi_2 y}\left\{\frac{\ell_2}{k^2}\cos(\eta_2 y-\theta+\tfrac{3\psi}{2})-(2-\nu)\cos(\eta_2 y-\theta+\tfrac{\psi}{2})\right\} A_5$$

$$+\sqrt{\frac{\ell_2}{k^2}}\, e^{\xi_2 y}\left\{\frac{\ell_2}{k^2}\sin(\eta_2 y-\theta+\tfrac{3\psi}{2})-(2-\nu)\sin(\eta_2 y-\theta+\tfrac{\psi}{2})\right\} A_6$$

$$-\sqrt{\frac{\ell_2}{k^2}}\, e^{-\xi_2 y}\left\{\frac{\ell_2}{k^2}\cos(\eta_2 y+\theta-\tfrac{3\psi}{2})-(2-\nu)\cos(\eta_2 y+\theta-\tfrac{\psi}{2})\right\} A_7$$

$$-\sqrt{\frac{\ell_2}{k^2}}\, e^{-\xi_2 y}\left\{\frac{\ell_2}{k^2}\sin(\eta_2 y+\theta-\tfrac{3\psi}{2})-(2-\nu)\sin(\eta_2 y+\theta-\tfrac{\psi}{2})\right\} A_8\Big]\sin(kx) \tag{50}$$

The values of the expressions (43) through (50) at $y = \pm \frac{R}{L}(\pi-\beta_1)$ will be used in the matching conditions (Eqns. (7) through (14)).

In the next section, analogous expressions for the flat panel region will be derived.

5b. Buckled State (Flat Panel)

From Equations (22)-(25), in the flat panel region

$$\nabla^4 f_p = 0 \tag{22}$$

$$\nabla^4 w_p + 2\lambda Z_p w_{p,xx} = 0 \tag{23}$$

where

$$Z_p = \left(\frac{h_s}{h_p}\right)^2 Z_s \tag{25}$$

$$Z_s = \left(\frac{L}{R}\right)^2\left(\frac{R}{h_s}\right)\sqrt{12(1-\nu^2)} \tag{24}$$

Again, as in section 5a,

let $$f_p = q_1(y)\sin(kx) \tag{51}$$

$$w_p = q_2(y)\sin(kx) \tag{52}$$

$0 \leq x \leq l$, $k = m\pi$, m = a positive integer,

where $q_1(y)$, $q_2(y)$ are functions of the circumferential coordinate y only. Substituting (51), (52) in (22) and (23), we get

$$(k^2 - \frac{dy^2}{dy^2})^2 \, q_1(y) = 0 \tag{53}$$

$$\left[(k^2 - \frac{d^2}{dy^2})^2 - 2\lambda Z_p k^2\right] q_2(y) = 0 \tag{54}$$

(53) $\Longrightarrow$

$$q_1(y) = \cosh(ky)B_1 + (ky)\cosh(ky)\frac{B_2}{k} + \sinh(ky)B_3 + (ky)\sinh(ky)\frac{B_4}{k} \tag{55}$$

Let $$q_2(y) = Be^{ay} \tag{56}$$

Substituting in (54),

$$\left[(k^2 - a^2)^2 - 2\lambda Z_p k^2\right] = 0$$

or

$$\left.\begin{aligned} a^2 &= k^2\left[1 - \sqrt{2\lambda\frac{Z_p}{k^2}}\right] & a^2 &= k^2\left[1 + \sqrt{2\lambda\frac{Z_p}{k^2}}\right] \\ &= \varsigma_1^2 & &= \varsigma_2^2 \end{aligned}\right\} \tag{57}$$

$$2\lambda\frac{Z_p}{k^2} \gtrless 1 \quad \text{implies} \quad \varsigma_1^2 \lessgtr 0\,, \qquad \varsigma_2^2 > 0 \tag{58}$$

Case I: $2\lambda \frac{Z_p}{k^2} > 1$ $\quad \zeta_1 = k\sqrt{\sqrt{2\lambda \frac{Z_p}{k^2}} - 1}$, $\quad \zeta_2 = k\sqrt{1+\sqrt{2\lambda \frac{Z_p}{k^2}}}$

$$q_2(y) = \cos(\zeta_1 y)B_5 + \sin(\zeta_1 y)B_6 + \cosh(\zeta_2 y)B_7 + \sinh(\zeta_2 y)B_8 \tag{59}$$

Case II: $2\lambda \frac{Z_p}{k^2} = 1$ $\quad \zeta_1 = 0$ $\quad \zeta_2 = 2k$

$$q_2(y) = B_5 + ky \frac{B_6}{k} + \cosh(2ky)\, B_7 + \sinh(2ky)B_8 \tag{60}$$

Case III: $2\lambda \frac{Z_p}{k^2} < 1$ $\quad \zeta_1 = k\sqrt{1 - \sqrt{2\lambda \frac{Z_p}{k^2}}}$ $\quad \zeta_2 = k\sqrt{1 + \sqrt{2\lambda \frac{Z_p}{k^2}}}$

$$q_2(y) = \cosh(\zeta_1 y)B_5 + \sinh(\zeta_1 y)B_6 + \cosh(\zeta_2 y)B_7 + \sinh(\zeta_2 y)B_8 \tag{61}$$

Using (55), (59), (60), (61) in (51), (52)

$$f_p = \left[\cosh(ky)B_1 + (ky)\cosh(ky)\frac{B_2}{k} + \cosh(ky)B_3 + (ky)\sinh(ky)\frac{B_4}{k}\right]\sin(kx) \tag{62}$$

Case I: $2\lambda \frac{Z_p}{k^2} > 1$ $\quad$ or $\quad \lambda > \frac{k^2}{2Z_p}$

$$w_p = \left[\cos(\zeta_1 y)B_5 + \sin(\zeta_1 y)B_6 + \cosh(\zeta_2 y)B_7 + \sinh(\zeta_2 y)B_8\right]\sin(kx) \tag{63}$$

Case II: $2\lambda \frac{Z_p}{k^2} = 1$ $\quad$ or $\quad \lambda = \frac{k^2}{2Z_p}$

$$w_p = \left[B_5 + (ky)\frac{B_6}{k} + \cosh(2ky)B_7 + \sinh(2ky)B_8\right]\sin(kx) \tag{64}$$

Case III: $2\lambda \frac{Z_p}{k^2} < 1$ $\quad$ or $\quad \lambda < \frac{k^2}{2Z_p}$

$$w_p = \left[\cosh(\zeta_1 y)B_5 + \sinh(\zeta_1 y)B_6 + \cosh(\zeta_2 y)B_7 + \sinh(\zeta_2 y)B_8\right]\sin(kx) \tag{65}$$

Strain in axial direction =

$$\epsilon_x = \frac{h_p}{L}\frac{\partial U_p}{\partial x} = \frac{h_p^2/L^2}{\sqrt{12(1-\nu^2)}}\left[F_{p,yy} - \nu F_{p,xx}\right]$$

or

$$\frac{\partial U_p}{\partial x} = \frac{h_p/L}{\sqrt{12(1-\nu^2)}}\left[F_{p,yy} - \nu F_{p,xx}\right] \tag{66}$$

Strain in circumferential direction =

$$\epsilon_y = \frac{h_p}{L}\frac{\partial V_p}{\partial y} = \frac{h_p^2/L^2}{\sqrt{12(1-\nu^2)}}\left[F_{p,xx} - \nu F_{p,yy}\right]$$

or

$$\frac{\partial V_p}{\partial y} = \frac{h_p/L}{\sqrt{12(1-\nu^2)}}\left[F_{p,xx} - \nu F_{p,yy}\right] \tag{67}$$

Here, from (18)

$$F_p = F_p' + f_p = -\frac{\sigma h_p L^2\sqrt{12(1-\nu^2)}}{2Eh_p^3}y^2 + f_p \tag{68}$$

$$W_p = W_p' + w_p = \frac{\nu\sigma R}{Eh_p}\cos\beta_1 + w_p \tag{69}$$

Using (68), (69) in (62) through (67), we can easily obtain the various terms to be used in the matching condition:

Case I: $\lambda > \frac{k^2}{2Z_p}$

$$W_p = \frac{\nu\sigma R}{Eh_p}\cos\beta_1 + \left[\cos(\zeta_1 y)B_5 + \sin(\zeta_1 y)B_6 + \cosh(\zeta_2 y)\beta_7 + \sinh(\zeta_2 y)B_8\right]\sin(kx) \tag{70}$$

$$U_p = -\frac{\sigma L x}{E h_p} - \frac{kh_p/L}{\sqrt{12(1-\nu^2)}}\left[(1+\nu)\cosh(ky)B_1+\left\{(1+\nu)(ky)\cosh(ky)\right.\right.$$

$$\left.+2\sinh(ky)\right\}\frac{B_2}{k} + (1+\nu)\sinh(ky)B_3$$

$$\left.+\left\{(1+\nu)(ky)\sinh(ky)+2\cosh(ky)\right\}\frac{B_4}{k}\right]\cos(kx) \qquad (71)$$

$$V_p = \frac{\nu\sigma L}{E h_p} y - \frac{kh_p/L}{\sqrt{12(1-\nu^2)}}\left[(1+\nu)\sinh(ky)B_1+\left\{(1+\nu)(ky)\sinh(ky)\right.\right.$$

$$\left.-(1-\nu)\cosh(ky)\right\}\frac{B_2}{k} +(1+\nu)\cosh(ky)B_3+\left\{(1+\nu)(ky)\cosh(ky)\right.$$

$$\left.-(1-\nu)\sinh(ky)\right\}\frac{B_4}{k}\Big]\sin(kx) \qquad (72)$$

$$\frac{\partial W_p}{\partial y} = k\left[-\frac{\zeta_1}{k}\sin(\zeta_1 y)B_5+\frac{\zeta_1}{k}\cos(\zeta_1 y)B_6+\frac{\zeta_2}{k}\sinh(\zeta_2 y)B_7\right.$$

$$\left.+\frac{\zeta_2}{k}\cosh(\zeta_2 y)B_8\right]\sin(kx) \qquad (73)$$

$$\left(\frac{\partial^2 W_p}{\partial y^2}+\nu\frac{\partial^2 W_p}{\partial x^2}\right) = -k^2\left[\left(\frac{\zeta_1^2}{k^2}+\nu\right)\cos(\zeta_1 y)B_5+\left(\frac{\zeta_1^2}{k^2}+\nu\right)\sin(\zeta_1 y)B_6\right.$$

$$\left.-\left(\frac{\zeta_2^2}{k^2}-\nu\right)\cosh(\zeta_2 y)B_7-\left(\frac{\zeta_2^2}{k^2}-\nu\right)\sinh(\zeta_2 y)B_8\right]\sin(kx) \qquad (74)$$

$$F_{p,xy} = k^2\left[\sinh(ky)B_1+\left\{(ky)\sinh(ky)+\cosh(ky)\right\}\frac{B_2}{k}\right.$$

$$\left.+\cosh(ky)B_3+\left\{(ky)\cosh(ky)+\sinh(ky)\right\}\frac{B_4}{k}\right]\cos(kx) \qquad (75)$$

$$F_{p,xx} = -k^2\left[\cosh(ky)B_1+(ky)\cosh(ky)\frac{B_2}{k}+\sinh(ky)B_3\right.$$

$$\left.+(ky)\sinh(ky)\frac{B_4}{k}\right]\sin(kx) \tag{76}$$

$$\left(\frac{\partial^3 W_p}{\partial y^3}+(2-\nu)\frac{\partial^3 W_p}{\partial y\,\partial x^2}\right) = k^3\left[\frac{\zeta_1}{k}\left\{\frac{\zeta_1^2}{k^2}+(2-\nu)\right\}\sin(\zeta_1 y)B_5\right.$$

$$-\frac{\zeta_1}{k}\left\{\frac{\zeta_1^2}{k^2}+(2-\nu)\right\}\cos(\zeta_1 y)B_6+\frac{\zeta_2}{k}\left\{\frac{\zeta_2^2}{k^2}-(2-\nu)\right\}\sinh(\zeta_2 y)B_7$$

$$\left.+\frac{\zeta_2}{k}\left\{\frac{\zeta_2^2}{k^2}-(2-\nu)\right\}\cosh(\zeta_2 y)B_8\right]\sin(kx) \tag{77}$$

Case II: $\lambda = \dfrac{k^2}{2Z_p}$

$$W_p = \frac{\nu\sigma R}{Eh_p}\cos\beta_1+\left[B_5+(ky)\frac{B_6}{k}+\cosh(2ky)B_7+\sinh(2ky)B_8\right]\sin(kx) \tag{78}$$

$$U_p = -\frac{\sigma L x}{Eh_p}-\frac{kh_p/L}{\sqrt{12(1-\nu^2)}}\left[(1+\nu)\cosh(ky)B_1+\left\{(1+\nu)(ky)\cosh(ky)\right.\right.$$

$$\left.+2\sinh(ky)\right\}\frac{B_2}{k}+(1+\nu)\sinh(ky)B_3+\left\{(1+\nu)(ky)\sinh(ky)\right.$$

$$\left.\left.+2\cosh(ky)\right\}\frac{B_4}{k}\right]\cos(kx) \tag{79}$$

$$V_p = \frac{\nu\sigma L}{Eh_p}y-\frac{kh_p/L}{\sqrt{12(1-\nu^2)}}\left[(1+\nu)\sinh(ky)B_1+\left\{(1+\nu)(ky)\sinh(ky)\right.\right.$$

$$\left.-(1-\nu)\cosh(ky)\right\}\frac{B_2}{k}+(1+\nu)\cosh(ky)B_3$$

$$\left.+\left\{(1+\nu)(ky)\cosh(ky)-(1-\nu)\sinh(ky)\right\}\frac{B_4}{k}\right]\sin(kx) \tag{80}$$

$$\frac{\partial W_p}{\partial y} = k\left[0\ B_5 + \frac{B_6}{k} + 2\sinh(2ky)B_7 + 2\cosh(2ky)B_8\right]\sin(kx) \tag{81}$$

$$\left(\frac{\partial^2 W_p}{\partial y^2} + \nu\ \frac{\partial^2 W_p}{\partial x^2}\right) = -k^2\left[\nu B_5 + \nu ky\ \frac{B_6}{k} + (4-\nu)\cosh(2ky)B_7\right.$$

$$\left. +(4-\nu)\sinh(2ky)\ B_8\right]\sin(kx) \tag{82}$$

$$F_{p,xy} = k^2\left[\sinh(ky)B_1 + \left\{(ky)\sinh(ky)+\cosh(ky)\right\}\frac{B_2}{k}\right.$$

$$\left. +\cosh(ky)B_3 + \left\{(ky)\cosh(ky)+\sinh(ky)\right\}\frac{B_4}{k}\right]\cos(kx) \tag{83}$$

$$F_{p,xx} = -k^2\left[\cosh(ky)B_1 + (ky)\cosh(ky)\ \frac{B_2}{k} + \sinh(ky)\ B_3\right.$$

$$\left. +(ky)\sinh(ky)\ \frac{B_4}{k}\right]\sin(kx) \tag{84}$$

$$\left(\frac{\partial^3 W_p}{\partial y^3} + (2-\nu)\ \frac{\partial^3 W_p}{\partial y \partial x^2}\right) = k^3\left[0\ B_5 - (2-\nu)\ \frac{B_6}{k} + 2\left\{4-(2-\nu)\right\}\sinh(2ky)B_7\right.$$

$$\left. +2\left\{4-(2-\nu)\right\}\cosh(2ky)B_8\right]\ \sin(kx) \tag{85}$$

Case III: $\lambda < \dfrac{k^2}{2Z_p}$

$$W_p = \frac{\nu\sigma R}{Eh_p}\cos\beta_1 + \left[\cosh(\zeta_1 y)B_5 + \sinh(\zeta_1 y)B_6\right.$$

$$\left. +\cosh(\zeta_2 y)B_7 + \sinh(\zeta_2 y)B_8\right]\sin(kx) \tag{86}$$

$$U_p = -\frac{\sigma L x}{E h_p} - \frac{k h_p/L}{\sqrt{12(1-\nu^2)}} \left[(1+\nu)\cosh(ky)B_1 + \left\{(1+\nu)(ky)\cosh(ky) + 2\sinh(ky)\right\}\frac{B_2}{k} + (1+\nu)\sinh(ky)B_3 + \left\{(1+\nu)(ky)\cosh(ky) + 2\cosh(ky)\right\}\frac{B_4}{k}\right]\cos(kx) \tag{87}$$

$$V_p = \frac{\nu\sigma L}{E h_p}\, y - \frac{k h_p/L}{\sqrt{12(1-\nu^2)}}\left[(1+\nu)\sinh(ky)B_1 + \left\{(1+\nu)(ky)\sinh(ky) - (1-\nu)\cosh(ky)\right\}\frac{B_2}{k} + (1+\nu)\cosh(ky)B_3 + \left\{(1+\nu)(ky)\cosh(ky) - (1-\nu)\sinh(ky)\right\}\frac{B_4}{k}\right]\sin(kx) \tag{88}$$

$$\frac{\partial W_p}{\partial y} = k\left[\frac{\zeta_1}{k}\sinh(\zeta_1 y)B_5 + \frac{\zeta_1}{k}\cosh(\zeta_1 y)B_6 + \frac{\zeta_2}{k}\sinh(\zeta_2 y)B_7 + \frac{\zeta_2}{k}\cosh(\zeta_2 y)B_8\right]\sin(kx) \tag{89}$$

$$\left(\frac{\partial^2 W_p}{\partial y^2} + \nu\frac{\partial^2 W_p}{\partial x^2}\right) = k^2\left[\left(\frac{\zeta_1^2}{k^2} - \nu\right)\cosh(\zeta_1 y)B_5 + \left(\frac{\zeta_1^2}{k^2} - \nu\right)\sinh(\zeta_1 y)B_6 + \left(\frac{\zeta_2^2}{k^2} - \nu\right)\cosh(\zeta_2 y)B_7 + \left(\frac{\zeta_2^2}{k^2} - \nu\right)\sinh(\zeta_2 y)B_8\right]\sin(kx) \tag{90}$$

$$F_{p,xy} = k^2 \left[\sinh(ky)B_1 + \left\{(ky)\sinh(ky)+\cosh(ky)\right\}\frac{B_2}{k} + \cosh(ky)B_3 + \left\{(ky)\cosh(ky)+\sinh(ky)\right\}\frac{B_4}{k} \right]\cos(kx) \tag{91}$$

$$F_{p,xx} = -k^2 \left[\cosh(ky)B_1 + (ky)\cosh(ky)\frac{B_2}{k} + \sinh(ky)B_3 + (ky)\sinh(ky)\frac{B_4}{k} \right]\sin(kx) \tag{92}$$

$$\left(\frac{\partial^3 W_p}{\partial y^3} + (2-\nu)\frac{\partial^3 W_p}{\partial y \partial x^2}\right) = k^3 \left[\frac{\zeta_1}{k}\left\{\frac{\zeta_1^2}{k^2} - (2-\nu)\right\}\sinh(\zeta_1 y)B_5 + \frac{\zeta_1}{k}\left\{\frac{\zeta_1^2}{k^2} - (2-\nu)\right\}\cosh(\zeta_1 y)B_6 + \frac{\zeta_2}{k}\left\{\frac{\zeta_2^2}{k^2} - (2-\nu)\right\}\sinh(\zeta_2 y)B_7 + \frac{\zeta_2}{k}\left\{\frac{\zeta_2^2}{k^2} - (2-\nu)\right\}\cosh(\zeta_2 y)B_8 \right]\sin(kx) \tag{93}$$

It can be easily observed that expressions for U_p, V_p, $F_{p,xy}$, $F_{p,xx}$ are identical in all three cases. This is because of the fact that f_p is independent of λ. The expressions have been repeated to make each set complete. In the next section we shall use these expressions in the matching conditions to obtain the eigenvalue problem.

5c. Matching Conditions and Evaluation of λ_{CR}

The expressions for displacements and forces in the curved and flat panels have 16 arbitrary constants of integration - $\{A_i\}$, $\{B_i\}$, $(i = 1, 8)$. From equations (43) through (50) for the curved

panel and Eqns. (70) through (77) or (78) through (85) or (86) through (93) for the flat panel, it is obvious that the perturbation parts of the forces and displacements identically satisfy the boundary conditions (15)-(16) at x = 0, 1. To evaluate the sixteen constants, therefore, we must match the appropriate forces and displacements at edges A($y_s = -\frac{R}{L}(\pi-\beta_1)$, $y_p = \frac{R}{L}\sin\beta_1$) and B($y_s = \frac{R}{L}(\pi-\beta_1)$, $y_p = -\frac{R}{L}\sin\beta_1$). (See Fig. 1). This gives sixteen equations for the sixteen unknowns, $\{A_i\}$, $\{B_i\}$, (i = 1, 8).

Using the proper expressions, we obtain the following equations from the matching conditions, Eqns. (7) through (14):

$$\begin{bmatrix} P_A \\ (8\times 8)\end{bmatrix}\begin{Bmatrix} A_i \\ 8\times 1\end{Bmatrix} = \begin{bmatrix} C_A \\ (8\times 8)\end{bmatrix}\begin{bmatrix} H \\ (8\times 8)\end{bmatrix}\begin{bmatrix} Q_A \\ (8\times 8)\end{bmatrix}\begin{Bmatrix} B_i \\ 8\times 1\end{Bmatrix}$$
$$\begin{bmatrix} P_B \\ (8\times 8)\end{bmatrix}\begin{Bmatrix} A_i \\ 8\times 1\end{Bmatrix} = \begin{bmatrix} C_B \\ (8\times 8)\end{bmatrix}\begin{bmatrix} H \\ (8\times 8)\end{bmatrix}\begin{bmatrix} Q_B \\ (8\times 8)\end{bmatrix}\begin{Bmatrix} B_i \\ 8\times 1\end{Bmatrix} \qquad (94)$$

where P_A, P_B, Q_A, Q_B, C_A, C_B and H are real 8 × 8 matrices. Row 1 through 8 of each of the matrices P_A, P_B, Q_A, Q_B has as its elements the coefficients of A_i (for the curved panel) or B_i (for the flat panel) in the expressions of W, U, V, $\frac{\partial w}{\partial y}$, $(\frac{\partial^2 W}{\partial y^2} + \nu\frac{\partial^2 W}{\partial x^2})$, $\frac{\partial^2 F_s}{\partial x\partial y}$, $\frac{\partial^2 F_s}{\partial x^2}$ and $\bar{h}(\frac{\partial^3 W}{\partial y^3} + (2-\nu)\frac{\partial^3 W}{\partial y\partial x^2})$ respectively. Here $\bar{h} = \frac{h/L}{\sqrt{12(1-\nu^2)}}$. In all the expressions, appropriate subscripts are implied and the expressions are evaluated using values of y_s and y_p corresponding to the edges A or B as the case may be.

The matrix C_A has the following form:

$$\left[C_A\right] = \begin{bmatrix} \cos\beta_1 & \sin\beta_1 & 0 & 0 & 0 & 0 & 0 & 0 \\ -\sin\beta_1 & \cos\beta_1 & 0 & 0 & 0 & 0 & 0 & 0 \\ 0 & 0 & 1 & 0 & 0 & 0 & 0 & 0 \\ 0 & 0 & 0 & 1 & 0 & 0 & 0 & 0 \\ 0 & 0 & 0 & 0 & 1 & 0 & 0 & 0 \\ 0 & 0 & 0 & 0 & 0 & 1 & 0 & 0 \\ 0 & 0 & 0 & 0 & 0 & 0 & \cos\beta_1 & \sin\beta_1 \\ 0 & 0 & 0 & 0 & 0 & 0 & -\sin\beta_1 & \cos\beta_1 \end{bmatrix} \tag{95}$$

Matrix C_B is identical to matrix C_A except that "sine" terms have signs opposite to those in C_A.

Matrix H is a diagonal matrix of the form

$$\left[H\right] = \begin{bmatrix} h' & h' & h' & h' & h'^4 & h'^3 & h'^3 & h'^3 \end{bmatrix} \tag{96}$$

Eqn. (94) forms a set of 16 homogeneous algebraic equations for 16 unknowns. For a non-trivial solution, the determinant of the 16 x 16 matrix of coefficients of $\{A_i\}$, $\{B_i\}$ must vanish. The lowest value of λ at which the determinant vanishes gives the critical load of the shell. The corresponding value of $\{A_i\}$, $\{B_i\}$ is the eigenmode and hence determines the variation of the state variables in the shell.

Symmetric and Antisymmetric Modes

The computation time for evaluating λ_{CR} can be considerably reduced if the order of the matrices is reduced. In this problem, if we introduce the following changes:

$$a_1 = \frac{A_1+A_3}{2},\ a_2 = \frac{A_2-A_4}{2},\ a_3 = \frac{A_5+A_7}{2},\ a_4 = \frac{A_6-A_8}{2},\ a_5 = B_1,\ a_6 = \frac{B_4}{k}$$

$$a_7 = B_5,\ a_8 = B_7 \tag{97}$$

$$b_1 = \frac{A_1-A_3}{2},\ b_2 = \frac{A_2+A_4}{2},\ b_3 = \frac{A_5-A_7}{2},\ b_4 = \frac{A_6+A_8}{2},\ b_5 = B_3,\ b_6 = \frac{B_2}{k}$$

$$b_7 = B_6,\ b_8 = B_8 \tag{98}$$

All the expressions in Eqns. (43) through (50) and (70) through (93), split into symmetric and antisymmetric parts - symmetric parts associated with coefficients a_i and antisymmetric parts with coefficients b_i. Here symmetry is considered in the circumferential direction with respect to the origin in each panel. When the change mentioned above is made, Eqn. (94) can be expressed in the form:

$$\begin{bmatrix} P_{(8\times8)} & 0 \\ 0 & Q_{(8\times8)} \end{bmatrix} \begin{Bmatrix} a_i \\ b_i \end{Bmatrix}_{(8\times1)} = \begin{Bmatrix} 0 \end{Bmatrix} \tag{99}$$

For non-trivial values of $\{a_i\}$, $\{b_i\}$,

$$\text{Det.} \begin{bmatrix} P & 0 \\ 0 & Q \end{bmatrix} = 0$$

or $\quad \text{Det. } [P] \ \text{Det. } [Q] = 0$

$$\text{This implies either} \quad \text{Det.}[P] = 0 \Longrightarrow \text{Symmetric Mode}$$
$$\text{or} \quad \text{Det.}[Q] = 0 \Longrightarrow \text{Antisymmetric Mode} \tag{100}$$
$$\text{or} \quad \text{both Det.}[P] = \text{Det.}[Q] = 0$$

Symmetric and antisymmetric modes are decoupled. Also, instead of one 16 x 16 matrix, we have 2 - 8 x 8 matrices which are comparatively easier to handle.

Matrices [P] and [Q] are listed in Appendix II.

6. NUMERICAL EVALUATION OF THE CRITICAL LOAD

At this point in the analysis, we can make the following observations about λ:

(i) $\lambda = \sigma/\sigma_{CL}(R, h_s)$ where $\sigma_{CL} = \dfrac{Eh_s/R}{\sqrt{3(1-\nu)^2}}$ is the buckling stress for a circular cylindrical shell of radius and thickness equal to that of the curved panel.

(ii) λ occurs non-linearly in every element of the matrices. For example θ, ℓ_1, ℓ_2, ξ_1, η_1, ξ_2, η_2, φ, ψ are non-linear functions of λ (see Eqns. (32) through (38)).

(iii) At $\lambda = 1$, i.e., an applied stress equal to $\sigma_{CL}(R, h_s)$, θ, η_1, η_2, φ, ψ vanish (Eqns. (32), (34), (36), (38)). This results in the vanishing of all "sine" terms in the expressions (43)-(50) for the curved panel. Therefore, from Eqn. (94), the determinant of the coefficient matrix is zero at $\lambda = 1$ and the upper limit for λ_{CR} is 1.

(iv) For $\lambda > 1$, from Eqn. (32), $\lambda = \cos\theta$ is no longer valid. Instead, $\lambda = \cosh\theta$ can be used. Proceeding as before, we obtain γ either real or pure imaginary and not complex ($\gamma = \xi + i\eta$) as in Eqn. (33).

This radically changes the character of the solution for f_s and w_s and hence all the state variables of the curved panel.

From (ii) above, it is fairly apparent that it is almost impossible to obtain a closed form value of λ_{CR} as a function of the geometric and material parameters of the shell. To obtain λ_{CR} numerically, we use the fact that λ_{CR} is the lowest value of λ for which at least one of the determinants (Eqn. (100)) vanishes. Let $g(\lambda)$ be one of the determinants as a function of λ. We can use the Method Of False Position (Ref. (9), p. 99) to pinpoint λ_{CR}. In this method, successive approximations to λ for which $g(\lambda) = 0$ are given by

$$\lambda_{j+1} = \lambda_j - g(\lambda_j) \frac{\lambda_j - \lambda_{j-1}}{g(\lambda_j) - g(\lambda_{j-1})} \qquad j = 1, 2, \ldots . \tag{101}$$

To start the iterative scheme we must guess the first two values, λ_1, λ_2. A geometric interpretation of the method is given in Fig. 5a . This method should work fairly well except when (a) there are more than one zeroes of $g(\lambda)$ between λ_{j-1} and λ_j; (b) one of the λ_j's in (101) is greater than 1, which in view of (iv), may mean trouble in our case. Therefore, we should use some other method.

From (iii) above, we know λ_{CR} lies between 0 and 1 and also we are interested in the lowest value of λ_{CR} in this range. So to compute λ_{CR}, we can divide the interval 0-1 into N parts. Starting from 0, we compute $g(\lambda)$ at each node and find two consecutive nodes between which $g(\lambda)$ changes sign. This means λ_{CR} lies between

those two nodes. Making the two nodes as the lower and upper limits of the interval, the process can be repeated to obtain λ_{CR} to any desired accuracy. A geometric representation of the method is given in Fig. 5b . The exact method followed is described below:

(a) For given values of L, R, h_s, h_p, ν, choose m, the number of half waves in the axial direction.

(b) For each value of β_1, find λ_{CR} corresponding to the assumed m.

(c) Vary m and repeat the process until, at the given β_1, λ_{CR} reaches a minimum with respect to m.

(d) When the information is required for a range of β_1's, plots of λ_{CR} vs. β_1 at different m can be obtained. The locus of the lowest λ_{CR} as a function of β_1 will be the final curve representing the shell. A representative plot to illustrate the method is shown in Fig. 6.

It may be pointed out that the problem of two or more zeroes of $g(\lambda)$ between two consecutive nodes is present in this method also. However the problem can be easily identified and corrected as follows: For a given shell, at a fixed m, the determinant g is a continuous function of λ and β_1 and λ_{CR} is determined by $g(\lambda_{CR}, \beta_1) = 0$. This implies λ_{CR} is a continuous function of β_1 for fixed R, L, h_s, h_p, ν and m. Therefore in the plot of λ_{CR} vs. β_1 at a given m, we can expect a sudden jump in the value of λ_{CR} at β_1, for which the lowest λ was missed because of multiple zeroes. We can find the actual value by specifying the obtained value for λ_{CR} as the upper limit and repeating the method described in (a), (b), (c) above.

7. RESULTS

Numerical results were obtained in order to study the effect of radius/length and radius/thickness ratios of the shell. For the sake of simplicity in all the computations, the thickness of the flat panel was taken to be the same as that of the curved panel, i.e.,

$h_s = h_p = h$ = thickness of the shell, $h' = 1.0$

In Table I, numerical values of λ_{CR} as a function of β_1 (half of the angle of flat spot) and m (no. of half waves in the axial direction) are presented for a shell of $R/h = 1000$, $R/L = 0.25$, $\nu = 0.3$. By examining this table we observe

(i) For a fixed β_1, there is a particular wave no. m for which λ_{CR} reaches a minimum (this λ_{CR} is underlined in the table).

(ii) This value of m and corresponding λ_{CR} decrease with an increase in β_1. Also for a fixed m, λ_{CR} decreases monotonically with increasing β_1.

Similar values of λ_{CR} for shells of the same thickness ratio and ν, but for $R/L = 0.50$ and $R/L = 1.0$ are given in Tables II and III. By comparing Tables I, II, III, it can be seen that, for the same R/h, ν and β_1, λ_{CR} remains unchanged if mR/L remains fixed, i.e., λ_{CR} for half waves m in case of $R/L = 1.0$, 2m for $R/L = 0.5$ and 4m for $R/L = 0.25$ have the same value. This point is justified analytically in Appendix III. It may be mentioned here that the last observation is strictly valid only when we consider λ_{CR} vs. β_1 at a fixed number of half waves and it may not hold generally for the general curves for shells having $R/L = 1.0$, 0.5 and 0.25. For

example, for some β_1, in the shell with R/L = 1.0, the lowest λ_{CR} is obtained for m = 2. For shells with R/L = 0.50, 0.25 at the same β_1, the same λ_{CR} will be obtained for m = 4 and 8 respectively, but these λ_{CR} may not be the lowest values for the shells at that β_1. It is possible that m = 3 or 5 (for R/L = 0.50) and m = 6, 7, 9, 10, etc. (for R/L = 0.25) may give the lowest critical loads.

Tables similar to I, II, III are presented for shells with R/h = 500 (Tables IV, V, VI) and R/h = 100 (Tables VII, VIII, IX). The discussion above equally applies to the results for the thicker shells.

The results presented in Tables I through IX, correspond to the symmetric buckling mode of the shell. They represent the lowest value of λ_{CR} for each β_1 and m, because it was found numerically that the antisymmetric mode always had a λ_{CR} higher than that for the symmetric mode at the same β_1 and m.

In Fig. 7 and Fig. 8, final plots of λ_{CR} vs. β_1 for shells of R/h = 1000, ν = 0.3, R/L = 0.25 and R/L = 1.0 respectively are presented. Numbers on each curve indicate the number of half waves m in the adjoining range of β_1. In addition to the plot for the shell, in each figure is plotted the λ_{CR} vs. β_1 variation for a simply-supported flat panel of width and thickness the same as that of the flat spot of the shell. λ_{CR} for a simply-supported flat panel is given by

$$\lambda_{CR} = \sigma_{CR}/\sigma_{CL}(R,h), \quad \sigma_{CR} = \frac{4\pi^2 Eh^2}{12(1-\nu^2)b^2} \tag{102}$$

b = width of the panel
= $2R\sin\beta_1$ (in the present case)

It can be seen that there is a wide difference between the results for the shell and the s. s. panel. This is especially true at low values of β_1 (small flat spots) when λ_{CR} for the shell is lower. However, agreement between the two improves for bigger flat spots (large β_1) and the λ_{CR} for the s. s. panel may be considered as a lower bound to the critical load of the shell.

In Fig. 9 , the out of plane or radial displacement distribution is plotted for some representative flat spot widths. It can be observed that, for small flat spots, the displacement is not limited to the flat panel only, but a very large portion (many times the width of the flat spot) of the curved panel is also affected. On the other hand, for very large β_1 (big flat spots), the buckling is essentially localized in the flat panel. Only a small region of the curved panel, near the common edges, is distorted in the buckling. This very much explains the better agreement between the λ_{CR} vs. β_1 curves for the shell and the panel, at larger values of β_1's.

In Fig. 10, 11 and 12 (for R/h = 500) and Fig. 13, 14 and 15 (for R/h = 100), analogous plots of λ_{CR} vs. β_1 and out of plane displacement distribution have been plotted. Further, in Fig. 16, the effect of very wide flat spot on λ_{CR} (for a shell of R/h = 100) is indicated and a representative set of radial displacement distributions are shown in Fig. 17. The comments and discussion for the shells of R/h = 1000, applies equally well to the thicker shells (R/h = 500, 100).

Finally, in Fig. 18 is presented a composite plot showing the effect of varying R/h on λ_{CR} vs. β_1. An analogous plot for the

simply-supported panels is also presented in the same figure for comparison. Fig. 19 shows the displacement distribution for a fixed flat spot width ($\beta_1 = 4.0$) as R/h changes. All these graphs show (i) for the same flat spot width, the thinner the shell, the more severe is the effect on the critical load, (ii) for the same flat spot widths, larger portions of curved panel are affected in thicker shells than in thinner shells.

8. CONCLUSIONS

In concluding this chapter, we can make the following observations:

(a) Cylindrical shells are indeed affected by the presence of flat spots. The severity of reduction of their critical loads increases with an increase in the width of the flat spot and the radius to thickness ratio of the shell. However the trend of the curve of λ_{CR} vs. width of flat spot is not substantially affected by changing the radius to length ratio of the shell.

(b) Beyond a certain width of the flat spot, the critical load of a simply-supported panel with thickness and width the same as those of the flat spot may provide a good lower bound to the critical load of the shell. The width beyond which this is true increases with the thickness of the shell.

(c) Koiter (Ref. 11) and Hutchinson (Ref. 8) in their analysis of axisymmetric imperfections, have shown that the critical load is very seriously affected by even very small amplitudes ($\epsilon \to 0$) of the imperfection. However, in the case of single flat spot prismatic

imperfections, this is not true. This is indicated by the horizontal tangent of the λ_{CR} vs. β_1 curve at $\lambda_{CR} = 1.0$, $\beta_1 = 0.0$. In fact, up to a certain β_1, λ_{CR} remains at unity. This value of β_1 decreases as the shells become thinner. If β_1 increases beyond this β_1, there is a rapid decrease in the critical load.

(d) This analysis of a very simple flat spot configuration has clearly indicated that prismatic imperfections in general, and flat spots in particular, are of importance, if we wish to predict the behavior of cylindrical shells under axial compression. It is certainly of great interest to find how a prismatic imperfection more general than a single flat spot would affect the critical load of a cylindrical shell.

II. BUCKLING OF IMPERFECT CIRCULAR CYLINDRICAL SHELL UNDER AXIAL COMPRESSION: SHELL WITH MULTIPLE FLAT SPOTS

1. INTRODUCTION

In the last chapter, buckling of a circular cylindrical shell with a single flat spot was considered. The principal conclusion was that the critical load of the shell is severely reduced because of the flat spot. However, in the analysis, it was assumed that there was no effect on the critical load of the shell due to the stress concentrations associated with the sharp corners between the panels. In actual structures, the designer tries to avoid unnecessary sharp corners to keep down problems of stress concentrations. In the introduction to the last chapter, it was mentioned that the shells may be formed by rolling flat sheets into the shape of the intended shells. This will help in eliminating the sharp corners. Also, we can expect that the imperfection will be more general than the single flat spot we considered in the last chapter.

Sometimes it may be possible to approximate a circle by a regular polygon with rounded corners. Or in other words, the shell may be formed from the flat sheet by bending it at discrete points instead of by continuous rolling. Let us for the moment assume that the inscribed radius of the shell has been prescribed. Now the obvious question arises: how does the critical load of the shell, so formed, vary with the number of sides of the polygon, the radius of the rounded corners, or the size of the flat panels? To illustrate

this point, in Fig.20 are shown only a few of the infinite ways to form the shell, having a given radius for the inscribed circle.

With the above considerations in view, in this chapter the imperfection again will be assumed in the form of flat spots. However, the shell will have two or more flat spots distributed uniformly along the circumference of the shell. Instead of sharp corners, two adjacent panels will join smoothly at their common edges. The analysis of this configuration will answer some of the questions posed above, while at the same time it will indicate the effect of more general (cyclic) prismatic imperfections.

2. DEFINITION OF THE PROBLEM

Let us consider a shell which has length L and r as the radius of the inscribed circle. Let the shell be formed from N identical flat panels and N identical uniform radius curved panels. Each flat panel has a thickness h_p and subtends an angle $2\beta_1$ at the center of the inscribed circle. The circular panels are of radius R, width = 2T and thickness h_s. The flat panels and the circular panels are so arranged that: (a) no two panels of the same kind are adjacent to each other, (b) two adjacent panels join smoothly without a sharp corner at their common edge. The configuration of the shell and details are shown in Fig. 21a.

If this shell is subjected to a uniform axial compressive stress σ, we shall study the effect of N (the number of panels of each kind), R/r (the radius of the circular panel as a fraction of the radius of the inscribed circle) and β_1 (width of the flat panels) on the value σ

at which the shell becomes unstable.

3. GEOMETRIC PRELIMINARIES

Angle subtended by each flat panel at the center of the inscribed circle = $2\beta_1$.

$$\text{Width of each flat panel} = 2b = 2r\tan\beta_1 \tag{103}$$

Let the angle subtended by the curved panel at the center of the inscribed circle = $2\beta_2$.

$$2(\beta_1+\beta_2) = \frac{2\pi}{N} \text{ or } (\beta_1+\beta_2) = \frac{\pi}{N} \tag{104}$$

From Fig.21a, the angle subtended by the curved panel at the center of its own circle = $2(\beta_1+\beta_2)$.

$$\therefore \quad 2(\beta_1+\beta_2) = \frac{2\pi}{N} = \frac{2T}{R}$$

$$\text{or} \quad (\beta_1+\beta_2) = \frac{\pi}{N} = \frac{T}{R} \tag{105}$$

Also from Fig. ,

$$\frac{r}{R} = \frac{r\tan\beta_1 + R\tan(\beta_1+\beta_2)}{R\tan(\beta_1+\beta_2)}$$

$$\text{or} \quad \tan\beta_1 = (1 - \frac{R}{r}) \tan (\frac{\pi}{N})$$

$$\text{or } b = r\tan\beta_1 = r(1 - \frac{R}{r}) \tan (\frac{\pi}{N}) \tag{106}$$

4. GOVERNING EQUATIONS

The method used to solve the problem will be exactly the same as that for the case of a single flat spot shell. Donnell's shallow

shell equations will be used in the curved panels and the flat plate equations in the flat panels of the shell. At the common edges between adjacent panels, matching conditions will be prescribed. Before proceeding further with the analysis, it will be appropriate to make the following comments on the notation used in the analysis:

(i) All the panels are identified by numbers from 1 to 2N and the panels are numbered consecutively. Thus all odd numbered panels will be curved panels, while the even numbered panels will be flat panels.

(ii) The coordinate system used is shown in Fig.2la. The origin for the coordinate system for a panel will be at the center of the panel.

(iii) The two edges of each panel will be identified by subscripts F (for the forward or positive y edge) and B (for the back or negative edge of the panel). Thus the forward edge of the ith panel will be in contact with the back edge of the (i+1)st panel. For example, W_{1F} is the displacement in the z direction at the forward edge of the first panel, while V_{iB} is the displacement in the circumferential direction at the back edge of the ith panel.

Since all the curved panels are identical, as are all flat panels, we can write, without any risk of confusion:

(a) In every curved panel

$$\nabla^4 F - Z_s W_{,xx} + \sqrt{12(1-\nu^2)}\,(W_{,xx}W_{,yy} - W^2_{,xy}) = 0 \qquad (107)$$

$$\nabla^4 W + Z_s F_{,xx} - \sqrt{12(1-\nu^2)}\,(F_{,xx}W_{,yy} - 2F_{,xy}W_{,xy} + F_{,yy}W_{,xx}) = 0 \qquad (108)$$

(b) In every flat panel

$$\nabla^4 F + \sqrt{12(1-\nu^2)}\,(W_{,xx}W_{,yy} - W^2_{,xy}) = 0 \qquad (109)$$

$$\nabla^4 W - \sqrt{12(1-\nu^2)}\,(F_{,xx}W_{,yy} - 2F_{,xy}W_{,xy} + F_{,yy}W_{,xx}) = 0 \qquad (110)$$

It is understood here that Eqns. (107), (108) are valid for all curved panels (numbered 1, 3, 5,....,2N-1), and Eqns. (109), (110) are valid for all flat panels (numbered 2, 4, 6,....,2N).

(c) At the common edges (see Fig. 21a)

In the curved panel, the forward edge is at $y = \frac{T}{L}$, back edge at $y = -\frac{T}{L}$ (111)

In the flat panel, the forward edge is at $y = \frac{r}{L}\tan\beta_1$, back edge at $y = -\frac{r}{L}\tan\beta_1$ (112)

If, in a panel, we define a vector $\{\underline{S}_i^T\}$ by

$$\{\underline{S}_i^T\} = \left\{ \begin{array}{l} W \\ \dfrac{\partial^2 W}{\partial y^2} + \nu \dfrac{\partial^2 W}{\partial x^2} \\ U \\ \dfrac{\partial^2 F}{\partial x^2} \\ \dfrac{\partial W}{\partial y} \\ \bar{h}\left(\dfrac{\partial^3 W}{\partial y^3} + (2-\nu)\dfrac{\partial^3 W}{\partial y \partial x^2}\right) \\ V \\ \dfrac{\partial^2 F}{\partial x \partial y} \end{array} \right\}, \quad \bar{h} = \frac{h/L}{\sqrt{12(1-\nu^2)}} \qquad (113)$$

Then we can write the matching conditions as

$$\{\underline{S}_i^T\}_F = [H_1]\ \{\underline{S}_{(i+1)}^T\}_B \qquad i = 1, 3, 5, \ldots, (2N-1) \qquad (114)$$

$$[H_1]\ \{\underline{S}_i^T\}_F = \{\underline{S}_{(i+1)}^T\}_B \qquad i = 2, 4, 6, \ldots, (2N) \qquad (115)$$

Panel No. 1 and (2N+1) refer to the same panel. $[H_1]$ is a real (8 x 8) diagonal matrix of the form

$$[H_1] = \begin{bmatrix} h' & h'^4 & h' & h'^3 & h' & h'^3 & h' & h'^3 \end{bmatrix} \qquad (117)$$

It may be noted here that the order of using various matching conditions is different in (113) than that used in (7) through (14). This is done so as to utilize fully the separation of the solution into symmetric and antisymmetric components. This will become apparent as the analysis progresses towards the numerical computation stage.

(d) Boundary conditions

As before, it is assumed that the boundary conditions at x = 0, 1 are applied only during the buckling process and they are given below:

At x = 0, 1 for all y

$$w = w_{,xx} = f_{,yy} = v = 0 \qquad (118)$$

in all panels. The lower case quantities are the perturbations (on the prebuckling state), which occur during the buckling process.

5. Prebuckling solution

It can be easily verified that the following is the solution of the governing equations:

In the curved panels

$$F' = -\frac{\sigma h_s}{2}\frac{L^2}{Eh_s^3}\sqrt{12(1-\nu^2)}\,y^2 \tag{119}$$

$$W' = \frac{\nu\sigma R}{Eh_s} + \frac{\nu\sigma r\tan(\beta_1)}{Eh_s\sin(\pi/N)}\cos(\frac{Ly}{R}) \tag{120}$$

The amplitude of $\cos(\frac{Ly}{R})$ in Eqn. (120) is the rigid body motion of the circular panel parallel to the line joining the centers of the inscribed circle and the circle of the curved panel.

In the flat panels

$$F' = -\frac{\sigma h_p}{2}\frac{L^2}{Eh_p^3}\sqrt{12(1-\nu^2)}\,y^2 \tag{121}$$

$$W' = \frac{\nu\sigma r}{Eh_p} = \text{rigid body motion of the flat panel normal to its plane} \tag{122}$$

Again, very simple calculations will show that Eqns. (119) through (122) imply a bending free stress state. (See Fig.21a for a pictorial representation of the prebuckling deformation.)

6. ANALYSIS OF THE BUCKLED STATE

Proceeding as in section 5 of Chapter I, let the buckled state in each panel be given by:

$$\left.\begin{aligned} F &= F' + f \\ W &= W' + w \end{aligned}\right\} \tag{124}$$

where F' and W' constitute the prebuckling solution and are given in Eqns. (119) through (123) of the last section and f and w are infinitesimal perturbations on the prebuckling solution. The compressive stress σ, at which non-vanishing values for f and w are possible, is the critical stress of the shell. Substituting (124) in Eqns. (107) through (110) and linearizing with respect to the infinitesimal quantities f and w, we obtain:

In every curved panel (panels numbered 1, 3, 5, ... , 2N-1)

$$\nabla^4 f - Z_s w_{,xx} = 0 \tag{125}$$

$$\nabla^4 w + Z_s f_{,xx} + 2\lambda_s Z_s w_{,xx} = 0 \tag{126}$$

In every flat panel (panels numbered 2, 4, 6, ... , 2N)

$$\nabla^4 f = 0 \tag{127}$$

$$\nabla^4 w + 2\lambda_s Z_p w_{,xx} = 0 \tag{128}$$

Here $Z_s = \left(\frac{L}{R}\right)^2 \left(\frac{R}{h_s}\right) \sqrt{12(1-\nu^2)}$, $Z_p = \left(\frac{h_s}{h_p}\right)^2 Z_s$, $\lambda_s = \sigma/\sigma_{CL}(R, h_s)$

$$\sigma_{CL}(R, h_s) = \frac{Eh_s/R}{\sqrt{3(1-\nu^2)}} \tag{129}$$

$$Z = \left(\frac{L}{r}\right)^2 \left(\frac{r}{h}\right) \sqrt{12(1-\nu^2)}\ , \quad \lambda = \sigma/\sigma_{CL}(r, h) \tag{130}$$

Eqns. (125) through (128) are identical to Eqns. (2) through (5) of Chapter I and we can write their solution and hence the matching condition expressions as follows:

In Every Curved Panel (from Eqns. (43) through (50))

$$W = \frac{\nu\sigma R}{Eh_s} + \frac{\nu\sigma r\tan(\beta_1)}{Eh_s\sin(\pi/N)}\cos\left(\frac{Ly}{R}\right)$$

$$-\Big[\Big\{e^{\xi_1 y}\cos(\eta_1 y+\theta)+e^{-\xi_1 y}\cos(\eta_1 y-\theta)\Big\}a_1$$

$$+\Big\{e^{\xi_1 y}\sin(\eta_1 y+\theta)-e^{-\xi_1 y}\sin(\eta_1 y-\theta)\Big\}a_2+\Big\{e^{\xi_2 y}\cos(\eta_2 y-\theta)$$

$$+e^{-\xi_2 y}\cos(\eta_2 y+\theta)\Big\}a_3+\Big\{e^{\xi_2 y}\sin(\eta_2 y-\theta)-e^{-\xi_2 y}\sin(\eta_2 y+\theta)\Big\}a_4$$

$$+\Big\{e^{\xi_1 y}\cos(\eta_1 y+\theta)-e^{-\xi_1 y}\cos(\eta_1 y-\theta)\Big\}a_5+\Big\{e^{\xi_1 y}\sin(\eta_1 y+\theta)$$

$$+e^{-\xi_1 y}\sin(\eta_1 y-\theta)\Big\}a_6+\Big\{e^{\xi_2 y}\cos(\eta_2 y-\theta)-e^{-\xi_2 y}\cos(\eta_2 y+\theta)\Big\}a_7$$

$$+\Big\{e^{\xi_2 y}\sin(\eta_2 y-\theta)+e^{-\xi_2 y}\sin(\eta_2 y+\theta)\Big\}a_8\Big]\sin(kx) \qquad (131)$$

$$\left(\frac{\partial^2 W}{\partial y^2}+\nu\frac{\partial^2 W}{\partial x^2}\right) = -k^2\Bigg[\Big\{e^{\xi_1 y}\left(\frac{\ell_1}{k^2}\cos(\eta_1 y+\theta+\varphi)-\nu\cos(\eta_1 y+\theta)\right)$$

$$+e^{-\xi_1 y}\left(\frac{\ell_1}{k^2}\cos(\eta_1 y-\theta-\varphi)-\nu\cos(\eta_1 y-\theta)\right)\Big\}a_1$$

$$+\Big\{e^{\xi_1 y}\left(\frac{\ell_1}{k^2}\sin(\eta_1 y+\theta+\varphi)-\nu\sin(\eta_1 y+\theta)\right)-e^{\xi_1 y}\left(\frac{\ell_1}{k^2}\sin(\eta_1 y-\theta-\varphi)\right.$$

$$\left.-\nu\sin(\eta_1 y-\theta)\right)\Big\}a_2+\Big\{e^{\xi_2 y}\left(\frac{\ell_2}{k^2}\cos(\eta_2 y-\theta+\psi)-\nu\cos(\eta_2 y-\theta)\right)$$

$$+e^{-\xi_2 y}\left(\frac{\ell_2}{k^2}\cos(\eta_2 y+\theta-\psi)-\nu\cos(\eta_2 y+\theta)\right)\Big\}a_3$$

$$+\left\{e^{\xi_2 y}\left(\frac{\ell_2}{k^2}\sin(\eta_2 y-\theta+\psi)-\nu\sin(\eta_2 y-\theta)\right)\right.$$

$$\left.-e^{-\xi_2 y}\left(\frac{\ell_2}{k^2}\sin(\eta_2 y+\theta-\psi)-\nu\sin(\eta_2 y+\theta)\right)\right\}a_4$$

$$+\left\{e^{\xi_1 y}\left(\frac{\ell_1}{k^2}\cos(\eta_1 y+\theta+\varphi)-\nu\cos(\eta_1 y+\theta)\right)\right.$$

$$\left.-e^{-\xi_1 y}\left(\frac{\ell_1}{k^2}\cos(\eta_1 y-\theta-\varphi)-\nu\cos(\eta_1 y-\theta)\right)\right\}a_5$$

$$+\left\{e^{\xi_1 y}\left(\frac{\ell_1}{k^2}\sin(\eta_1 y+\theta+\varphi)-\nu\sin(\eta_1 y+\theta)\right)\right.$$

$$\left.+e^{-\xi_1 y}\left(\frac{\ell_1}{k^2}\sin(\eta_1 y-\theta-\varphi)-\nu\sin(\eta_1 y-\theta)\right)\right\}a_6$$

$$+\left\{e^{\xi_2 y}\left(\frac{\ell_2}{k^2}\cos(\eta_2 y-\theta+\psi)-\nu\cos(\eta_2 y-\theta)\right)\right.$$

$$\left.-e^{-\xi_2 y}\left(\frac{\ell_2}{k^2}\cos(\eta_2 y+\theta-\psi)-\nu\cos(\eta_2 y+\theta)\right)\right\}a_7$$

$$+\left\{e^{\xi_2 y}\left(\frac{\ell_2}{k^2}\sin(\eta_2 y-\theta+\psi)-\nu\sin(\eta_2 y-\theta)\right)\right.$$

$$\left.+e^{-\xi_2 y}\left(\frac{\ell_2}{k^2}\sin(\eta_2 y+\theta-\psi)-\nu\sin(\eta_2 y+\theta)\right)\right\}a_8\Bigg]\sin(kx) \qquad (132)$$

$$U = -\frac{\sigma Lx}{Eh_s} - \frac{kh_s/L}{\sqrt{12(1-\nu^2)}}\left[\left\{e^{\xi_1 y}\left(\frac{\ell_1}{k^2}\cos(\eta_1 y+\varphi)+\nu\cos(\eta_1 y)\right)\right.\right.$$

$$\left.+e^{-\xi_1 y}\left(\frac{\ell_1}{k^2}\cos(\eta_1 y-\varphi)+\nu\cos(\eta_1 y)\right)\right\}a_1$$

$$+\left\{e^{\xi_1 y}\left(\frac{\ell_1}{k^2}\sin(\eta_1 y+\varphi)+\nu\sin(\eta_1 y)\right)\right.$$

$$
\begin{aligned}
&-e^{-\xi_1 y}\left(\frac{\ell_1}{k^2}\sin(\eta_1 y-\varphi)+\nu\sin(\eta_1 y)\right)\Big\}a_2\\
&+\Big\{e^{\xi_2 y}\left(\frac{\ell_2}{k^2}\cos(\eta_2 y+\psi)+\nu\cos(\eta_2 y)\right)\\
&+e^{-\xi_2 y}\left(\frac{\ell_2}{k^2}\cos(\eta_2 y-\psi)+\nu\cos(\eta_2 y)\right)\Big\}a_3\\
&+\Big\{e^{\xi_2 y}\left(\frac{\ell_2}{k^2}\sin(\eta_2 y+\psi)+\nu\sin(\eta_2 y)\right)\\
&-e^{-\xi_2 y}\left(\frac{\ell_2}{k^2}\sin(\eta_2 y-\psi)+\nu\sin(\eta_2 y)\right)\Big\}a_4\\
&+\Big\{e^{\xi_1 y}\left(\frac{\ell_1}{k^2}\cos(\eta_1 y+\varphi)+\nu\cos(\eta_1 y)\right)\\
&-e^{-\xi_1 y}\left(\frac{\ell_1}{k^2}\cos(\eta_1 y-\varphi)+\nu\cos(\eta_1 y)\right)\Big\}a_5\\
&+\Big\{e^{\xi_1 y}\left(\frac{\ell_1}{k^2}\sin(\eta_1 y+\varphi)+\nu\sin(\eta_1 y)\right)\\
&+e^{-\xi_1 y}\left(\frac{\ell_1}{k^2}\sin(\eta_1 y-\varphi)+\nu\sin(\eta_1 y)\right)\Big\}a_6\\
&+\Big\{e^{\xi_2 y}\left(\frac{\ell_2}{k^2}\cos(\eta_2 y+\psi)+\nu\cos(\eta_2 y)\right)\\
&-e^{-\xi_2 y}\left(\frac{\ell_2}{k^2}\cos(\eta_2 y-\psi)+\nu\cos(\eta_2 y)\right)\Big\}a_7\\
&+\Big\{e^{\xi_2 y}\left(\frac{\ell_2}{k^2}\sin(\eta_2 y+\psi)+\nu\sin(\eta_2 y)\right)\\
&+e^{-\xi_2 y}\left(\frac{\ell_2}{k^2}\sin(\eta_2 y-\psi)+\nu\sin(\eta_2 y)\right)\Big\}a_8\Big]\cos(kx)
\end{aligned}
\tag{133}
$$

$$F_{,xx} = -k^2\Big[\Big\{e^{\xi_1 y}\cos(\eta_1 y)+e^{-\xi_1 y}\cos(\eta_1 y)\Big\}a_1$$

$$+\Big\{e^{\xi_1 y}\sin(\eta_1 y)-e^{-\xi_1 y}\sin(\eta_1 y)\Big\}a_2$$

$$+\Big\{e^{\xi_2 y}\cos(\eta_2 y)+e^{-\xi_2 y}\cos(\eta_2 y)\Big\}a_3$$

$$+\Big\{e^{\xi_2 y}\sin(\eta_2 y)-e^{-\xi_2 y}\sin(\eta_2 y)\Big\}a_4$$

$$+\Big\{e^{\xi_1 y}\cos(\eta_1 y)-e^{-\xi_1 y}\cos(\eta_1 y)\Big\}a_5$$

$$+\Big\{e^{\xi_1 y}\sin(\eta_1 y)+e^{-\xi_1 y}\sin(\eta_1 y)\Big\}a_6$$

$$+\Big\{e^{\xi_2 y}\cos(\eta_2 y)-e^{-\xi_2 y}\cos(\eta_2 y)\Big\}a_7$$

$$+\Big\{e^{\xi_2 y}\cos(\eta_2 y)+e^{-\xi_2 y}\cos(\eta_2 y)\Big\}a_8\Big]\sin(kx) \qquad (134)$$

$$\frac{\partial W_s}{\partial y} = -k\Big[\sqrt{\frac{\ell_1}{k^2}}\Big\{e^{\xi_1 y}\cos(\eta_1 y+\theta+\tfrac{\varphi}{2})-e^{-\xi_1 y}\cos(\eta_1 y-\theta-\tfrac{\varphi}{2})\Big\}a_1$$

$$+\sqrt{\frac{\ell_1}{k^2}}\Big\{e^{\xi_1 y}\sin(\eta_1 y+\theta+\tfrac{\varphi}{2})+e^{-\xi_1 y}\sin(\eta_1 y-\theta-\tfrac{\varphi}{2})\Big\}a_2$$

$$+\sqrt{\frac{\ell_2}{k^2}}\Big\{e^{\xi_2 y}\cos(\eta_2 y-\theta+\tfrac{\psi}{2})-e^{-\xi_2 y}\cos(\eta_2 y+\theta-\tfrac{\psi}{2})\Big\}a_3$$

$$+\sqrt{\frac{\ell_2}{k^2}}\Big\{e^{\xi_2 y}\sin(\eta_2 y-\theta+\tfrac{\psi}{2})+e^{-\xi_2 y}\sin(\eta_2 y+\theta-\tfrac{\psi}{2}\Big\}a_4$$

$$+\sqrt{\frac{\ell_1}{k^2}}\left\{e^{\xi_1 y}\cos(\eta_1 y+\theta+\frac{\varphi}{2})+e^{-\xi_1 y}\cos(\eta_1 y-\theta-\frac{\varphi}{2})\right\}a_5$$

$$+\sqrt{\frac{\ell_1}{k^2}}\left\{e^{\xi_1 y}\sin(\eta_1 y+\theta+\frac{\varphi}{2})-e^{-\xi_1 y}\sin(\eta_1 y-\theta-\frac{\varphi}{2})\right\}a_6$$

$$+\sqrt{\frac{\ell_2}{k^2}}\left\{e^{\xi_2 y}\cos(\eta_2 y-\theta+\frac{\psi}{2})+e^{-\xi_2 y}\cos(\eta_2 y+\theta-\frac{\psi}{2})\right\}a_7$$

$$+\sqrt{\frac{\ell_2}{k^2}}\left\{e^{\xi_2 y}\sin(\eta_2 y-\theta+\frac{\psi}{2})-e^{-\xi_2 y}\sin(\eta_2 y+\theta-\frac{\psi}{2})\right\}a_8\Bigg]\sin(kx) \tag{135}$$

$$\bar{h}_s\left(\frac{\partial^3 W}{\partial y^3}+(2-\nu)\frac{\partial^3 W}{\partial y\,\partial x^2}\right)=-k^3\cdot\frac{h_s/L}{\sqrt{12(1-\nu^2)}}$$

$$\Bigg[\sqrt{\frac{\ell_1}{k^2}}\left\{e^{\xi_1 y}\left(\frac{\ell_1}{k^2}\cos(\eta_1 y+\theta+\frac{3\varphi}{2})-(2-\nu)\cos(\eta_1 y+\theta+\frac{\varphi}{2})\right)\right.$$

$$\left.-e^{-\xi_1 y}\left(\frac{\ell_1}{k^2}\cos(\eta_1 y-\theta-\frac{3\varphi}{2})-(2-\nu)\cos(\eta_1 y-\theta-\frac{\varphi}{2})\right)\right\}a_1$$

$$+\sqrt{\frac{\ell_1}{k^2}}\left\{e^{\xi_1 y}\left(\frac{\ell_1}{k^2}\sin(\eta_1 y+\theta+\frac{3\varphi}{2})-(2-\nu)\sin(\eta_1 y+\theta+\frac{\varphi}{2})\right)\right.$$

$$\left.+e^{-\xi_1 y}\left(\frac{\ell_1}{k^2}\sin(\eta_1 y-\theta-\frac{3\varphi}{2})-(2-\nu)\sin(\eta_1 y-\theta-\frac{\varphi}{2})\right)\right\}a_2$$

$$+\sqrt{\frac{\ell_2}{k^2}}\left\{e^{\xi_2 y}\left(\frac{\ell_2}{k^2}\cos(\eta_2 y-\theta+\frac{3\psi}{2})-(2-\nu)\cos(\eta_2 y-\theta+\frac{\psi}{2})\right)\right.$$

$$\left.-e^{-\xi_2 y}\left(\frac{\ell_2}{k^2}\cos(\eta_2 y+\theta-\frac{3\psi}{2})-(2-\nu)\cos(\eta_2 y+\theta-\frac{\psi}{2})\right)\right\}a_3$$

$$+\sqrt{\frac{\ell_2}{k^2}}\left\{e^{\xi_2 y}\left(\frac{\ell_2}{k^2}\sin(\eta_2 y-\theta+\frac{3\psi}{2})-(2-\nu)\sin(\eta_2 y-\theta+\frac{\psi}{2})\right)\right.$$

$$+e^{-\xi_2 y}\left(\frac{\ell_2}{k^2}\sin(\eta_2 y+\theta-\frac{3\psi}{2})-(2-\nu)\sin(\eta_2 y+\theta-\frac{\psi}{2})\right)\Big\}\,a_4$$

$$+\sqrt{\frac{\ell_1}{k^2}}\left\{e^{\xi_1 y}\left(\cos(\eta_1 y+\theta+\frac{3\varphi}{2})-(2-\nu)\cos(\eta_1 y+\theta+\frac{\varphi}{2})\right)\right.$$

$$+e^{-\xi_1 y}\left(\cos(\eta_1 y-\theta-\frac{3\varphi}{2})-(2-\nu)\cos(\eta_1 y-\theta-\frac{\varphi}{2})\right)\Big\}a_5$$

$$+\sqrt{\frac{\ell_1}{k^2}}\left\{e^{\xi_1 y}\left(\sin(\eta_1 y+\theta+\frac{3\varphi}{2})-(2-\nu)\sin(\eta_1 y+\theta+\frac{\varphi}{2})\right)\right.$$

$$-e^{-\xi_1 y}\left(\sin(\eta_1 y-\theta-\frac{3\varphi}{2})-(2-\nu)\sin(\eta_1 y-\theta-\frac{\varphi}{2})\right)\Big\}a_6$$

$$+\sqrt{\frac{\ell_2}{k^2}}\left\{e^{\xi_2 y}\left(\cos(\eta_2 y-\theta+\frac{3\psi}{2})-(2-\nu)\cos(\eta_2 y-\theta+\frac{\psi}{2})\right)\right.$$

$$+e^{-\xi_2 y}\left(\cos(\eta_2 y+\theta-\frac{3\psi}{2})-(2-\nu)\cos(\eta_2 y+\theta-\frac{\psi}{2})\right)\Big\}a_7$$

$$+\sqrt{\frac{\ell_2}{k^2}}\left\{e^{\xi_2 y}\left(\sin(\eta_2 y-\theta+\frac{3\psi}{2})-(2-\nu)\sin(\eta_2 y-\theta+\frac{\psi}{2})\right)\right.$$

$$-e^{-\xi_2 y}\left(\sin(\eta_2 y+\theta-\frac{3\psi}{2})-(2-\nu)\sin(\eta_2 y+\theta-\frac{\psi}{2})\right)\Big\}a_8\Big]\sin(kx) \quad (136)$$

$$V = -\frac{\nu\sigma r\tan(\beta_1)}{Eh_s\sin(\pi/N)}\sin(\frac{Ly}{R})+\frac{kh_s/L}{\sqrt{12(1-\nu^2)}}$$

$$\Big[\sqrt{\frac{\ell_1}{k^2}}\left(e^{\xi_1 y}\left\{\frac{\ell_1}{k^2}\cos(\eta_1 y+\frac{3\varphi}{2})-(2+\nu)\cos(\eta_1 y+\frac{\varphi}{2})\right\}\right.$$

$$-e^{-\xi_1 y}\left\{\frac{\ell_1}{k^2}\cos(\eta_1 y-\frac{3\varphi}{2})-(2+\nu)\cos(\eta_1 y-\frac{\varphi}{2})\right\}\Big)a_1$$

$$+\sqrt{\frac{\ell_1}{k^2}}\left(e^{\xi_1 y}\left\{\frac{\ell_1}{k^2}\sin(\eta_1 y+\frac{3\varphi}{2})-(2+\nu)\sin(\eta_1 y+\frac{\varphi}{2})\right\}\right.$$

$$+e^{-\xi_1 y}\left\{\frac{\ell_1}{k^2}\sin(\eta_1 y-\frac{3\varphi}{2})-(2+\nu)\sin(\eta_1 y-\frac{\varphi}{2})\right\}\Bigg)a_2$$

$$+\sqrt{\frac{\ell_2}{k^2}}\left(e^{\xi_2 y}\left\{\frac{\ell_2}{k^2}\cos(\eta_2 y+\frac{3\psi}{2})-(2+\nu)\cos(\eta_2 y+\frac{\psi}{2})\right\}\right.$$

$$\left.-e^{-\xi_2 y}\left\{\frac{\ell_2}{k^2}\cos(\eta_2 y-\frac{3\psi}{2})-(2+\nu)\cos(\eta_2 y-\frac{\psi}{2})\right\}\right)a_3$$

$$+\sqrt{\frac{\ell_2}{k^2}}\left(e^{\xi_2 y}\left\{\frac{\ell_2}{k^2}\sin(\eta_2 y+\frac{3\psi}{2})-(2+\nu)\sin(\eta_2 y+\frac{\psi}{2})\right\}\right.$$

$$\left.+e^{-\xi_2 y}\left\{\frac{\ell_2}{k^2}\sin(\eta_2 y-\frac{3\psi}{2})-(2+\nu)\sin(\eta_2 y-\frac{\psi}{2})\right\}\right)a_4$$

$$+\sqrt{\frac{\ell_1}{k^2}}\left(e^{\xi_1 y}\left\{\frac{\ell_1}{k^2}\cos(\eta_1 y+\frac{3\varphi}{2})-(2+\nu)\cos(\eta_1 y+\frac{\varphi}{2})\right\}\right.$$

$$\left.+e^{-\xi_1 y}\left\{\frac{\ell_1}{k^2}\cos(\eta_1 y-\frac{3\varphi}{2})-(2+\nu)\cos(\eta_1 y-\frac{\varphi}{2})\right\}\right)a_5$$

$$+\sqrt{\frac{\ell_1}{k^2}}\left(e^{\xi_1 y}\left\{\frac{\ell_1}{k^2}\sin(\eta_1 y+\frac{3\varphi}{2})-(2+\nu)\sin(\eta_1 y+\frac{\varphi}{2})\right\}\right.$$

$$\left.-e^{-\xi_1 y}\left\{\frac{\ell_1}{k^2}\sin(\eta_1 y-\frac{3\varphi}{2})-(2+\nu)\sin(\eta_1 y-\frac{\varphi}{2})\right\}\right)a_6$$

$$+\sqrt{\frac{\ell_2}{k^2}}\left(e^{\xi_2 y}\left\{\frac{\ell_2}{k^2}\cos(\eta_2 y+\frac{3\psi}{2})-(2+\nu)\cos(\eta_2 y+\frac{\psi}{2})\right\}\right.$$

$$\left.+e^{-\xi_2 y}\left\{\frac{\ell_2}{k^2}\cos(\eta_2 y-\frac{3\psi}{2})-(2+\nu)\cos(\eta_2 y-\frac{\psi}{2})\right\}\right)a_7$$

$$+\sqrt{\frac{\ell_2}{k^2}}\left(e^{\xi_2 y}\left\{\frac{\ell_2}{k^2}\sin(\eta_2 y+\frac{3\psi}{2})-(2+\nu)\sin(\eta_2 y+\frac{\psi}{2})\right\}\right.$$

$$\left.-e^{-\xi_2 y}\left\{\frac{\ell_2}{k^2}\sin(\eta_2 y-\frac{3\psi}{2})-(2+\nu)\sin(\eta_2 y-\frac{\psi}{2})\right\}\right)a_8\Bigg]\quad\sin(kx)\quad(137)$$

$$
\begin{aligned}
F_{,xy} = k^2\Bigg[& \sqrt{\frac{\ell_1}{k^2}}\left\{e^{\xi_1 y}\cos(\eta_1 y+\tfrac{\varphi}{2})-e^{-\xi_1 y}\cos(\eta_1 y-\tfrac{\varphi}{2})\right\}a_1 \\
& +\sqrt{\frac{\ell_1}{k^2}}\left\{e^{\xi_1 y}\sin(\eta_1 y+\tfrac{\varphi}{2})+e^{-\xi_1 y}\sin(\eta_1 y-\tfrac{\varphi}{2})\right\}a_2 \\
& +\sqrt{\frac{\ell_2}{k^2}}\left\{e^{\xi_2 y}\cos(\eta_2 y+\tfrac{\psi}{2})-e^{-\xi_2 y}\cos(\eta_2 y-\tfrac{\psi}{2})\right\}a_3 \\
& +\sqrt{\frac{\ell_2}{k^2}}\left\{e^{\xi_2 y}\sin(\eta_2 y+\tfrac{\psi}{2})+e^{-\xi_2 y}\sin(\eta_2 y-\tfrac{\psi}{2})\right\}a_4 \\
& +\sqrt{\frac{\ell_1}{k^2}}\left\{e^{\xi_1 y}\cos(\eta_1 y+\tfrac{\varphi}{2})+e^{-\xi_1 y}\cos(\eta_1 y-\tfrac{\varphi}{2})\right\}a_5 \\
& +\sqrt{\frac{\ell_1}{k^2}}\left\{e^{\xi_1 y}\sin(\eta_1 y+\tfrac{\varphi}{2})-e^{-\xi_1 y}\sin(\eta_2 y-\tfrac{\varphi}{2})\right\}a_6 \\
& +\sqrt{\frac{\ell_2}{k^2}}\left\{e^{\xi_2 y}\cos(\eta_2 y+\tfrac{\psi}{2})+e^{-\xi_2 y}\cos(\eta_2 y-\tfrac{\psi}{2})\right\}a_7 \\
& +\sqrt{\frac{\ell_2}{k^2}}\left\{e^{\xi_2 y}\sin(\eta_2 y+\tfrac{\psi}{2})-e^{-\xi_2 y}\sin(\eta_2 y-\tfrac{\psi}{2})\right\}a_8\Bigg]\cos(kx) \qquad (138)
\end{aligned}
$$

By examining Eqns. (131), (132), (135) and (136), one may observe that, in the last three equations, there are no terms corresponding to the term $\frac{\nu\sigma r\tan(\beta_1)}{Eh_s\sin(\pi/N)}\cos(\frac{Ly}{R})$ of Eqn. (131). It was mentioned in Section 5 (Prebuckling Solution) that this term is contributed by the rigid body motion of the curved panel, and it should not contribute anything to forces and moments, etc. However, the expression for the w-contribution of the rigid body motion

is a function of y and apparently should affect Eqns. (132), (135) and (136). The last mentioned equations are, in effect, equations for equilibrium of moment, continuity of tangent, and equilibrium of out-of-plane shear respectively. As indicated in Appendix I, in the Donnell's shallow shell equations, the terms provided by the in-plane displacements to curvature, etc. are neglected. This is true only if in-plane displacements are small. It can be seen from expression (137) for V, that the perturbation part is of the order of h_s/L times the perturbation part of W, but the prebuckling solutions are of the same order for V and W. Therefore, if we use the full expressions for slope and curvature with V and W as listed in (131), (137) and then use Donnell's assumption, we will obtain the expressions (132), (135) and (136). Details for this can be found in Appendix I.

In Every Flat Panel

Case I $\lambda_s > \frac{k^2}{2Z_p}$, (from Eqns. (70) through (77))

$$W = \frac{\nu\sigma r}{Eh_p} + [\cos(\zeta_1 y)a_3 + \cosh(\zeta_2 y)a_4 + \sin(\zeta_1 y)a_7 + \sinh(\zeta_2 y)a_8]\sin(kx) \tag{139}$$

$$\left(\frac{\partial^2 W}{\partial y^2} + \nu\frac{\partial^2 W}{\partial x^2}\right) = k^2[-(\frac{\zeta_1^2}{k^2} + \nu)\cos(\zeta_1 y)a_3 + (\frac{\zeta_2^2}{k^2} - \nu)\cosh(\zeta_2 y)a_4$$
$$-(\frac{\zeta_1^2}{k^2} + \nu)\sin(\zeta_1 y)a_7 + (\frac{\zeta_2^2}{k^2} - \nu)\sinh(\zeta_2 y)a_8]\sin(kx) \tag{140}$$

$$U = -\frac{\sigma Lx}{Eh_p} - \frac{kh_p/L}{\sqrt{12(1-\nu^2)}}[(1+\nu)\cosh(ky)a_1 + \{(1+\nu)(ky)\sinh(ky) + 2\cosh(ky)\}a_2$$
$$+\{(1+\nu)(ky)\cosh(ky) + 2\sinh(ky)\}a_5 + (1+\nu)\sinh(ky)a_6]\cos(kx) \tag{141}$$

$$F_{,xx} = -k^2[\cosh(ky)a_1 + (ky)\sinh(ky)a_2$$
$$+(ky)\cosh(ky)a_5 + \sinh(ky)a_6]\sin(kx) \tag{142}$$

$$\frac{\partial W}{\partial y} = k[-\frac{\zeta_1}{k}\sin(\zeta_1 y)a_3 + \frac{\zeta_2}{k}\sinh(\zeta_2 y)a_4 + \frac{\zeta_1}{k}\cos(\zeta_1 y)a_7$$
$$+\frac{\zeta_2}{k}\cosh(\zeta_2 y)a_8]\sin(kx) \tag{143}$$

$$\bar{h}_p\left(\frac{\partial^3 W}{\partial y^3} + (2-\nu)\frac{\partial^3 W}{\partial y \partial x^2}\right) = k^3\frac{h_p/L}{\sqrt{12(1-\nu^2)}}\left[\frac{\zeta_1}{k}\left\{\frac{\zeta_1^2}{k^2} + (2-\nu)\right\}\sin(\zeta_1 y)a_3\right.$$
$$+\frac{\zeta_2}{k}\left\{\frac{\zeta_2^2}{k^2} - (2-\nu)\right\}\sinh(\zeta_2 y)a_4 - \frac{\zeta_1}{k}\left\{\frac{\zeta_1^2}{k^2} + (2-\nu)\right\}\cos(\zeta_1 y)a_7$$

$$+\frac{\zeta_2}{k}\left\{\frac{\zeta_2^2}{k^2}-(2-\nu)\right\}\cosh(\zeta_2 y)a_8\Big]\sin(kx) \qquad (144)$$

$$V=\frac{\nu\sigma L}{Eh_p}y-\frac{kh_p/L}{\sqrt{12(1-\nu^2)}}\Big[(1+\nu)\sinh(ky)a_1+\Big\{(1+\nu)(ky)\cosh(ky)$$

$$-(1-\nu)\sinh(ky)\Big\}a_2+\Big\{(1+\nu)(ky)\sinh(ky)-(1-\nu)\cosh(ky)\Big\}a_5$$

$$+(1+\nu)\cosh(ky)a_6\Big]\sin(kx) \qquad (145)$$

$$F_{p,xy}=k^2\Big[\sinh(ky)a_1+\Big\{(ky)\cosh(ky)+\sinh(ky)\Big\}a_2$$

$$+\Big\{(ky)\sinh(ky)+\cosh(ky)\Big\}a_5+\cosh(ky)a_6\Big]\cos(kx) \qquad (146)$$

Case II $\qquad \lambda_s=\dfrac{k^2}{2Z_p}$ $\qquad$ (from Eqns. (78) through (85))

$$W=\frac{\nu\sigma r}{Eh_p}+\Big[a_3+\cosh(2ky)a_4+(ky)a_7+\sinh(2ky)a_8\Big]\sin(kx) \qquad (147)$$

$$\left(\frac{\partial^2 W}{\partial y^2}+\nu\frac{\partial^2 W}{\partial x^2}\right)=k^2\Big[-\nu a_3+(4-\nu)\cosh(2ky)a_4-\nu(ky)a_7$$

$$+(4-\nu)\sinh(2ky)a_8\Big]\sin(kx) \qquad (148)$$

$$U=-\frac{\sigma L}{Eh_p}x-\frac{kh_p/L}{\sqrt{12(1-\nu^2)}}\Big[(1+\nu)\cosh(ky)a_1+\Big\{(1+\nu)(ky)\sinh(ky)$$

$$+2\cosh(ky)\Big\}a_2+\Big\{(1+\nu)(ky)\cosh(ky)+2\sinh(ky)\Big\}a_5$$

$$+(1+\nu)\sinh(ky)a_6\Big]\cos(kx) \qquad (149)$$

$$F_{,xx} = -k^2[\cosh(ky)a_1 + (ky)\sinh(ky)a_2 + (ky)\cosh(ky)a_5 + \sinh(ky)a_6]\sin(kx) \tag{150}$$

$$\frac{\partial W}{\partial y} = k[0\ a_3 + 2\sinh(2ky)a_4 + a_7 + 2\cosh(2ky)a_8]\sin(kx) \tag{151}$$

$$\bar{h}_p\left(\frac{\partial^3 W}{\partial y^3} + (2-\nu)\frac{\partial^3 W}{\partial y \partial x^2}\right) = k^3 \frac{h_p/L}{\sqrt{12(1-\nu^2)}}[0\,a_3 + 2\left\{4-(2-\nu)\right\}\sinh(2ky)a_4$$

$$-(2-\nu)a_7 + 2\left\{4-(2-\nu)\right\}\cosh(2ky)a_8]\sin(kx) \tag{152}$$

$$V = \frac{\nu\sigma L}{Eh_p}y - \frac{kh_p/L}{\sqrt{12(1-\nu^2)}}[(1+\nu)\sinh(ky)a_1 + \left\{(1+\nu)(ky)\cosh(ky)\right.$$

$$\left.-(1-\nu)\sinh(ky)\right\}a_2 + \left\{(1+\nu)(ky)\sinh(ky) - (1-\nu)\cosh(ky)\right\}a_5$$

$$+(1+\nu)\cosh(ky)a_6]\ \sin(kx) \tag{153}$$

$$F_{,xy} = k^2[\sinh(ky)a_1 + \left\{(ky)\cosh(ky) + \sinh(ky)\right\}a_2$$

$$+\left\{(ky)\sinh(ky) + \cosh(ky)\right\}a_5 + \cosh(ky)a_6]\ \cos(kx) \tag{154}$$

<u>Case III</u> $\qquad \lambda_s < \dfrac{k^2}{2Z_p}$ $\qquad$ (from Eqns. (86) through (93))

$$W = \frac{\nu\sigma r}{Eh_p} + [\cosh(\zeta_1 y)a_3 + \cosh(\zeta_2 y)a_4 + \sinh(\zeta_1 y)a_7$$

$$+\sinh(\zeta_2 y)a_8]\sin(kx) \tag{155}$$

$$\left(\frac{\partial^2 W}{\partial y^2} + \nu \frac{\partial^2 W}{\partial x^2}\right) = k^2 \left[\left(\frac{\zeta_1^2}{k^2} - \nu\right)\cosh(\zeta_1 y)a_3 + \left(\frac{\zeta_2^2}{k^2} - \nu\right)\cosh(\zeta_2 y)a_4 + \left(\frac{\zeta_1^2}{k^2} - \nu\right)\sinh(\zeta_1 y)a_7 + \left(\frac{\zeta_2^2}{k^2} - \nu\right)\sinh(\zeta_2 y)a_8\right] \sin(kx) \quad (156)$$

$$U = -\frac{\sigma L}{E h_p} x - \frac{k h_p/L}{\sqrt{12(1-\nu^2)}} \left[(1+\nu)\cosh(ky)a_1 + \left\{(1+\nu)(ky)\sinh(ky) + 2\cosh(ky)\right\}a_2 + \left\{(1+\nu)(ky)\cosh(ky) + 2\sinh(ky)\right\}a_5 + (1+\nu)\sinh(ky)a_6\right] \cos(kx) \quad (157)$$

$$F_{p,xx} = -k^2 \left[\cosh(ky)a_1 + (ky)\sinh(ky)a_2 + (ky)\cosh(ky)a_5 + \sinh(ky)a_6\right] \sin(kx) \quad (158)$$

$$\frac{\partial W}{\partial y} = k\left[\frac{\zeta_1}{k}\sinh(\zeta_1 y)a_3 + \frac{\zeta_2}{k}\sinh(\zeta_2 y)a_4 + \frac{\zeta_1}{k}\cosh(\zeta_1 y)a_7 + \frac{\zeta_2}{k}\cosh(\zeta_2 y)a_8\right] \sin(kx) \quad (159)$$

$$\bar{h}_p \left(\frac{\partial^3 W}{\partial y^3} + (2-\nu)\frac{\partial^3 W}{\partial y \partial x^2}\right) = k^3 \frac{h_p/L}{\sqrt{12(1-\nu^2)}} \left[\frac{\zeta_1}{k}\left\{\frac{\zeta_1^2}{k^2} - (2-\nu)\right\}\sinh(\zeta_1 y)a_3 + \frac{\zeta_2}{k}\left\{\frac{\zeta_2^2}{k^2} - (2-\nu)\right\}\sinh(\zeta_2 y)a_4 + \frac{\zeta_1}{k}\left\{\frac{\zeta_1^2}{k^2} - (2-\nu)\right\}\cosh(\zeta_1 y)a_7 + \frac{\zeta_2}{k}\left\{\frac{\zeta_2^2}{k^2} - (2-\nu)\right\}\cosh(\zeta_2 y)a_8\right] \sin(kx) \quad (160)$$

$$V = \frac{\nu\sigma L}{Eh_p}\, y - \frac{kh_p/L}{\sqrt{12(1-\nu^2)}} \left[(1+\nu)\sinh(ky)a_1 + \left\{(1+\nu)(ky)\cosh(ky)\right.\right.$$

$$\left. -(1-\nu)\sinh(ky)\right\} a_2 + \left\{(1+\nu)(ky)\sinh(ky) - (1-\nu)\cosh(ky)\right\} a_5$$

$$\left. +(1+\nu)\cosh(ky)a_6\right] \sin(kx) \qquad (161)$$

$$F_{,xy} = k^2 \left[\sinh(ky)a_1 + \left\{(ky)\cosh(ky)+\sinh(ky)\right\} a_2\right.$$

$$\left. + \left\{(ky)\sinh(ky)+\cosh(ky)\right\} a_5 + \cosh(ky)a_6\right] \cos(kx) \qquad (162)$$

In Eqns. (131) through (138) and Eqns. (139) through (162), the expressions for the state variables have been split into symmetric and antisymmetric components. Using Eqn. (113), we can write for the ith panel:

$$\{\underline{S}_i^T\} = \left\{ \begin{array}{l} W \\ \dfrac{\partial^2 W}{\partial y^2} + \nu \dfrac{\partial^2 W}{\partial x^2} \\ U \\ \dfrac{\partial^2 F}{\partial x^2} \\ \dfrac{\partial W}{\partial y} \\ \overline{h}\left(\dfrac{\partial^3 W}{\partial y^3} + (2-\nu)\dfrac{\partial^3 W}{\partial y \partial x^2}\right) \\ V \\ \dfrac{\partial^2 F}{\partial x \partial y} \end{array} \right\} = \{\underline{S}_i^\circ\} + \{\underline{S}_i\} \qquad (163)$$

where $\{S_i^\circ\}$ and $\{S_i\}$ are the prebuckling solution and the perturbation respectively. From Eqns. (131) through (162), $\{S_i\}$ can be represented in matrix form as:

$$\{\underline{S}_i(y)\} = [P_i(y)]\{\underline{a}_i\}, \{\underline{a}_i\} = \begin{Bmatrix} \underline{a}_i' \\ \underline{a}_i'' \end{Bmatrix} = \begin{Bmatrix} a_{1i} \\ a_{2i} \\ a_{3i} \\ a_{4i} \\ \hline a_{5i} \\ a_{6i} \\ a_{7i} \\ a_{8i} \end{Bmatrix} \tag{164}$$

where a_{1i} through a_{8i} are the same as a_1 through a_8 respectively in Eqns. (131)-(162).

$$\left.\begin{aligned} [P_i(y)] &= \left[\begin{array}{c:c} P_{i1} & P_{i2} \\ \hdashline P_{i3} & P_{i4} \end{array}\right] \\ [P_{i1}(-y)] &= [P_{i1}(y)] \qquad [P_{i2}(-y)] = -[P_{i2}(y)] \\ [P_{i3}(-y)] &= -[P_{i3}(y)] \qquad [P_{i4}(-y)] = [P_{i4}(y)] \end{aligned}\right\} \tag{165}$$

The left half of matrix $[P_i]$ represents the symmetric mode, while the right half is the antisymmetric mode. Again, symmetry and antisymmetry are considered with respect to the circumferential coordinate y about the origin in each panel.

Each set of Eqns. (131) through (138) for the curved panels and Eqns. (139) through (146) or (147) through (154) or (155) through (162) for the flat panels, has eight constants of integration $a_i (i = 1, 2, \ldots, 8)$. Thus in all, we have 2N x 8 constants to determine. It is obvious from the x-dependence of various state variables in expressions (131) through (162) that, in each panel, the boundary conditions at x = 0, 1 are identically satisfied. Therefore, as before, we must match various forces and displacements at 2N common edges to arrive at 2N x 8 equations for 2N sets of unknowns of type a_i $(i = 1, 2, \ldots, 8)$.

6a. Matching Conditions and the Formulation of the Eigenvalue Problem

The matching conditions at the common edges are given in (114) and (115) as follows:

$$\left\{\underline{S}_i^T\right\}_F = [H_1] \left\{\underline{S}_{(i+1)}^T\right\}_B \qquad i = 1, 3, 5, \ldots, (2N-1) \qquad (114)$$

$$[H_1] \left\{\underline{S}_i^T\right\}_F = \left\{\underline{S}_{(i+1)}^T\right\}_B \qquad i = 2, 4, 6, \ldots, (2N) \qquad (115)$$

where from (163)

$$\left\{\underline{S}_i^T\right\} = \left\{\underline{S}_i^\circ\right\} + \left\{\underline{S}_i\right\} = \begin{matrix}\text{Prebuckling} \\ \text{solution}\end{matrix} + \begin{matrix}\text{Perturbation} \\ \text{solution}\end{matrix} \qquad (163)$$

We may repeat here that:

(i) All the odd numbered panels are curved panels and Eqns. (131) through (138) apply. All the even numbered panels are flat panels and, depending on the value of λ, Eqns. (134)-(146) or (147)-(154) or (155)-(162) apply.

(ii) The subscripts F and B denote that the expressions are evaluated at the front and back edges of the panel respectively. The front edge is at $y = \frac{T}{L}$ (or $y = \frac{r}{L}\tan\beta_1$) and the back edge at $y = -\frac{T}{L}$ (or $y = -\frac{r}{L}\tan\beta_1$) for each of the curved (or flat) panels.

Substituting (163) in the matching conditions (114) and (115), it can be seen that the prebuckling parts $\{\underline{S}_i^\circ\}$ of vectors $\{\underline{S}_i^T\}$ identically satisfy Eqns. (114) and (115) and we obtain

$$\{\underline{S}_i\}_F = [H_1]\{\underline{S}_{(i+1)}\}_B \qquad (i = 1, 3, 5, \ldots, (2N-1)) \qquad (166)$$

$$[H_1]\{\underline{S}_i\}_F = \{\underline{S}_{(i+1)}\}_B \qquad (i = 2, 4, 6, 8, \ldots, 2N) \qquad (167)$$

Panels numbered 1 and (2N+1) refer to the same panel. Using Eqn. (164) in (166) and (167) and rearranging the matrix equations

$$\left.\begin{aligned}
&[P_{1F}]\{\underline{a}_1\} = [H_1][P_{2B}]\{\underline{a}_2\}\\
&[H_1][P_{2F}]\{\underline{a}_2\} = [P_{3B}]\{\underline{a}_3\}\\
&[P_{3F}]\{\underline{a}_3\} = [H_1][P_{4B}]\{\underline{a}_4\}\\
&\text{----------}\\
&\text{----------}\\
&\text{----------}\\
&[P_{(2N-1)F}]\{\underline{a}_{(2N-1)}\} = [H_1][P_{(2N)B}]\{\underline{a}_{(2N)}\}\\
&[H_1][P_{(2N)F}]\{\underline{a}_{(2N)}\} = [P_{1B}]\{\underline{a}_1\}
\end{aligned}\right\} \qquad (168)$$

Each of the matrices in [ ] is an (8 x 8) real non-singular matrix. Thus we have 2N x 8 equations for 2N eight component vectors $\{\underline{a}_i\}$ (i = 1, 2, ... , 2N). The last of the matrix equations (168) is the closure condition, indicating that we are considering a closed shell. Equation (168) is a set of 16(N) homogeneous equations in 16(N) unknown a's. For non-trivial values of a's, the determinant of the 16(N) x 16(N) coefficient matrix must vanish. The determinant is a function of N (number of panels of each kind), $\frac{R}{r}$ (radius of the curved panels), $\frac{2b}{r}$ (width of the panel) and other geometric parameters like r/h_s, h_s/h_p, etc. The lowest value of λ_s for given geometric parameters at which the determinant vanishes gives the critical load for the shell. The corresponding eigenvector of a's determines the displacement distribution at the critical load. To actually locate the lowest λ, we may use the method employed in the case of a shell with single flat spot (Section 6, Chapter I).

6b. Simplifications for Numerical Evaluation of λ_{CR}

It is obvious from (168) that the order of the final matrix, for which the determinant has to be found, is 16 times N (the number of panels of each kind). Evidently, for large N, the storage requirements in the computer may become prohibitive. This situation can be improved by rearranging the equations and making full use of the large number of zeroes in the matrix. The final form of (168) becomes:

For N = 5 (for example)

$$
\begin{bmatrix}
x & x & & & & & & & & \\
x & & x & & & & & & & \\
 & x & & x & & & & & & \\
 & & x & & x & & & & & \\
 & & & x & & x & & & & \\
 & & & & x & & x & & & \\
 & & & & & x & & x & & \\
 & & & & & & x & & x & \\
 & & & & & & & x & & x \\
 & & & & & & & & x & x
\end{bmatrix}
\begin{Bmatrix}
\underline{a}_1 \\ \underline{a}_2 \\ \underline{a}_{10} \\ \underline{a}_3 \\ \underline{a}_9 \\ \underline{a}_4 \\ \underline{a}_8 \\ \underline{a}_5 \\ \underline{a}_7 \\ \underline{a}_6
\end{Bmatrix}
=
\begin{Bmatrix}
 \\ \\ \\ \\ \underline{0} \\ \\ \\ \\ \\
\end{Bmatrix}
\qquad (169)
$$

Here x's denote 8 x 8 real non-singular matrices. All the empty squares indicate (8 x 8) null matrices. The same procedure applies to any value of 2N. The order of vectors in the general case is $\underline{a}_1$, $\underline{a}_2$, $\underline{a}_{(2N)}$, $\underline{a}_3$, $\underline{a}_{(2N-1)}$, $\underline{a}_4$, $\underline{a}_{(2N-2)}$, etc. Format (169) reduces the storage requirements for the final matrix and is valid in general, even if all the panels are different. However, in the problem under consideration, all the odd numbered panels are identical and so are the even numbered panels. Every panel of either type is identically positioned along the circumference of the shell. In fact, in the numbering of the panels, the location of panel number one is completely arbitrary. This arrangement of the panels implies certain symmetries in the shell configuration and hence in the

buckling modes of the shell as discussed below.

The problem of the shell with a single flat spot was reduced to solving a set of 16 homogeneous algebraic equations in 16 unknowns (Eqn. (94)). By redefining the unknown coefficients (Eqns. (97), (98)), Eqn. (94) was reduced to Eqn. (99) in which the symmetric and antisymmetric modes had been decoupled. This meant that the buckled configuration of the shell was either symmetric or antisymmetric with respect to the line joining the centers of the flat panel and the curved panel. This line was also the line of symmetry of the undeformed shell. Now if a multi-flat spot shell with N panels of each kind is considered, it can be easily shown that it has N lines of symmetry. In Fig. 21b, the lines of symmetry for shells with N = 3 and N = 4 are shown. Reversing the arguments of the single flat spot case, it may be expected that the buckling modes of the shell with N-lines of symmetry will also exhibit certain symmetries.

It may be mentioned here that this method of using symmetry of geometry and loading, has been extensively used in the numerical solution (e.g., by finite difference or by finite elements method) of certain problems. There, by symmetry considerations, the problem of complete structure is reduced to that of a part of the structure. In the problem under consideration, for very large N it may not be easy to take into account and analyze all the symmetries, so that the buckling analysis of a part of the shell will give the lowest critical load. With this in mind, the study of the symmetries will not be carried further. Instead, a systematic reduction of matrix

equations employing the properties of matrices and the roots of unity will be used to reduce the orders of matrices and hence, the computations. In Section 9 of this chapter, it will be shown that the solutions so obtained do have the required symmetries.

In (168) matrices $[P_{iF}]$, $[P_{iB}]$, $(i = 1, 2, \ldots, 2N)$ and $[H_1]$ are non-singular. Therefore, by the elimination process, we can write

$$[P_{1F}]\{\underline{a}_1\} = [H_1][P_{2B}][P_{2F}^{-1}][H_1^{-1}][P_{3B}][P_{3F}^{-1}][H_1][P_{4B}][P_{4F}^{-1}][H_1^{-1}]\ldots$$
$$\ldots. [H_1][P_{(2N)B}][P_{(2N)F}^{-1}][H_1^{-1}][P_{1B}]\{\underline{a}_1\} \qquad (170)$$

or

$$\Big[I-[H_1][P_{2B}][P_{2F}^{-1}][H_1^{-1}][P_{3B}][P_{3F}^{-1}][H_1]\ldots..$$
$$\ldots [H_1][P_{(2N)B}][P_{(2N)F}^{-1}][H_1^{-1}][P_{1B}][P_{1F}^{-1}]\Big][P_{1F}]\{\underline{a}_1\} = \{\underline{0}\} \qquad (171)$$

Here

$$\left.\begin{aligned} [P_{2F}^{-1}][P_{2F}] &= [I] = \text{Identity matrix} \\ [H_1^{-1}][H_1] &= [I] \qquad \text{etc.} \end{aligned}\right\} \qquad (172)$$

For non-trivial $\{\underline{a}_1\}$

$$\text{Det.}\Big[I-[H_1][P_{2B}][P_{2F}^{-1}][H_1^{-1}]\ldots..[P_{1B}][P_{1F}^{-1}]\Big]\cdot \text{Det}(P_{1F}] = 0 \qquad (173)$$

Incidentally, the method for block-tridiagonal matrices, described in Ref. (9), p. 58, can be applied to the matrix in (169)

to reduce it to a product of a block lower triangular matrix and a block upper triangular matrix. The determinant of this matrix product can be shown to be the same as (173) with some rearrangement of terms.

Since all the odd numbered panels are identical, as are all the even numbered panels, in (168)

$$\begin{aligned}
&[P_{1B}] = [P_{3B}] = [P_{5B}] = \cdots = [P_{(2N-1)B}] \\
&[P_{1F}] = [P_{3}F] = [P_{5F}] = \cdots = [P_{(2N-1)F}] \\
&[P_{2B}] = [P_{4B}] = [P_{6B}] = \cdots = [P_{(2N)B}] \\
&[P_{2F}] = [P_{4F}] = [P_{6F}] = \cdots = [P_{(2N)F}]
\end{aligned} \tag{174}$$

Using (174) in (173), for non-trivial $\{\underline{a}_1\}$

$$\text{Det.}\left[I-\left([H_1][P_{2B}][P_{2F}^{-1}][H_1^{-1}][P_{1B}][P_{1F}]^{-1}\right)^N\right]\text{Det.}[P_{1F}] = 0 \tag{175}$$

For the sake of brevity, let

$$[P] = [H_1][P_{2B}][P_{2F}^{-1}][H_1^{-1}][P_{1B}][P_{1F}]^{-1} \tag{176}$$

Then (175) $\Longrightarrow$ Det. $[I-[P]^N]$ Det. $[P_{1F}] = 0$

Det. $[P_{1F}] \neq 0$, because $[P_{1F}]$ is non-singular.

This implies that the eigenvalue problem (168) can be posed as

$$[P]^N\{\underline{b}\} = \{\underline{b}\} \quad \text{where} \quad \{\underline{b}\} = [P_{1F}]\{\underline{a}_1\} \tag{177}$$

Now, we must find the lowest λ for which one of the eigenvalues of $[P]^N$ is unity.

By using a well-known theorem for the eigenvalues of a matrix and its powers, (177) $\Longrightarrow$

$$[P]\ \{\underline{b}\} = \alpha\{\underline{b}\} \tag{178}$$

where

α = Nth root of unity

$$= \cos(\Gamma)+i\sin(\Gamma),\ \Gamma = \frac{2n\pi}{N}\ ,\quad (n = 0, 1, 2, \ldots, \frac{N}{2} \text{or} \frac{N-1}{2}) \tag{179}$$

$\frac{N}{2}$ if N is even

and $\frac{N-1}{2}$ if N is odd

If α is the Nth root of unity, so is $\bar{\alpha}$ where $\bar{\alpha}$ is the complex conjugate of α. Also $\bar{\alpha} = 1/\alpha$.

Therefore, from (177)

$$[P]\ \{\underline{b}\} = \alpha\{\underline{b}\}$$

$$[P]\ [P_{1F}]\ \{\underline{a}_1\} = \alpha\,[P_{1F}]\ \{\underline{a}_1\}$$

or using (176)

$$[H_1]\,[P_{2B}][P_{2F}^{-1})[H_1^{-1}]\,[P_{1B}]\ \{\underline{a}_1\} = \alpha\,[P_{1F}]\{\underline{a}_1\}$$

or $$\bar{\alpha}\,[P_{1B}]\{\underline{a}_1\} = [H_1][P_{2F}][P_{2B}^{-1}][H_1^{-1}][P_{1F}]\{\underline{a}_1\}$$

By interchanging α and $\bar{\alpha}$

$$\alpha[P_{1B}]\{\underline{a}_1\} = [H_1][P_{2F}][P_{2B}^{-1}][H_1^{-1}][P_{1F}]\{\underline{a}_1\} \qquad (180)$$

From the first two sets of (168) and (174),

$$[P_{1B}]\{\underline{a}_3\} = [H_1][P_{2F}][P_{2B}^{-1}][H_1^{-1}][P_{1F}]\{\underline{a}_1\} \qquad (181)$$

(180), (181) $\Longrightarrow$

$$\{\underline{a}_3\} = \alpha\{\underline{a}_1\}$$

Similarly $\{\underline{a}_5\} = \alpha\{\underline{a}_3\} = \alpha^2\{\underline{a}_1\}$, $\{\underline{a}_1\} = \alpha^3\{\underline{a}_1\}$ etc.

And also $\{\underline{a}_4\} = \alpha\{\underline{a}_2\}$, $\{\underline{a}_6\} = \alpha^2\{\underline{a}_2\}$, etc. (182)

or $\{\underline{a}_{(2N-1)}\} = \bar{\alpha}\{\underline{a}_1\}$, $\{\underline{a}_{(2N)}\} = \bar{\alpha}\{\underline{a}_2\}$

Using (182), (174), (165), (164) in (168), we get

$$[P_{1F}]\{\underline{a}_1\} = [H_1][P_{2B}]\{\underline{a}_2\}$$

$$\alpha[P_{1B}]\{\underline{a}_1\} = [H_1][P_{2F}]\{\underline{a}_2\}$$

or

$$\left[\begin{array}{c|c} P_{11} & P_{12} \\ \hline P_{13} & P_{14} \end{array}\right]\left\{\begin{array}{c} \underline{a}'_1 \\ \hline \underline{a}''_1 \end{array}\right\} = [H_1]\left[\begin{array}{c|c} P_{21} & -P_{22} \\ \hline -P_{23} & P_{24} \end{array}\right]\left\{\begin{array}{c} \underline{a}'_2 \\ \hline \underline{a}''_2 \end{array}\right\}$$

$$\alpha\left[\begin{array}{c|c} P_{11} & -P_{12} \\ \hline -P_{13} & P_{14} \end{array}\right]\left\{\begin{array}{c} \underline{a}'_1 \\ \hline \underline{a}''_1 \end{array}\right\} = [H_1]\left[\begin{array}{c|c} P_{21} & P_{22} \\ \hline P_{23} & P_{24} \end{array}\right]\left\{\begin{array}{c} \underline{a}'_2 \\ \hline \underline{a}''_2 \end{array}\right\}$$

Since $[H_1]$ is a diagonal matrix, we can write the two matrix equations

$$\left[\begin{array}{c|c} P_{11} & P_{12} \\ \hline P_{13} & P_{14} \end{array}\right] \left\{\begin{array}{c} \underline{a}'_1 \\ \hline \underline{a}''_1 \end{array}\right\} = [H_1] \left[\begin{array}{c|c} P_{21} & -P_{22} \\ \hline -P_{23} & P_{24} \end{array}\right] \left\{\begin{array}{c} \underline{a}'_2 \\ \hline \underline{a}''_2 \end{array}\right\} \quad \text{(a)}$$

$$\alpha \left[\begin{array}{c|c} P_{11} & P_{12} \\ \hline P_{13} & P_{14} \end{array}\right] \left\{\begin{array}{c} \underline{a}'_1 \\ \hline -\underline{a}''_1 \end{array}\right\} = [H_1] \left[\begin{array}{c|c} P_{21} & -P_{22} \\ \hline -P_{23} & P_{24} \end{array}\right] \left\{\begin{array}{c} \underline{a}'_2 \\ \hline -\underline{a}''_2 \end{array}\right\} \quad \text{(b)} \tag{183}$$

(183) can be further reduced to

$$\left[\begin{array}{c|c} P_{11} & P_{12} \\ \hline P_{13} & P_{14} \end{array}\right] \left\{\begin{array}{c} (1+\alpha)\,\underline{a}'_1 \\ \hline (1-\alpha)\,\underline{a}''_1 \end{array}\right\} = [H_1] \left[\begin{array}{c|c} P_{21} & -P_{22} \\ \hline -P_{23} & P_{24} \end{array}\right] \left\{\begin{array}{c} 2\underline{a}'_2 \\ \hline 0 \end{array}\right\} = \left[\begin{array}{c|c} Q_{21} & -Q_{22} \\ \hline -Q_{23} & Q_{24} \end{array}\right] \left\{\begin{array}{c} 2\underline{a}'_2 \\ \hline 0 \end{array}\right\} \quad \text{(a)}$$

$$\left[\begin{array}{c|c} P_{11} & P_{12} \\ \hline P_{13} & P_{14} \end{array}\right] \left\{\begin{array}{c} (1-\alpha)\underline{a}'_1 \\ \hline (1-\alpha)\underline{a}''_1 \end{array}\right\} = [H_1] \left[\begin{array}{c|c} P_{21} & -P_{22} \\ \hline -P_{23} & P_{24} \end{array}\right] \left\{\begin{array}{c} 0 \\ \hline 2\underline{a}''_2 \end{array}\right\} = \left[\begin{array}{c|c} Q_{21} & -Q_{22} \\ \hline -Q_{23} & Q_{24} \end{array}\right] \left\{\begin{array}{c} 0 \\ \hline 2\underline{a}''_2 \end{array}\right\} \quad \text{(b)} \tag{184}$$

Eliminating $\{\underline{a}'_2\}$ and $\{\underline{a}''_2\}$ in (a) and (b) above,

$$\left([Q_{21}^{-1}][P_{11}] + [Q_{23}^{-1}][P_{13}]\right)\{\underline{a}'_1\} + \frac{(1-\alpha)}{(1+\alpha)}\left([Q_{21}^{-1}][P_{12}] + [Q_{23}^{-1}][P_{14}]\right)\{\underline{a}''_1\} = \{\underline{0}\} \tag{185a}$$

$$\left([Q_{22}^{-1}][P_{11}] + [Q_{24}^{-1}][P_{13}]\right)\{\underline{a}'_1\}$$

$$+\frac{(1+\alpha)}{(1-\alpha)}\left([Q_{22}^{-1}][P_{12}] + [Q_{24}^{-1}][P_{14}]\right)\{\underline{a}''_1\} = \{\underline{0}\} \qquad (185b)$$

or in matrix form

$$\left[\begin{array}{c|c} [Q_{21}^{-1}][P_{11}]+[Q_{23}^{-1}][P_{13}] & (\frac{1-\alpha}{1+\alpha})^2\,[Q_{21}^{-1}][P_{12}]+[Q_{23}^{-1}][P_{14}] \\ \hline [Q_{22}^{-1}][P_{11}]+[Q_{24}^{-1}][P_{13}] & [Q_{22}^{-1}][P_{12}]+[Q_{24}^{-1}][P_{14}] \end{array}\right]\left\{\begin{array}{c} \underline{a}'_1 \\ \hline \frac{(1+\alpha)}{(1-\alpha)}\,\underline{a}''_1 \end{array}\right\} = \underline{0} \qquad (185)$$

From (179) $\alpha = \cos(\Gamma) + i\sin(\Gamma)$ $\quad \Gamma = \frac{2n\pi}{N}$

$$(n=0, 1, 2, \ldots, \frac{N}{2} \text{ or } \frac{N-1}{2})$$

$$\text{or } \frac{1+\alpha}{1-\alpha} = \frac{1+\cos(\Gamma)+i\sin(\Gamma)}{1-\cos(\Gamma)-i\sin(\Gamma)}$$

$$= \frac{i\sin(\Gamma)}{i-\cos(\Gamma)} = i\cot(\frac{\Gamma}{2})$$

$$\text{or } (\frac{1-\alpha}{1+\alpha})^2 = -\tan^2(\frac{\Gamma}{2}) \qquad (186)$$

Using (186) in (185), the matrix is found to be a real matrix.

(185) is a set of 8 homogeneous equations for the 8 components of the vector $\{\underline{a}_1\}$. For a non-trivial vector $\{\underline{a}\}$, the determinant of the matrix must vanish. The lowest value of λ_s at which this happens is the critical load of the shell and the corresponding $\{\underline{a}\}$ gives the eigenmode.

From (185) we can see that now, instead of a 16N x 16N matrix as in (168), the order of the matrix to be considered is at most 8.

In fact, for some special cases below, it can be further reduced to 4.

Special Cases

(i) $\alpha = 1,\ n = 0$

This corresponds to the buckling mode in which all the curved panels have identical displacement distributions--symmetric or antisymmetric. From (184), (185) the matrix for this case reduces to

$$\left[\begin{array}{c|c} [Q_{21}^{-1}][P_{11}] + [Q_{23}^{-1}][P_{13}] & 0 \\ \hline 0 & [Q_{22}^{-1}][P_{12}] + [Q_{24}^{-1}][P_{14}] \end{array}\right] \left\{\begin{array}{c} \underline{a}_1' \\ \hline \underline{a}_1'' \end{array}\right\} = \left\{\begin{array}{c} \underline{0} \\ \\ \end{array}\right\} \tag{187}$$

With $\alpha = 1$, there are two possibilities, namely symmetric modes and antisymmetric modes of buckling. They are uncoupled and the order of corresponding matrices is reduced to 4.

(ii) $\alpha = -1,\ n = \frac{N}{2}$ (Possible only when N is even)

This mode occurs when the consecutive panels of the same kind have the same type of deflection distribution, but of opposite sign. If the curved panels have a symmetric mode, the flat panels will have an antisymmetric mode and vice versa. Again, from (184), (185), the final matrix reduces to:

$$\left[\begin{array}{c|c} 0 & [Q_{21}^{-1}][P_{12}] + [Q_{23}^{-1}][P_{14}] \\ \hline [Q_{22}^{-1}][P_{11}] + [Q_{24}^{-1}][P_{13}] & 0 \end{array}\right] \left\{\begin{array}{c} \underline{a}_1' \\ \hline \underline{a}_1'' \end{array}\right\} = \left\{\begin{array}{c} \underline{0} \\ \\ \end{array}\right\} \tag{188}$$

Again the symmetric and antisymmetric modes are uncoupled and the order for their matrices is 4. From (184), it can be observed that for $\alpha = -1$, the symmetric mode in panel 1 is associated with an

antisymmetric mode in panel 2 and antisymmetric in 1 with symmetric in 2.

7. SHELL MADE UP OF FLAT PANELS ONLY

In this case, the shell is in the form of a regular polygon without any rounded corners. The critical load for such a shell should be the limit for the critical load for the shell considered in the previous sections of this chapter as the radius of the curved panels is reduced to zero. The analysis for this shell follows exactly that used for the shell with both flat and curved panels and it will not be repeated here. Only the points of departure from the last analysis and the final form of the equations will be presented.

(i) Numbering of Panels

To maintain the uniformity of notation, the panels will be numbered $2, 4, 6, \ldots\ldots, 2N$, because all of the N panels are flat plates. Again the front and the back edges will be differentiated by subscripts F and B respectively. The coordinate system remains unchanged.

(ii) Reference Shell

In the previous analysis of the flat panels, the critical load was defined by $\lambda_s = \sigma/\sigma_{CL}(R, h_s)$ (Eqn. (129)), where $\sigma_{CL}(R, h_s) = \frac{Eh_s/R}{\sqrt{3(1-\nu^2)}}$ is the buckling stress of a circular cylindrical shell of radius and thickness equal to those of the curved panels. Similarly, from Eqn. (129), $Z_p = (\frac{h_s}{h_p})^2 Z_s$ where $Z_s = (\frac{L}{R})^2(\frac{R}{h_s})\sqrt{12(1-\nu^2)}$. However, in the present case, there are no curved panels. Hence $R = 0$. For the purpose of analysis, we define:

$$\left.\begin{aligned} &\lambda = \sigma/\sigma_{CL}(r,h_p),\ \sigma_{CL}(r,h_p) = \frac{Eh_p/r}{\sqrt{3(1-\nu^2)}} \\ &Z_p = Z = \left(\frac{L}{r}\right)^2 \left(\frac{r}{h_p}\right) \sqrt{12(1-\nu^2)} \end{aligned}\right\} \qquad (189)$$

Using this information in the analysis of the flat panels, we arrive at expressions similar to Eqns. (139) through (146), Eqns. (147) through (154) and Eqns. (155) through (162).

(iii) Matching Conditions at the Common Edges

In this shell, as in the case of the shell with a single flat spot, the adjacent panels do not join smoothly at the common edge. With reference to Fig. 4b , we can write the matching conditions (analogous to Eqns. (115)) as follows:

$$\left\{S^T_{(i+2)}\right\}_B = [C(2\beta_1)] \left\{S^T_i\right\}_F \qquad (i = 2, 4, 6, 8, \ldots, 2N) \qquad (190)$$

Panels numbered 2 and (2N+2) refer to the same panel. If we use expressions similar to Eqn. (139) through (162) with changes mentioned in (ii) above and Eqn. (190), we obtain matrix equations similar to (168):

$$\left.\begin{aligned} &[P_{4B}]\{\underline{a}_4\} = [C(2\beta_1)]\,[P_{2F}]\,\{\underline{a}_2\} \\ &[P_{6B}]\,\{\underline{a}_6\} = [C(2\beta_1)]\,[P_{4F}]\,\{\underline{a}_4\} \\ &[P_{8B}]\,\{\underline{a}_8\} = [C(2\beta_1)]\,[P_{6F}]\,\{\underline{a}_6\} \\ &\text{----------} \\ &\text{----------} \\ &\text{----------} \\ &[P_{(2N1)B}]\{\underline{a}_{(2N)}\} = [C(2\beta_1)]\,[P_{(2N-2)F}]\,\{\underline{a}_{(2N-2)}\} \\ &[P_{2B}]\{\underline{a}_2\} = [C(2\beta_1)]\,[P_{(2N)F}]\,\{\underline{a}_{(2N)}\} \end{aligned}\right\} \qquad (191)$$

The last of (191) is again the closure condition. As before, all the matrices $[P_{iB}]$ or $[P_{iF}]$ are 8 x 8 real nonsingular matrices. Matrix [C] is also an (8 x 8) matrix analogous to matrix $[C_A]$ of Eqn. (94) for the shell with a single flat spot and is given below:

$$\left[C(2\beta_1)\right]=\left[\begin{array}{c|c} C_1(2\beta_1) & C_2(2\beta_1) \\ \hline C_3(2\beta_1) & C_4(2\beta_1) \end{array}\right]= \left[\begin{array}{cccc|cccc} \cos(2\beta_1) & 0 & 0 & 0 & 0 & 0 & \sin(2\beta_1) & 0 \\ 0 & 1 & 0 & 0 & 0 & 0 & 0 & 0 \\ 0 & 0 & 1 & 0 & 0 & 0 & 0 & 0 \\ 0 & 0 & 0 & \cos(2\beta_1) & 0 & \sin(2\beta_1) & 0 & 0 \\ \hline 0 & 0 & 0 & 0 & 1 & 0 & 0 & 0 \\ 0 & 0 & 0 & -\sin(2\beta_1) & 0 & \cos(2\beta_1) & 0 & 0 \\ -\sin(2\beta_1) & 0 & 0 & 0 & 0 & 0 & \cos(2\beta_1) & 0 \\ 0 & 0 & 0 & 0 & 0 & 0 & 0 & 1 \end{array}\right] \tag{192}$$

Matrix [C] has the following properties

$$\text{Det. } [C] = 1$$

$$\left[\begin{array}{c|c} C_1(\beta_1) & C_2(\beta_1) \\ \hline C_3(\beta_1) & C_4(\beta_1) \end{array}\right]^2 = \left[\begin{array}{c|c} C_1(2\beta_1) & C_2(2\beta_1) \\ \hline C_3(2\beta_1) & C_4(2\beta_1) \end{array}\right]$$

$$\left[\begin{array}{c|c} C_1(\beta_1) & C_2(\beta_1) \\ \hline C_3(\beta_1) & C_4(\beta_1) \end{array}\right]^{-1} = \left[\begin{array}{c|c} C_1(\beta_1) & -C_2(\beta_1) \\ \hline -C_3(\beta_1) & C_4(\beta_1) \end{array}\right] \tag{193}$$

Here $2\beta_1$ = Angle subtended by each of the N flat panels at the center of the inscribed circle

$$2\beta_1 = \frac{2\pi}{N} \quad \text{or} \quad \beta_1 = \frac{\pi}{N} \quad (N \geq 3) \tag{194}$$

(iv) Analysis and the Final Equations

From the fact that all the N panels are identical and by using arguments similar to those in the last section,

$$\{\underline{a}_4\} = \alpha\{\underline{a}_2\},\ \{\underline{a}_6\} = \alpha^2\{\underline{a}_2\},\ \ldots\ldots,\ \{\underline{a}_{(2N)}\} = \alpha^{N-1}\{\underline{a}_2\}$$

$$\alpha^N = 1,\quad \alpha = \cos(\Gamma) + i\sin(\Gamma),\quad \Gamma = \frac{2n\pi}{N}\ , \tag{179}$$

$$(n = 0, 1, 2, \ldots\ldots, \frac{N}{2} \text{ or } \frac{N-1}{2})$$

$$\left.\begin{aligned} &\frac{1+\alpha}{1-\alpha} = i\cot(\Gamma/2) \\ &(\frac{1-\alpha}{1+\alpha})^2 = -\tan^2(\Gamma/2) \end{aligned}\right\} \tag{186}$$

Also from (191)

$$\alpha\begin{bmatrix} P_{2B} \end{bmatrix}\left\{\underline{a}_2\right\} = \left[\begin{array}{c|c} C_1(2\beta_1) & C_2(2\beta_1) \\ \hline C_3(2\beta_1) & C_4(2\beta_1) \end{array}\right]\begin{bmatrix} P_{2F} \end{bmatrix}\left\{\underline{a}_2\right\}$$

Using (193) and (191),

$$\alpha\left[\begin{array}{c|c} C_1(\beta_1) & -C_2(\beta_1) \\ \hline -C_3(\beta_1) & C_4(\beta_1) \end{array}\right]\left[\begin{array}{c|c} P_{21} & -P_{22} \\ \hline P_{23} & P_{24} \end{array}\right]\left\{\begin{array}{c} \underline{a}'_2 \\ \hline \underline{a}''_2 \end{array}\right\} = \left[\begin{array}{c|c} C_1(\beta_1) & C_2(\beta_1) \\ \hline C_3(\beta_1) & C_4(\beta_1) \end{array}\right]\left[\begin{array}{c|c} P_{21} & P_{22} \\ \hline P_{23} & P_{24} \end{array}\right]\left\{\begin{array}{c} \underline{a}'_2 \\ \hline \underline{a}''_2 \end{array}\right\}$$

or by rearranging

$$\Big([C_3(\beta_1)][P_{21}] + [C_4(\beta_1)[P_{23}]\Big)\{\underline{a}'_2\}$$

$$+ (\frac{1-\alpha}{1+\alpha})\Big([C_3(\beta_1)][P_{22}] + [C_4(\beta_1)][P_{24}]\Big)\{\underline{a}_2''\} = \{\underline{0}\} \tag{195a}$$

$$\left([C_1(\beta_1)][P_{21}] + [C_2(\beta_1)][P_{23}]\right) \{\underline{a}'_2\}$$

$$+ \frac{(1+\alpha)}{(1-\alpha)}\left([C_1(\beta_1)][P_{22}] + [C_2(\beta_1)][P_{24}]\right) \{\underline{a}''_2\} = \{\underline{0}\} \qquad (195b)$$

or

$$\left[\begin{array}{c|c} \left([C_3(\beta_1)][P_{21}] + [C_4(\beta_1)][P_{23}]\right) & \frac{(1-\alpha)^2}{(1+\alpha)}\left([C_3(\beta_1)][P_{22}] + [C_4(\beta_1)][P_{24}]\right) \\ \hline \left([C_1(\beta_1)][P_{21}] + [C_2(\beta_1)][P_{23}]\right) & \left([C_1(\beta_1)][P_{22}] + [C_2(\beta_1)][P_{24}]\right) \end{array}\right] x$$

$$x \left\{\begin{array}{c} \underline{a}'_2 \\ \hline \frac{(1+\alpha)}{(1-\alpha)}\,\underline{a}_2'' \end{array}\right\} = \left\{\begin{array}{c} \underline{0} \\ \\ \end{array}\right\} \qquad (195)$$

Special Cases

$\alpha = 1,\ n = 0$

As before, this corresponds to the buckling mode in which all the panels have identical displacement distributions and the symmetric and the antisymmetric modes are decoupled. The corresponding matrix (195) becomes, in view of (195a) and (195b):

$$\left[\begin{array}{c|c} \left([C_3(\beta_1)][P_{21}] + [C_4(\beta_1)][P_{23}]\right) & 0 \\ \hline 0 & \left([C_1(\beta_1)][P_{22}] + [C_2(\beta_1)][P_{24}]\right) \end{array}\right] \left\{\begin{array}{c} \underline{a}'_2 \\ \hline \underline{a}''_2 \end{array}\right\} = \left\{\begin{array}{c} \underline{0} \\ \\ \end{array}\right\} \qquad (196)$$

$\alpha = -1,\ n = \frac{N}{2}$ (Possible only if N is even)

In this case, matrix (195) becomes:

$$\left[\begin{array}{c|c} 0 & \left([C_3(\beta_1)][P_{22}] + [C_4(\beta_1)][P_{24}]\right) \\ \hline \left([C_1(\beta_1)][P_{21}] + [C_2(\beta_1)][P_{23}]\right) & 0 \end{array}\right] \left\{\begin{array}{c} \underline{a}'_2 \\ \hline \underline{a}''_2 \end{array}\right\} = \left\{\begin{array}{c} \underline{0} \\ \\ \end{array}\right\} \qquad (197)$$

Comparing Eqns. (195), (196), (197) to (185), (187), (188), it is easily observed that the equations are similar and the orders of matrices in similar cases is identical. Because of this similarity, the method of obtaining λ_{CR} numerically, outlined in the next section, is equally applicable to the shells with multiple flat spots and the shells with flat panels only.

8. NUMERICAL EVALUATION OF THE CRITICAL LOAD

The method used to obtain the critical value of the load parameter λ is similar to the one used in the case of the shell with a single flat spot. The arguments given in the last chapter, for using that method, apply equally well in the present case. The variables in the present case are the number of panels of each kind (N), the radius of the curved panel (R/r), the width of the flat panels (b/r) and the other material and geometric characteristics of the shell. N is greater than or equal to two in the case of the multiple flat spot shell. Therefore, unlike the case of single flat spot shells, the buckling modes for multiple flat spot shells are no longer limited to one symmetric and one antisymmetric mode. In fact, $\frac{N}{2}$ (or $\frac{N-1}{2}$ for N odd) different modes have to be investigated to obtain the lowest critical load for the shell for a fixed set of geometric constants and every wave number in the axial direction.

In order to use the method of the last chapter, we have to know the upper and the lower bounds to λ_{CR}. Between these two values, λ_{CR} is that λ at which the determinant of the appropriate matrix changes sign. The vanishing of all the "sine" terms in

Eqns. (131) through (138), at the compressive stress $\sigma_{CL}(R, h_s)$ indicates that $\lambda_s = \sigma/\sigma_{CL}(R, h_s) = 1$ can be taken as a suitable upper bound. For the case of a shell with flat panels only, $\lambda = \sigma/\sigma_{CL}(r, h_p) = 1$ is a suitable upper bound. The lower bound may be fixed at any positive value of λ less than the upper bounds mentioned above. In the absence of better information, a positive value close to zero is a good choice. At a fixed R/r and for a particular number of half waves in the axial direction, λ_{CR} has to be determined as n (in Eqn. (179)) varies as $0, 1, 2, 3, \ldots\ldots, \frac{N}{2}$ or $\frac{N-1}{2}$. If only the lowest λ_{CR} is required and not λ_{CR} for every n, we can use the upper and the lower bounds mentioned above for n = 0. For the higher values of n, the upper bound may be fixed at the λ_{CR} obtained for the previous value of n.

With the above remarks in view, the various steps in obtaining λ_{CR} are summarized below:

(i) For a fixed R/r (or $\frac{b}{r}$ in the case of N = 2, for which $\frac{R}{r} = 1.0$ and the shell configuration is changed by varying flat spot width) and at a constant m, the lowest value of λ_{CR} is obtained as n is varied from 0 to $\frac{N}{2}$ (for N even) or $\frac{N-1}{2}$ (for N odd).

(ii) Step (i) is repeated at the same $\frac{R}{r}$ for various values of m until the lowest λ_{CR} of step (i) as a function of m reaches a minimum. This minimum λ_{CR} is the critical load of the shell with a given $\frac{R}{r}$. The corresponding values for m, n determines the eigenmode and hence the displacement distribution in the buckling mode at that critical load.

(iii) Steps (i) and (ii) are repeated for different values of R/r or b/r. Half waves, for which the computations are to be carried out, may be selected to be in the neighborhood of m, at which a minimum is expected to be reached. (This information may be guessed from the data corresponding to the previous values of R/r or b/r.) A typical set of data points is shown plotted in Fig. 22.

(iv) All the values of λ_{CR} are reduced to a common basis. In the present case, the reference stress is $\sigma_{CL}(r, h_s)$, i.e., the critical stress of a circular cylindrical shell with a radius equal to that of the inscribed circle and thickness the same as that of the curved panel.

(v) Plots of λ_{CR} vs. R/r or b/r or β_1 are obtained with m as a parameter. The locus of the minimum λ_{CR} is obtained and is the final curve for the shell indicating the critical load as a function of R/r or b/R or β_1.

9. EIGENMODES AND DISPLACEMENT DISTRIBUTIONS AT CRITICAL LOADS

Equations (185) and (195) give the final form of the equations, the satisfaction of which determines λ_{CR} for the shell with both curved and flat panels and the shell with flat panels only respectively. Either of (185) and (195) is a set of 8 homogeneous equations. After obtaining λ_{CR}, we can regenerate the corresponding matrices for λ_{CR} and solve for the eigenvector $\{\underline{a}_1\}$ and $\{\underline{a}_2\}$ respectively. If we examine the matrices of coefficients in (185) and (195), it is easy to see that they are real matrices, although α is complex. This is

because of Eqn. (186). For a real matrix, the solution of the unknown vector of coefficients has real components. Therefore,

$$\begin{Bmatrix} \underline{a}'_1 \\ \left(\frac{1+\alpha}{1-\alpha}\right)\underline{a}''_1 \end{Bmatrix} \quad \text{and} \quad \begin{Bmatrix} \underline{a}'_2 \\ \left(\frac{1+\alpha}{1-\alpha}\right)\underline{a}''_2 \end{Bmatrix}$$

are real vectors, and so are $\{\underline{a}'_1\}$ and $\{\underline{a}'_2\}$. From Eqns. (186), $\frac{1+\alpha}{1-\alpha} = i \cot(\Gamma/2)$ is an imaginary number. Therefore $\{\underline{a}''_1\}$ and $\{\underline{a}''_2\}$ are also imaginary, but all the state variables of the shell have to be real quantities.

In Eqn. (179), it was mentioned that, if α is the Nth root of unity, so is $\bar{\alpha}$, the complex conjugate of α. From Eqn. (178), it is easy to show that

$$[P]\{\bar{\underline{b}}\} = \bar{\alpha}\{\bar{\underline{b}}\} \tag{198}$$

where $\{\bar{\underline{b}}\}$ is the complex conjugate to vector $\{\underline{b}\}$. Using (177), $\{\bar{\underline{b}}\}$ can be written as:

$$\{\bar{\underline{b}}\} = [P_{1F}]\{\bar{\underline{a}}_1\} \tag{199}$$

Eqns. (198) and (199) imply that at a λ_{CR}, if $\{\underline{a}_1\}$ is a solution of Eqn. (185), then so is its complex conjugate vector $\{\bar{\underline{a}}_1\}$.

From Eqns. (131) through (138), the state variables in the curved panel are of the form

$$\begin{Bmatrix} \underline{S}_i^T \end{Bmatrix} = \begin{bmatrix} \quad \end{bmatrix} \begin{Bmatrix} \underline{a}_i \end{Bmatrix}$$

where the elements of matrix [ ] are functions of x and y. For panel 1, if $\{\underline{a}_1\}$ and $\{\bar{\underline{a}}_1\}$ are the solutions of (185) at a particular

λ_{CR}, a linear combination of $\{\underline{a}_1\}$ and $\{\bar{\underline{a}}\}$ is also a solution.

Therefore, to obtain real values for the state variables,

$$\left|\begin{matrix}\underline{S}_1^T\\ \underline{\bar{S}}_1\end{matrix}\right| = \frac{1}{2}\begin{bmatrix} & \\ & \end{bmatrix}\left(\left|\begin{matrix}\underline{a}_1\\ \underline{\bar{a}}_1\end{matrix}\right| + \left|\begin{matrix}\underline{\bar{a}}_1\\ \underline{a}_1\end{matrix}\right|\right) \tag{200}$$

From Eqn. (182), for other panels

$$\{\underline{a}_{(2i-1)}\} = \alpha^i \{\underline{a}_1\} \text{ and } \{\underline{\bar{a}}_{(2i-1)}\} = (\bar{\alpha})^i \{\underline{\bar{a}}_1\} \tag{201}$$

$$(i = 2, 3, 4, \ldots . N)$$

Formats similar to (200) may be used to obtain the variation of the state variables in all the odd numbered panels. The vectors $\{\underline{a}_i\}$ for the even numbered panels can be obtained from (168) after substituting the vectors for the odd numbered panels. This procedure can be applied to the case of a shell with flat panels only.

Symmetries of the Eigenmodes

In Section 6b of this chapter, it was mentioned that a cylindrical shell with N panels of each kind, has N lines of symmetry. This implies that the buckling modes will also be symmetric and antisymmetric about these axes. This is demonstrated qualitatively below:

N = 2 (Two Panels of Each Kind)

From (179),

$n = 0, \quad \alpha = 1, \qquad n = 1, \quad \alpha = -1$

As shown in (187) and (188), for these values of α, the symmetric and antisymmetric modes of panels (here symmetry is implied

in the sense of local symmetry in the panel about the origin) decouple. Therefore we can consider them separately. Let the panels 1 and 3 be curved and 2 and 4 be flat panels.

(a) $\alpha = 1$ Symmetric Mode

Let $\{\underline{a}_1\} = \left\{\begin{matrix}\underline{a}'_1 \\ \hline \underline{0}\end{matrix}\right\}$ sym. mode

Then $\{\underline{a}_3\} = \alpha\{\underline{a}_1\} = \left\{\begin{matrix}\underline{a}'_1 \\ \hline \underline{0}\end{matrix}\right\}$ = sym. mode of same sign as $\{\underline{a}_1\}$.

This means $\{\underline{a}_2\}$ and $\{\underline{a}_4\}$ are also symmetric modes and have the same sign (not necessarily similar to $\{\underline{a}_3\}$. In other words, the buckling mode of the shell considered as a whole is symmetric about its two axes of symmetry, viz., lines joining centers of 1 and 3 and centers of 2 and 4.

(b) $\alpha = -1$ Antisymmetric Mode

Let $\{\underline{a}_1\} = \left\{\begin{matrix}\underline{0} \\ \hline \underline{a}''_1\end{matrix}\right\}$ antisym. mode

As before $\{\underline{a}_3\} = \left\{\begin{matrix}\underline{0} \\ \hline \underline{a}''_1\end{matrix}\right\}$ antisym. mode of same sign as $\{\underline{a}_1\}$

Similarly $\{\underline{a}_2\}$ and $\{\underline{a}_4\}$ are antisymmetric modes and have the same sign. Now, if we keep in mind that the forward edge of panel 1 is a mirror image of the back edge of panel 3 with respect to the line of symmetry through panels 2 and 4 and the back edge of panel 1 is the mirror image of the front edge of panel 3 (and similarly for panels 2 and 4 with respect to the axis through 1 and 3), the above arguments for the vectors indicate that the buckling mode of the shell is antisymmetric about the two axes of symmetry of the shell.

(c) $\alpha = -1$, Symmetric Mode

Proceeding as in (a) and (b) above, it can be easily shown that this mode is symmetric about an axis of symmetry through

panels 1 and 3 and antisymmetric about the axis through 2 and 4.

(d) $\alpha = 1$ Antisymmetric Mode

This mode is symmetric about the axis through 2 and 4, but antisymmetric about the axis of symmetry through panels 1 and 3.

In exactly the same way, the symmetry (antisymmetry) of the various modes of buckling of the shell can be demonstrated for the cases when N is greater than 2.

10. RESULTS

Numerical results have been obtained to evaluate the effect of the following on the critical stress of a shell:

(i) The number of panels of each kind, (ii) the radius of curvature of the circular panels and the width of every flat panel, and (iii) the inscribed radius to thickness ratio of the shell.

All the results to be presented in this section are for a shell with $r/L = 1.0$ and $h_s = h_p = h$, $h' = 1$, i.e., the same thickness in the curved and flat panels. The discussion in Section 7 of Chapter I and the analysis of Appendix III regarding the effect of r/L on λ_{CR} is easily applicable in the present case also. It may be mentioned here that one may not get detailed results for a shell with $r/L \neq 1.0$ from the results corresponding to $r/L = 1.0$, yet the final envelope of λ_{CR} vs. R/r of b/r or β_1 at $r/L = 1.0$, does represent, to a very good approximation, similar curves at r/L values other than unity. In the latter curves however, the number of half waves in the axial direction have to be adjusted suitably (see Appendix III).

In Table X, numerical values of λ_{CR} as a function of m and $\beta_1(\frac{2b}{r})$ are presented for a shell with N = 2, r/h = 1000, ν = 0.3. For N = 2, $\frac{R}{r}$ is always 1.0 and the configuration of the shell is changed by varying β_1. (This is not true for shells with N equal to or greater than 3. In that case, by Eqn. (106), there is a unique β_1 and $\frac{2b}{r}$ for every R/r.) The observations made in the case of a single flat spot shell are borne out by the results of a shell with 2 flat spots (and also by the later results of shells with N equal to or larger than 3). There is a certain m for which λ_{CR} reaches a minimum; the m at which the minimum is reached decreases with increasing β_1 and for a fixed m, λ_{CR} decreases monotonically with increasing flat spot width. In Fig. 23 are plotted the above results in the form of λ_{CR} vs. width of the flat spot $\frac{2b}{r}$. It indicates a quite rapid decrease in the buckling load of the shell. In the same figure a similar plot is given for a simply supported panel having a width equal to that of the flat spot. The critical load for the simply supported panel is considerably larger than the critical load of the shell for small flat spots, but the agreement improves as the width of the flat spots increases. Even then, the λ_{CR} for a s. s. panel is greater than that for the shell. This result may seem to be at variance with the observations of the last chapter. There, it is mentioned that, for single spot shells, λ_{CR} for a s. s. panel is higher than that for the shell having small flat spot widths, but lower for large flat spots. That this difference in results of single and multiple flat spot shells is justified and should be expected, is explained in the next paragraphs.

Due to a larger moment of inertia, an angle section has a higher bending rigidity than a flat plate of the same thickness and cross-sectional area. The bending rigidity is the same as that of the flat plate when the angle between the two limbs is 180° and it increases as the angle is reduced. The flat panels of the shells have, at their edges, constraints on the out-of-plane displacement and the slope in the circumferential direction due to the adjoining panels. For the same width of the flat panel, the slope constraint is of the same order in the single flat spot (sharp corners) and multi-flat spot (rounded corners) shells. However, due to the angle section effect, the support in the w-displacement direction, for the flat panel in the single flat spot shell is stiffer than that in the multi-spot shell. Moreover, in the former this stiffness increases with the width of the flat panel while, in the latter, it is fairly constant. The result is that in the single spot case, for small flat panel widths, the increase in the buckling load due to small slope constraint does not compensate the reduction in the critical load due to weak out-of-plane displacement support (compared to the rigid support in the simply supported panel). Therefore, the critical load of the flat panel and hence, of the single spot shell, is lower than that for the simply supported panel. For larger flat panel widths, the angle at the edges is much less than 180°. This means a stiffer support in the w-displacement direction. This, coupled with the slope restraint, increases the critical load of the single flat spot panel above that of the simply supported panel.

For the case of multiple flat spot shells (rounded corners), there is no change in the support conditions at the edges as the flat spot width increases. As a result, the critical load of the flat panels and hence, of the multiple flat spot shells, continues to be lower than that of the s. s. panels. For large flat panel widths, however, the difference from simply supported panels decreases and this is in agreement with the results for a compressed plate supported by elastic beams (Ref. 13, pp. 368-369). The difference between the critical loads for an elastically supported plate and a rigidly supported plate is small at large widths and decreases as the width increases. The above discussion thus establishes qualitatively the validity of difference between the results of a single flat spot shell, multi-flat spot shell and a simply supported panel. Comparison of single and two flat spot shells illustrating the above points, is presented in Fig. 32.

Returning to the results of multiple flat spot shells, in Tables XI, XII, XIII λ_{CR} is presented as a function of R/r, $\frac{2b}{r}$ and m for 3, 4 and 8 panels of each kind. The above results are presented in Fig. 24 through Fig. 26 as λ_{CR} vs. width $\frac{2b}{r}$ of the flat panel. ($\frac{R}{r}$ is related to $\frac{2b}{r}$ by Eqn. 106.) As before, in each figure is plotted λ_{CR} vs. $\frac{2b}{r}$ for a simply supported panel of thickness and width the same as those of each flat panel in the shell. In Fig. 27 is given a composite plot of λ_{CR} vs. $\frac{2b}{r}$ for the above cases. In addition, λ_{CR} values are given for shells with no curved panels ($\frac{R}{r} = 0.0$), but with a very high number of flat panels. These shells are of the same thickness ratio and inscribed radius to length ratio as above.

In Table XIV and Fig. 28 , values of λ_{CR} are given for a shell with r/h = 100, r/L = 1.0 and 8 panels of each kind. In this figure is also plotted λ_{CR} vs. $\frac{2b}{r}$ for a similar shell with r/h = 1000 and for simply supported panels of thickness r/h = 100 and r/h = 1000. As expected, the rate of decrease in the critical load with the flat spot width is considerably less for the thicker shells and the mode shape is limited to a low number of half waves in axial direction.

One of the questions posed in the introduction to this chapter was: How does the critical load of the shell change with the radius of curvature of the circular panels? In Fig. 29 and Fig. 30 are presented plots for λ_{CR} vs. R/r for shells with different numbers of panels of each kind and different thicknesses. It can be easily observed that the smaller the number of panels and the thinner the shell, the sharper is the decrease in the critical load.

The effect of the number of panels of each kind is presented in Table XV. For the sake of simplicity it is assumed that there are no circular panels ($\frac{R}{r} = 0.0$) and the shell is an N sided regular polygon. These results were plotted in Fig. 27 of λ_{CR} vs. $\frac{2b}{r}$, but are presented again in Fig. 31 as the variation of λ_{CR} with the number of panels at a constant radius of the circular panels. Though N, the number of panels, is an integral number, a continuous curve is drawn to emphasize the trend of the results. In Fig. 31, are also plotted values of λ_{CR} for a simply supported panel. From the curves, it is apparent that λ_{CR} for an N sided regular polygon approaches asymptotically to the critical load of a shell of radius and thickness the same as the inscribed radius and the thickness of the polygonal

shell. As an incidental result, the curves indicate a limit on the common assumption of simple support condition at a sharp corner between two flat panels. As shown, this assumption may not hold when the angle between the two panels approaches 180°.

11. CONCLUSIONS

In concluding this chapter, we can make the following remarks regarding the stability of shells with flat spots:

(a) The performance of the shell is better if it is formed from the flat sheet by bending into large numbers of small flat panels joined by curved panels. In other words, this means that the continuous rolling method to form shells is better than bending at discrete points.

(b) If the shell has to be formed by discrete bending, the radius of curvature of the bend should be as close to the inscribed radius of the shell as possible. The critical load is very sensitive to this, and becomes more so as the thickness of the shell and the number of panels of each kind decrease.

(c) From the comparison of the results of single spot shells (sharp corners) and two flat spot shells (rounded corners), a possible conclusion may be drawn that the flat spots with sharp corners give higher critical loads. However it may be mentioned that, in the analysis, the effect of stress concentrations on the critical loads have not been considered. Although they may not be serious by themselves, they may trigger collapse of the shell.

(d) In this and the last chapters, the effect of the prismatic imperfections in the form of flat spots has been studied. The results indicate sharp reductions in the critical loads. If we express these flat spots as imperfections on the perfect circular cylindrical shell, and compare the results with those for axisymmetric imperfections (Koiter (11), Hutchinson (8)), we may conclude that the flat spots are not as damaging as the axisymmetric imperfections. However, it must be kept in mind that, even the multiple spot case considered in this chapter is not the general form of a distributed prismatic imperfection and also, the prismatic imperfections occur more commonly than the axisymmetric imperfections (Abrocz and Babcock (3)).

This analysis was started with some questions regarding the effects of flat spots and prismatic imperfections. The results demonstrate the reductions in critical loads due to the former and give an indication of the effects of the latter. Only a detailed analysis of general prismatic imperfections may be able to give information regarding which imperfections are the most critical.

REFERENCES

1. Almroth, B. O., Holmes, A. M. C., and Brush, D. O., An Experimental Study of the Buckling of Cylinders Under Axial Compression, Proceedings of the Society of Experimental Stress Analysis, v. 21, No. 2, 1964, p. 263.

2. Arbocz, J., The Effect of General Imperfections on the Buckling of Cylindrical Shells, Ph. D. Thesis, California Institute of Technology, Pasadena, California, 1968.

3. Arbocz, J. and Babcock, C. D., The Effect of General Imperfections on the Buckling of Cylindrical Shells, Journal of Applied Mechanics, v. 36, 1969, p. 28.

4. Babcock, C. D. and Sechler, E. E., The Effect of Initial Imperfections on the Buckling Stress of Cylindrical Shells. In Collected Papers on Instability of Shell Structures, NASA TN-D 1510, 1962. Also NASA TN-D 2005, 1963.

5. Donnell, L. H., A New Theory for the Buckling of Thin Cylinders under Axial Compression and Bending, Transactions A. S. M. E., v. 56, 1936, p. 795.

6. Donnell, L. H. and Wan, C. C., Effect of Imperfections on Buckling of Thin Cylinders and Columns under Axial Compression, Journal of Applied Mechanics, v. 17, 1950, p. 73.

7. Horton, W. H. and Durham, S. C., Imperfections, a Main Contributor to Scatter in Experimental Values of Buckling Load, Int. Journal of Solids and Structures, v. 1, 1965, p. 59.

8. Hutchinson, J., Axial Buckling of Pressurized Imperfect Cylindrical Shells, AIAA Journal, v. 3, 1965, p. 1461.

9. Isaacson, E. and Keller, H. B., Analysis of Numerical Methods, John Wiley and Sons, New York, 1966.

10. Koiter, W. T., On the Stability of Elastic Equilibrium, Ph. D. Thesis, Polytechnic Inst., Delft, 1945. Also NASA-TT-F 10833, 1967.

11. Koiter, W. T., The Effect of Axisymmetric Imperfections on the Buckling of Cylindrical Shells under Axial Compression, Proceedings of Konin. Nederl. Akademie van Wetenschappen-Amsterdam, Series B, v. 66, No. 5, 1963, p. 265.

12. Tennyson, R. C., A Note on the Classical Buckling Load of Circular Cylindrical Shells under Axial Compression, AIAA Journal, v. 1, 1963, p. 475.

13. Timoshenko, S. and Gere, J. M., Theory of Elastic Stability, McGraw Hill Book Company, New York, 1961.

14. von Karman, T. and Tsien, H. S., The Buckling of Thin Cylindrical Shells under Axial Compression, Journal of Aero. Sciences, v. 8, 1941, p. 303.

APPENDIX I

GOVERNING EQUATIONS AND MATCHING CONDITIONS

(i) Donnell's Equations :

The common form of Donnell's shallow shell equations in the dimensional form is :

$$\frac{1}{Eh_s}\nabla^4 F_1 - \frac{1}{R}W_{1,xx} + (W_{1,xx}W_{1,yy} - W_{1,xy}^2) = 0$$

$$\frac{Eh_s^3}{12(1-\nu^2)}\nabla^4 W_1 + \frac{1}{R}F_{1,xx} - (F_{1,xx}W_{1,yy} - 2F_{1,xy}W_{1,xy} + F_{1,yy}W_{1,xx}) = 0$$

If we non-dimensionalize x and y with respect to the length L of the shell and introduce the following changes :

$$F_1 = \frac{Eh_s^3}{\sqrt{12(1-\nu^2)}}F_s, \quad W_1 = h_s W_s, \quad Z_s = (\frac{L}{R})^2(\frac{R}{h_s})\sqrt{12(1-\nu^2)}$$

the equations become

$$\nabla^4 F_s - Z_s W_{s,xx} + \sqrt{12(1-\nu^2)}\,(W_{s,xx}W_{s,yy} - W_{s,xy}^2) = 0 \quad \text{(a)}$$

$$\nabla^4 W_s + Z_s F_{s,xx} - \sqrt{12(1-\nu^2)}\,(F_{s,xx}W_{s,yy} - 2F_{s,xy}W_{s,xy} + F_{s,yy}W_{s,xx}) = 0 \quad \text{(b)}$$

(ii) von Karman's Plate Equations :

$$\frac{1}{Eh_p}\nabla^4 F_2 + (W_{2,xx}W_{2,yy} - W_{2,xy}^2) = 0$$

$$\frac{Eh_p^3}{12(1-\nu^2)}\nabla^4 W_2 - (F_{2,xx}W_{2,yy} - 2F_{2,xy}W_{2,xy} + F_{2,yy}W_{2,xx}) = 0$$

Again non-dimensionalizing x and y with respect to L and introducing the following:

$$F_2 = \frac{Eh_p^3}{\sqrt{12(1-\nu^2)}} F_p, \quad W_2 = h_p w_p ,$$

the equations reduce to

$$\nabla^4 F_p + \sqrt{12(1-\nu^2)}\,(W_{p,xx} W_{p,yy} - W_{p,xy}^2) = 0 \qquad (c)$$

$$\nabla^4 W_p - \sqrt{12(1-\nu^2)}\,(F_{p,xx} W_{p,yy} - 2F_{p,xy} W_{p,xy} + F_{p,yy} W_{p,xx}) = 0 \qquad (d)$$

(iii) Matching Conditions

In a single flat spot shell, the following are the matching conditions which must be satisfied to insure continuity of displacements and equilibrium of forces across the common edge:

At Edge A $\left(y_s = -\frac{R}{L}(\pi - \beta_1),\ y_p = \frac{R}{L}\sin\beta_1\right)$

$W_1 = W_2\cos\beta_1 + V_2\sin\beta_1$	out-of-plane displacement
$V_1 = V_2\cos\beta_1 - W_2\sin\beta_1$	circumferential or y displacement
$U_1 = U_2$	axial displacement
$(\phi_y)_1 = (\phi_y)_2$	rotation about x-axis
$(M_y)_1 = (M_y)_2$	moment in y-direction
$(N_{xy})_1 = (N_{xy})_2$	inplane shear
$(N_{yy})_1 = (N_{yy})_2\cos\beta_1 - (Q_y)_2\sin\beta_1$	y-direction normal force
$(Q_y)_1 = (Q_y)_2\cos\beta_1 + (N_{yy})_2\sin\beta_1$	out-of-plane shear

In the above expressions:

$$(\phi_y)_1 = -\frac{\partial W_1}{\partial y} + \underline{\frac{1}{R} V_1} \qquad (\phi_y)_2 = -\frac{\partial W_2}{\partial y}$$

$$(M_y)_1 = \frac{Eh_s^3}{12(1-\nu^2)} (\kappa_{yy} + \nu\kappa_{xx})_1 \qquad (M_y)_2 = \frac{Eh_p^3}{12(1-\nu^2)} (\kappa_{yy}+\nu\kappa_{xx})_2$$

$$(\kappa_{xx})_1 = -\frac{\partial^2 W_1}{\partial x^2}, \qquad (\kappa_{xx})_2 = -\frac{\partial^2 W_2}{\partial x^2}$$

$$(\kappa_{yy})_1 = -\frac{\partial^2 W_1}{\partial y^2} + \underline{\frac{1}{R}\frac{\partial V_1}{\partial y}}, \qquad (\kappa_{yy})_2 = -\frac{\partial^2 W_2}{\partial y^2}$$

$$(N_{xy})_1 = -\frac{\partial^2 F_1}{\partial x \partial y}, \qquad (N_{xy})_2 = -\frac{\partial^2 F_2}{\partial x \partial y}$$

$$(N_{yy})_1 = \frac{\partial^2 F_1}{\partial x^2}, \qquad (N_{yy})_2 = \frac{\partial^2 F_2}{\partial x^2}$$

$$(Q_y)_1 = \frac{\partial (M_y)_1}{\partial y} + \frac{\partial (M_{xy})_1}{\partial x}$$

$$= D_s\left[\frac{\partial}{\partial y}(\kappa_{yy}+\nu\kappa_{xx})_1 + \frac{\partial}{\partial x}(\kappa_{xy})_1\right], \quad (\kappa_{xy})_1 = -\frac{\partial^2 W_1}{\partial x \partial y} + \underline{\frac{1}{2R}\frac{\partial V_1}{\partial x}}$$

$$(Q_y)_2 = D_p\left[\frac{\partial}{\partial y}(\kappa_{yy}+\kappa_{xx})_2 + \frac{\partial}{\partial x}(\kappa_{xy})_2\right], \quad (\kappa_{xy})_2 = -\frac{\partial^2 W_2}{\partial x \partial y}$$

The underlined quantities are neglected in the Donnell's approximation of shell curvatures and slopes by the corresponding flat plate curvatures and slopes.

Making the following changes:

$$W_1 = h_s W_s, \; V_1 = h_s V_s, \; U_1 = h_s U_s, \; F_1 = \frac{Eh_s^3}{\sqrt{12(1-\nu^2)}} F_s \text{ and}$$

$$W_2 = h_p W_p,\quad V_2 = h_p V_p,\quad U_2 = h_p U_p,\quad F_2 = \frac{Eh_p^3}{\sqrt{12(1-\nu^2)}} F_p,\quad h' = h_p/h_s$$

The matching conditions reduce to:

$$W_s = h'(W_p \cos\beta_1 + V_p \sin\beta_1) \tag{e}$$

$$V_s = h'(V_p \cos\beta_1 - W_p \sin\beta_1) \tag{f}$$

$$U_s = h' U_p \tag{g}$$

$$\frac{\partial W_s}{\partial y} = h' \frac{\partial W_p}{\partial y}$$

$$\left(\frac{\partial^2 W_s}{\partial y^2} + \nu \frac{\partial^2 W_s}{\partial x^2}\right) = h'^4 \left(\frac{\partial^2 W_p}{\partial y^2} + \nu \frac{\partial^2 W_p}{\partial x^2}\right) \tag{h}$$

$$\frac{\partial^2 F_s}{\partial x \partial y} = h'^3 \frac{\partial^2 F_p}{\partial x \partial y} \tag{i}$$

$$\frac{\partial^2 F_s}{\partial x^2} = \left[\frac{\partial^2 F_p}{\partial x^2} \cos\beta_1 + \frac{h_p/L}{\sqrt{12(1-\nu^2)}} \left(\frac{\partial^3 W_p}{\partial y^3} + (2-\nu) \frac{\partial^3 W_p}{\partial y \partial x^2}\right) \sin\beta_1\right] h'^3 \tag{j}$$

$$\frac{h_s/L}{\sqrt{12(1-\nu^2)}} \left(\frac{\partial^3 W_s}{\partial y^3} + (2-\nu) \frac{\partial^3 W_s}{\partial y \partial x^2}\right) = \left[\frac{h_p/L}{\sqrt{12(1-\nu^2)}} \left(\frac{\partial^3 W_p}{\partial y^3} + (2-\nu) \frac{\partial^3 W_p}{\partial y \partial x^2}\right) \cos\beta_1 \right. \tag{k}$$

$$\left. - \frac{\partial^2 F_p}{\partial x^2} \sin\beta_1\right] h'^3 \tag{l}$$

<u>At Edge B</u> $\left(y_s = \frac{R}{L}(\pi - \beta_1),\ y_p = -\frac{R}{L}\sin\beta_1\right)$

The matching conditions at edge B are obtained by changing β_1 to $-\beta_1$.

Multiple Flat Spot Shells

In the multi-spot shells with rounded corners, the matching conditions are obtained by setting $\beta_1 = 0$.

(iv) Rigid Body Motion of Curved Panels

In the case of multiple flat spot shells, the prebuckling solution admits a rigid body motion of the curved panels, viz. the panel moving parallel to the line joining the centers of the circle of the curved panel and the inscribed circle. This motion contributes y-dependent components to W_s and V_s in the expressions (e) through (l) above.

Prebuckling solution

$$W' = \frac{\nu\sigma R}{Eh_s} + \frac{\nu\sigma r\tan(\beta_1)}{Eh_s\sin(\pi/N)} \cos\left(\frac{Ly}{R}\right) \tag{120}$$

$$V' = -\frac{\nu\sigma r\tan(\beta_1)}{Eh_s\sin(\pi/N)} \sin\left(\frac{Ly}{R}\right)$$

There are no similar terms contributed by the flat panels. Therefore, this W', V' substituted directly in the matching conditions will remain unbalanced. However, if we do not apply the Donnell's approximation and retain the underlined terms in slopes and curvatures, the contributions of W' and V' to the slopes and curvature cancel each other. Now applying the Donnell's approximation, we obtain the matching condition in the form of Eqns. (e) through (l) with $\beta_1 = 0$.

APPENDIX II

FINAL MATRICES FOR SINGLE FLAT SPOT SHELLS

In Eqn. (99), the eigenvalue problem for the single spot shells was reduced to the solution of the following:

$$\left[\begin{array}{c|c} P_{(8\times8)} & 0 \\ \hline 0 & Q_{(8\times8)} \end{array}\right] \left\{\begin{array}{c} a_i \\ (8\times1) \\ \hline b_i \\ (8\times1) \end{array}\right\} = \left\{\begin{array}{c} 0 \\ \\ \end{array}\right\}$$

Matrix $[P]$ and vector $\{a_i\}$ are associated with symmetric modes and $[Q]$ and $\{b_i\}$ with antisymmetric modes of buckling. In the flat plate region, the form of W_p and its functions changes depending on λ. If $\lambda > \frac{k^2}{2Z_p}$ (Case I), W_p has both trigonometric and hyperbolic terms (Eqn. (70)), while for $\lambda < \frac{k^2}{2Z_p}$ (Case III), there are only hyperbolic terms (Eqn. (86)). $\lambda = \frac{k^2}{2Z_p}$ (Case II) is the intermediate case with constant, linear in y and hyperbolic terms (Eqn. (78)). $\lambda = \frac{k^2}{2Z_p}$ corresponds to Euler buckling of a panel in m half waves. However, due to the constraints at the edges, we can expect $\lambda_{CR} > \frac{k^2}{2Z_p}$. Therefore, final matrices $[P]$ and $[Q]$ will be presented for the case of $\lambda > \frac{k^2}{2Z_p}$ only. For the other two cases, the matrices can be easily formed in a similar way by the use of Eqns. (70) through (93).

As before

$$\left.\begin{array}{l} 2\beta_1 = \text{angle subtended by the flat} \\ \qquad\qquad \text{spot at the center of the circle} \end{array}\right| \qquad \text{(a)}$$

Let $2\beta_2$ = angle subtended by the curved panel at the center of the circle

$= 2(\pi - \beta_1)$

or $\beta_2 = \pi - \beta_1$ (b)

Also let

$2T = 2R(\pi - \beta_1)$ = width of the curved panel

$2b = 2R \sin\beta_1$ = width of the flat panel (c)

$$\bar{h}_s = \frac{h_s/L}{\sqrt{12(1-\nu^2)}}, \quad \bar{h}_p = \frac{h_p/L}{\sqrt{12(1-\nu^2)}}, \quad h' = \frac{h_p}{h_s} \qquad (d)$$

With this notation in mind, the final matrices [P] and [Q] are given in the following pages.

Matrix [P]

$$P(1,1) = +\left[e^{-\xi_1 \frac{T}{L}} \cos\left(\eta_1 \frac{T}{L} - \theta\right) + e^{\xi_1 \frac{T}{L}} \cos\left(\eta_1 \frac{T}{L} + \theta\right)\right]$$

$$P(1,2) = -\left[e^{-\xi_1 \frac{T}{L}} \sin\left(\eta_1 \frac{T}{L} - \theta\right) - e^{\xi_1 \frac{T}{L}} \sin\left(\eta_1 \frac{T}{L} + \theta\right)\right]$$

$$P(1,3) = +\left[e^{-\xi_2 \frac{T}{L}} \cos\left(\eta_2 \frac{T}{L} + \theta\right) + e^{\xi_2 \frac{T}{L}} \cos\left(\eta_2 \frac{T}{L} - \theta\right)\right]$$

$$P(1,4) = -\left[e^{-\xi_2 \frac{T}{L}} \sin\left(\eta_2 \frac{T}{L} + \theta\right) - e^{-\xi_2 \frac{T}{L}} \sin\left(\eta_2 \frac{T}{L} - \theta\right)\right]$$

$$P(1,5) = -\, h' \overline{h}_p k(1+\nu)\sinh\left(\frac{kb}{L}\right)\sin\beta_1$$

$$P(1,6) = -h' \overline{h}_p k\left[(1+\nu)\frac{kb}{L}\cosh\left(\frac{kb}{L}\right) - (1-\nu)\sinh\left(\frac{kb}{L}\right)\right]\sin\beta_1$$

$$P(1,7) = +h' \cos\left(\zeta_1 \frac{b}{L}\right)\cos\beta_1$$

$$P(1,8) = +h' \cosh\left(\zeta_2 \frac{b}{L}\right)\cos\beta_1$$

$$P(2,1) = +\overline{h}_s k\left[\sqrt{\frac{\ell_1}{k^2}}\left\{e^{-\xi_1 \frac{T}{L}}\left[\frac{\ell_1}{k^2}\cos\left(\eta_1 \frac{T}{L} - \frac{3\varphi}{2}\right) - (2+\nu)\cos\left(\eta_1 \frac{T}{L} - \frac{\varphi}{2}\right)\right]\right.\right.$$
$$\left.\left. - e^{\xi_1 \frac{T}{L}}\left[\frac{\ell_1}{k^2}\cos\left(\eta_1 \frac{T}{L} + \frac{3\varphi}{2}\right) - (2+\nu)\cos\left(\eta_1 \frac{T}{L} + \frac{\varphi}{2}\right)\right]\right\}\right]$$

$$P(2,2) = -\overline{h}_s k\left[\sqrt{\frac{\ell_1}{k^2}}\left\{e^{-\xi_1 \frac{T}{L}}\left[\frac{\ell_1}{k^2}\sin\left(\eta_1 \frac{T}{L} - \frac{3\varphi}{2}\right) - (2+\nu)\sin\left(\eta_1 \frac{T}{L} - \frac{\varphi}{2}\right)\right]\right.\right.$$
$$\left.\left. + e^{\xi_1 \frac{T}{L}}\left[\frac{\ell_1}{k^2}\sin\left(\eta_1 \frac{T}{L} + \frac{3\varphi}{2}\right) - (2+\nu)\sin\left(\eta_1 \frac{T}{L} + \frac{\varphi}{2}\right)\right]\right\}\right]$$

$$P(2,3) = +\bar{h}_s k\left[\sqrt{\frac{\ell_2}{k^2}}\left\{e^{-\xi_2\frac{T}{L}}\left[\frac{\ell_2}{k^2}\cos(\eta_2\frac{T}{L}-\frac{3\psi}{2})-(2+\nu)\cos(\eta_2\frac{T}{L}-\frac{\psi}{2})\right]\right.\right.$$
$$\left.\left.-e^{\xi_2\frac{T}{L}}\left[\frac{\ell_2}{k^2}\cos(\eta_2\frac{T}{L}+\frac{3\psi}{2})-(2+\nu)\cos(\eta_2\frac{T}{L}+\frac{\psi}{2})\right]\right\}\right]$$

$$P(2,4) = -\bar{h}_s k\left[\sqrt{\frac{\ell_2}{k^2}}\left\{e^{-\xi_2\frac{T}{L}}\left[\frac{\ell_2}{k^2}\sin(\eta_2\frac{T}{L}-\frac{3\psi}{2})-(2+\nu)\sin(\eta_2\frac{T}{L}-\frac{\psi}{2})\right]\right.\right.$$
$$\left.\left.+e^{\xi_2\frac{T}{L}}\left[\frac{\ell_2}{k^2}\sin(\eta_2\frac{T}{L}+\frac{3\psi}{2})-(2+\nu)\sin(\eta_2\frac{T}{L}+\frac{\psi}{2})\right]\right\}\right]$$

$$P(2,5) = +h'\,\bar{h}_p k\,(1+\nu)\sinh(\frac{kb}{L})\cos\beta_1$$

$$P(2,6) = +h'\,\bar{h}_p k\left[(1+\nu)\frac{kb}{L}\cosh(\frac{kb}{L})-(1-\nu)\sinh(\frac{kb}{L})\right]\cos\beta_1$$

$$P(2,7) = +h'\cos(\zeta_1\frac{b}{L})\sin\beta_1$$

$$P(2,8) = +h'\cosh(\zeta_2\frac{b}{L})\sin\beta_1$$

$$P(3,1) = +\bar{h}_s k\left[e^{-\xi_1\frac{T}{L}}\left\{\frac{\ell_1}{k^2}\cos(\eta_1\frac{T}{L}-\varphi)+\nu\cos(\eta_1\frac{T}{L})\right\}\right.$$
$$\left.+e^{\xi_1\frac{T}{L}}\left\{\frac{\ell_1}{k^2}\cos(\eta_1\frac{T}{L}+\varphi)+\nu\cos(\eta_1\frac{T}{L})\right\}\right]$$

$$P(3,2) = -\bar{h}_s k\left[e^{-\xi_1\frac{T}{L}}\left\{\frac{\ell_1}{k^2}\sin(\eta_1\frac{T}{L}-\varphi)+\nu\sin(\eta_1\frac{T}{L})\right\}\right.$$
$$\left.-e^{\xi_1\frac{T}{L}}\left\{\frac{\ell_1}{k^2}\sin(\eta_1\frac{T}{L}+\varphi)+\nu\sin(\eta_1\frac{T}{L})\right\}\right]$$

$$P(3,3) = +\bar{h}_s k\left[e^{-\xi_2\frac{T}{L}}\left\{\frac{\ell_2}{k^2}\cos(\eta_2\frac{T}{L}-\psi)+\nu\cos(\eta_2\frac{T}{L})\right\}\right.$$

$$\left.+e^{\xi_2\frac{T}{L}}\left\{\frac{\ell_2}{k^2}\cos(\eta_2\frac{T}{L}+\psi)+\nu\cos(\eta_2\frac{T}{L})\right\}\right]$$

$$P(3,4) = -\bar{h}_s k\left[e^{-\xi_2\frac{T}{L}}\left\{\frac{\ell_2}{k^2}\sin(\eta_2\frac{T}{L}-\psi)+\nu\sin(\eta_2\frac{T}{L})\right\}\right.$$

$$\left.-e^{\xi_2\frac{T}{L}}\left\{\frac{\ell_2}{k^2}\sin(\eta_2\frac{T}{L}+\psi)+\nu\sin(\eta_2\frac{T}{L})\right\}\right]$$

$$P(3,5) = -h'\bar{h}_p k\cosh(\frac{kb}{L})$$

$$P(3,6) = -h'\bar{h}_p k\left[(1+\nu)\frac{kb}{L}\sinh(\frac{kb}{L})+2\cosh(\frac{kb}{L})\right]$$

$$P(3,7) = 0.0$$

$$P(3,8) = 0.0$$

$$P(4,1) = +\sqrt{\frac{\ell_1}{k^2}}\left\{e^{-\xi_1\frac{T}{L}}\cos(\eta_1\frac{T}{L}-\theta-\frac{\varphi}{2})-e^{\xi_1\frac{T}{L}}\cos(\eta_1\frac{T}{L}+\theta+\frac{\varphi}{2})\right\}$$

$$P(4,2) = -\sqrt{\frac{\ell_1}{k^2}}\left\{e^{-\xi_1\frac{T}{L}}\sin(\eta_1\frac{T}{L}-\theta-\frac{\varphi}{2})+e^{\xi_1\frac{T}{L}}\sin(\eta_1\frac{T}{L}+\theta+\frac{\varphi}{2})\right\}$$

$$P(4,3) = +\sqrt{\frac{\ell_2}{k^2}}\left\{e^{-\xi_2\frac{T}{L}}\cos(\eta_2\frac{T}{L}+\theta-\frac{\psi}{2})-e^{\xi_2\frac{T}{L}}\cos(\eta_2\frac{T}{L}-\theta+\frac{\psi}{2})\right\}$$

$$P(4,4) = -\sqrt{\frac{\ell_2}{k^2}}\left\{e^{-\xi_2\frac{T}{L}}\sin(\eta_2\frac{T}{L}+\theta-\frac{\psi}{2})-e^{\xi_2\frac{T}{L}}\sin(\eta_2\frac{T}{L}-\theta+\frac{\psi}{2})\right\}$$

$$P(4,5) = 0.0$$

$$P(4,6) = 0.0$$

$$P(4,7) = -h' \frac{\zeta_1}{k} \sin(\zeta_1 \frac{b}{L})$$

$$P(4,8) = h' \frac{\zeta_2}{k} \sinh(\zeta_2 \frac{b}{L})$$

$$P(5,1) = + \left[e^{-\xi_1 \frac{T}{L}} \left\{ - \frac{\ell_1}{k^2} \cos(\eta_1 \frac{T}{L} - \theta - \varphi) + \nu \cos(\eta_1 \frac{T}{L} - \theta) \right\} \right.$$
$$\left. + e^{\xi_1 \frac{T}{L}} \left\{ - \frac{\ell_1}{k^2} \cos(\eta_1 \frac{T}{L} + \theta + \varphi) + \nu \cos(\eta_1 \frac{T}{L} + \theta) \right\} \right]$$

$$P(5,2) = - \left[e^{-\xi_1 \frac{T}{L}} \left\{ - \frac{\ell_1}{k^2} \sin(\eta_1 \frac{T}{L} - \theta - \varphi) + \nu \sin(\eta_1 \frac{T}{L} - \theta) \right\} \right.$$
$$\left. - e^{\xi_1 \frac{T}{L}} \left\{ - \frac{\ell_1}{k^2} \sin(\eta_1 \frac{T}{L} + \theta + \varphi) + \nu \sin(\eta_1 \frac{T}{L} + \theta) \right\} \right]$$

$$P(5,3) = + \left[e^{-\xi_2 \frac{T}{L}} \left\{ - \frac{\ell_2}{k^2} \cos(\eta_2 \frac{T}{L} + \theta - \psi) + \nu \cos(\eta_2 \frac{T}{L} + \theta) \right\} \right.$$
$$\left. + e^{\xi_2 \frac{T}{L}} \left\{ - \frac{\ell_2}{k^2} \cos(\eta_2 \frac{T}{L} - \theta + \psi) + \nu \cos(\eta_2 \frac{T}{L} - \theta) \right\} \right]$$

$$P(5,4) = - \left[e^{-\xi_2 \frac{T}{L}} \left\{ - \frac{\ell_2}{k^2} \sin(\eta_2 \frac{T}{L} + \theta - \psi) + \nu \sin(\eta_2 \frac{T}{L} + \theta) \right\} \right.$$
$$\left. - e^{\xi_2 \frac{T}{L}} \left\{ - \frac{\ell_2}{k^2} \sin(\eta_2 \frac{T}{L} - \theta + \psi) + \nu \sin(\eta_2 \frac{T}{L} - \theta) \right\} \right]$$

$$P(5,5) = 0.0$$

$$P(5,6) = 0.0$$

$$P(5,7) = h'^4 \left(\frac{\zeta_1^2}{k^2} + \nu\right) \cos\left(\frac{\zeta_1 b}{L}\right)$$

$$P(5,8) = -h'^4 \left(\frac{\zeta_2^2}{k^2} - \nu\right) \cosh\left(\frac{\zeta_2 b}{L}\right)$$

$$P(6,1) = +\sqrt{\frac{\ell_1}{k^2}} \left[e^{-\xi_1 \frac{T}{L}} \cos\left(\eta_1 \frac{T}{L} - \frac{\varphi}{2}\right) - e^{\xi_1 \frac{T}{L}} \cos\left(\eta_1 \frac{T}{L} + \frac{\varphi}{2}\right)\right]$$

$$P(6,2) = -\sqrt{\frac{\ell_1}{k^2}} \left[e^{-\xi_1 \frac{T}{L}} \sin\left(\eta_1 \frac{T}{L} - \frac{\varphi}{2}\right) + e^{\xi_1 \frac{T}{L}} \sin\left(\eta_1 \frac{T}{L} + \frac{\varphi}{2}\right)\right]$$

$$P(6,3) = +\sqrt{\frac{\ell_2}{k^2}} \left[e^{-\xi_2 \frac{T}{L}} \cos\left(\eta_2 \frac{T}{L} - \frac{\psi}{2}\right) - e^{\xi_2 \frac{T}{L}} \cos\left(\eta_2 \frac{T}{L} + \frac{\psi}{2}\right)\right]$$

$$P(6,4) = -\sqrt{\frac{\ell_2}{k^2}} \left[e^{-\xi_2 \frac{T}{L}} \sin\left(\eta_2 \frac{T}{L} - \frac{\psi}{2}\right) + e^{\xi_2 \frac{T}{L}} \sin\left(\eta_2 \frac{T}{L} + \frac{\psi}{2}\right)\right]$$

$$P(6,5) = -h'^3 \sinh\left(\frac{kb}{L}\right)$$

$$P(6,6) = -h'^3 \left[\frac{kb}{L} \cosh\left(\frac{kb}{L}\right) + \sinh\left(\frac{kb}{L}\right)\right]$$

$$P(6,7) = 0.0$$

$$P(6.8) = 0.0$$

$$P(7,1) = + \left[e^{-\xi_1 \frac{T}{L}} \cos(\eta_1 \frac{T}{L}) + e^{\xi_1 \frac{T}{L}} \cos(\eta_1 \frac{T}{L}) \right]$$

$$P(7,2) = - \left[e^{-\xi_1 \frac{T}{L}} \sin(\eta_1 \frac{T}{L}) - e^{\xi_1 \frac{T}{L}} \sin(\eta_1 \frac{T}{L}) \right]$$

$$P(7,3) = + \left[e^{-\xi_2 \frac{T}{L}} \cos(\eta_2 \frac{T}{L}) + e^{\xi_2 \frac{T}{L}} \cos(\eta_2 \frac{T}{L}) \right]$$

$$P(7,4) = - \left[e^{-\xi_2 \frac{T}{L}} \sin(\eta_2 \frac{T}{L}) - e^{\xi_2 \frac{T}{L}} \sin(\eta_2 \frac{T}{L}) \right]$$

$$P(7,5) = -h'^3 \cosh(\frac{kb}{L}) \cos \beta_1$$

$$P(7,6) = - h'^3 \frac{kb}{L} \sinh(\frac{kb}{L}) \cos\beta_1$$

$$P(7,7) = +h'^3 \overline{h}_p k \left(\frac{\zeta_1^3}{k^3} + (2-\nu) \frac{\zeta_1}{k} \right) \sin(\frac{\zeta_1 b}{L}) \sin\beta_1$$

$$P(7,8) = +h'^3 \overline{h}_p k \left(\frac{\zeta_2^3}{k^3} - (2-\nu) \frac{\zeta_2}{k} \right) \sinh(\frac{\zeta_2 b}{L}) \sin\beta_1$$

$$P(8,1) = +\overline{h}_s k \sqrt{\frac{\ell_1}{k^2}} \left[e^{-\xi_1 \frac{T}{L}} \left\{ - \frac{\ell_1}{k^2} \cos(\eta_1 \frac{T}{L} - \theta - \frac{3\varphi}{2}) + (2-\nu) \cos(\eta_1 \frac{T}{L} - \theta - \frac{\varphi}{2}) \right\} \right.$$
$$\left. - e^{\xi_1 \frac{T}{L}} \left\{ - \frac{\ell_1}{k^2} \cos(\eta_1 \frac{T}{L} + \theta + \frac{3\varphi}{2}) + (2-\nu) \cos(\eta_1 \frac{T}{L} + \theta + \frac{\varphi}{2}) \right\} \right]$$

$$P(8,2) = - \overline{h}_s k \sqrt{\frac{\ell_1}{k^2}} \left[e^{-\xi_1 \frac{T}{L}} \left\{ - \frac{\ell_1}{k^2} \sin(\eta_1 \frac{T}{L} - \theta - \frac{3\varphi}{2}) + (2-\nu) \sin(\eta_1 \frac{T}{L} - \theta - \frac{\varphi}{2}) \right\} \right.$$
$$\left. + e^{\xi_1 \frac{T}{L}} \left\{ - \frac{\ell_1}{k^2} \sin(\eta_1 \frac{T}{L} + \theta + \frac{3\varphi}{2}) + (2-\nu) \sin(\eta_1 \frac{T}{L} + \theta + \frac{\varphi}{2}) \right\} \right]$$

$$P(8,3) = \bar{h}_s k\sqrt{\frac{\ell_2}{k^2}}\left[e^{-\xi_2\frac{T}{L}}\left\{-\frac{\ell_2}{k^2}\cos(\eta_2\frac{T}{L}+\theta-\frac{3\psi}{2})+(2-\nu)\cos(\eta_2\frac{T}{L}+\theta-\frac{\psi}{2})\right\}\right.$$
$$\left.-e^{\xi_2\frac{T}{L}}\left\{-\frac{\ell_2}{k^2}\cos(\eta_2\frac{T}{L}-\theta+\frac{3\psi}{2})+(2-\nu)\cos(\eta_2\frac{T}{L}-\theta+\frac{\psi}{2})\right\}\right]$$

$$P(8,4) = -\bar{h}_s k\sqrt{\frac{\ell_2}{k^2}}\left[e^{-\xi_2\frac{T}{L}}\left\{-\frac{\ell_2}{k^2}\sin(\eta_2\frac{T}{L}+\theta-\frac{3\psi}{2})+(2-\nu)\sin(\eta_2\frac{T}{L}+\theta-\frac{\psi}{2})\right\}\right.$$
$$\left.+e^{\xi_2\frac{T}{L}}\left\{-\frac{\ell_2}{k^2}\sin(\eta_2\frac{T}{L}-\theta+\frac{3\psi}{2})+(2-\nu)\sin(\eta_2\frac{T}{L}-\theta+\frac{\psi}{2})\right\}\right]$$

$$P(8,5) = -h'^3\cosh(\frac{kb}{L})\sin\beta_1$$

$$P(8,6) = -h'^3\frac{kb}{L}\sinh(\frac{kb}{L})\sin\beta_1$$

$$P(8,7) = -h'^3\bar{h}_p k\left(\frac{\zeta_1^3}{k^3}+(2-\nu)\frac{\zeta_1}{k}\right)\sin(\frac{\zeta_1 b}{L})\cos\beta_1$$

$$P(8,8) = -h'^3\bar{h}_p k\left(\frac{\zeta_2^3}{k^3}-(2-\nu)\frac{\zeta_2}{k}\right)\sinh(\frac{\zeta_2 b}{L})\cos\beta_1$$

Matrix [Q]

This matrix can be formed from the elements of the matrix [P] by making the following changes:

(i) Change $e^{\xi_1\frac{T}{L}}$ to $-e^{\xi_1\frac{T}{L}}$, $e^{\xi_2\frac{T}{L}}$ to $-e^{\xi_2\frac{T}{L}}$. Signs of $e^{-\xi_1\frac{T}{L}}$ and $e^{-\xi_2\frac{T}{L}}$ terms remain the same.

(ii) Except for the elements given below, change

$\cos(\frac{\zeta_1 b}{L})$ to $\sin(\frac{\zeta_1 b}{L})$, $\sin(\frac{\zeta_1 b}{L})$ to $\cos(\frac{\zeta_1 b}{L})$,

$\cosh(\frac{kb}{L})$ to $\sinh(\frac{kb}{L})$, $\sinh(\frac{kb}{L})$ to $\cosh(\frac{kb}{L})$,

$\cosh(\frac{\zeta_2 b}{L})$ to $\sinh(\frac{\zeta_2 b}{L})$ and $\sinh(\frac{\zeta_2 b}{L})$ to $\cosh(\frac{\zeta_2 b}{L})$.

Exceptions are:

$P(4, 7) = -h' \frac{\zeta_1}{k} \sin(\frac{\zeta_1 b}{L})$ changes to $Q(4, 7) = h' \frac{\zeta_1}{k} \cos(\frac{\zeta_1 b}{L})$

$P(7, 7) = +h'^3 \bar{h}_p k \left(\frac{\zeta_1^3}{k^3} + (2-\nu)\frac{\zeta_1}{k}\right) \sin(\frac{\zeta_1 b}{L}) \sin\beta_1$ changes to

$Q(7, 7) = -h'^3 \bar{h}_p k \left(\frac{\zeta_1^3}{k^3} + (2-\nu)\frac{\zeta_1}{k}\right) \cos(\frac{\zeta_1 b}{L}) \sin\beta_1$

$P(8, 7) = -h'^3 \bar{h}_p k \left(\frac{\zeta_1^3}{k^3} + (2-\nu)\frac{\zeta_1}{k}\right) \sin(\frac{\zeta_1 b}{L}) \cos\beta_1$ changes to

$Q(8, 7) = +h'^3 \bar{h}_p k \left(\frac{\zeta_1^3}{k^3} + (2-\nu)\frac{\zeta_1}{k}\right) \cos(\frac{\zeta_1 b}{L}) \cos\beta_1$.

APPENDIX III

EFFECT OF CHANGING RADIUS TO LENGTH RATIO

In the analysis of the single flat spot shell, we had:

$$Z_s = \left(\frac{L}{R}\right)^2 \left(\frac{R}{h_s}\right) \sqrt{12(1-\nu^2)} \tag{24}$$

$$k = m\pi \tag{27}$$

$$\frac{\ell_1}{k^2} = \sqrt{1 + 2\sqrt{\frac{Z_s}{k^2}} \cos\frac{\theta}{2} + \frac{Z_s}{k^2}} \tag{35}$$

$$\tan\varphi = \frac{\sqrt{\frac{Z_s}{k^2}} \sin\frac{\theta}{2}}{1+\sqrt{\frac{Z_s}{k^2}} \cos\frac{\theta}{2}} \tag{36}$$

$$\frac{\ell_2}{k^2} = \sqrt{1 - 2\sqrt{\frac{Z_s}{k^2}} \cos\frac{\theta}{2} + \frac{Z_s}{k^2}} \tag{37}$$

$$\tan\psi = \frac{\sqrt{\frac{Z_s}{k^2}} \sin\frac{\theta}{2}}{1-\sqrt{\frac{Z_s}{k^2}} \cos\frac{\theta}{2}} \tag{38}$$

$$\left.\begin{aligned} \frac{\xi_1}{k} &= \sqrt{\frac{\ell_1}{k^2}} \cos\frac{\varphi}{2}\ , \quad \frac{\eta_1}{k} = \sqrt{\frac{\ell_1}{k^2}} \sin\frac{\varphi}{2} \\ \frac{\xi_2}{k} &= \sqrt{\frac{\ell_2}{k^2}} \cos\frac{\psi}{2}\ , \quad \frac{\eta_2}{k} = \sqrt{\frac{\ell_2}{k^2}} \sin\frac{\psi}{2} \end{aligned}\right\} \tag{39}$$

$$Z_p = \left(\frac{h_s}{h_p}\right)^2 Z_s \tag{25}$$

$$\frac{\zeta_1}{k} = \sqrt{1 - \sqrt{2\lambda \frac{Z_p}{k^2}}} \qquad \frac{\zeta_2}{k} = \sqrt{1 + \sqrt{2\lambda \frac{Z_p}{k^2}}} \tag{57}$$

Also from Appendix II,

$$\frac{kT}{L} = \frac{kR}{L}(\pi - \beta_1), \quad \frac{kb}{L} = \frac{kR}{L} \sin \beta_1 \tag{II (c)}$$

$$k\bar{h}_s = \frac{kh_s/L}{\sqrt{12(1-\nu^2)}} = \frac{1}{\sqrt{12(1-\nu^2)}} \left(\frac{h_s}{R}\right)\left(\frac{kR}{L}\right)$$

$$k\bar{h}_p = \frac{kh_p/L}{\sqrt{12(1-\nu^2)}} = \frac{1}{\sqrt{12(1-\nu^2)}} \left(\frac{h_p}{R}\right)\left(\frac{kR}{L}\right) \tag{II (d)}$$

$$h' = h_p/h_s$$

Now, if for a single flat spot shell, R/h_s, h_p/h_s and ν remain fixed, (24) and (25) imply that Z_s/k^2 will remain unchanged as long as m (the number of half waves in the axial direction) and $\frac{R}{L}$ change such that $\frac{mR}{L}$ is constant. For a given $\lambda \leqslant 1$, θ is fixed. Therefore, at a particular value of λ and fixed $\frac{mR}{L}$, $\frac{\ell_1}{k^2}$, φ, $\frac{\ell_2}{k^2}$, ψ, $\frac{\xi_1}{k}$, $\frac{\eta_1}{k}$, $\frac{\xi_2}{k}$, $\frac{\eta_2}{k}$, $\frac{\zeta_1}{k}$, $\frac{\zeta_2}{k}$ remain unchanged. If in addition, $2\beta_1$, the angle of the flat spot is prescribed, it can be easily observed that all the elements of matrix [P] (and also of matrix [Q]) in Appendix II are unchanged and so is the determinant of [P]. Reversing the argument, for a fixed R/h_s, h_p/h_s, ν, β_1, the value of λ at which the determinants of [P] and [Q] vanish, remain the same as long as m and $\frac{R}{L}$

vary such that $\frac{mR}{L}$ is constant. Thus, if λ_{CR} is the value of the critical load of a shell at a particular m, the critical load of a similar but twice as long shell will be the same for 2m half waves in the axial direction. It may be pointed out again that the results of this section can be used only to relate λ_{CR} vs. β_1 (or width of flat spot) variation of a shell at a fixed m to a similar variation of different length shell at a corresponding m. The results do not apply to the final envelope of λ_{CR} vs. β_1 curves of the two shells.

It can be easily proved that the results obtained above also apply to the multiple flat spot shells, which are identical except for their lengths. The wave number m and length L vary such that $\frac{mr}{L}$ is constant, where r is the inscribed radius of the shell.

TABLE I - λ_{CR} for a Single Flat Spot Shell (R/L = 0.25, R/h = 1000, ν = 0.3)

β_1 \ m	57	56	55	54	53	52	51	50	49	48
0.90	0.99000	0.98990	0.99000	0.99000						
1.10	0.97260	0.97250	0.97240	0.97240	0.97260	0.97280				
1.30		0.94250	0.94220	0.94200	0.94200	0.94220	0.94250			
1.50				0.90010	0.89970	0.89940	0.89940	0.89970	0.90020	
1.70						0.84880	0.84810	0.84780	0.84780	0.84810
1.90								0.79230	0.79150	0.79110
2.10								0.73710	0.73540	0.73410

β_1 \ m	47	46	45	44	43	42	41	40	39	38
1.90	0.79110	0.79142	0.79220							
2.10	0.73320	0.73279	0.73280	0.73316	0.73410					
2.30		0.67690	0.67600	0.67553	0.67550	0.67602	0.67710			
2.50				0.62226	0.62130	0.62088	0.62100	0.62163		
2.70						0.57111	0.57030	0.56999	0.57030	0.57110
2.90								0.52395	0.52330	0.52320
3.10								0.48329	0.48180	0.48090
3.30								0.44773	0.44550	0.44380
3.50								0.41667	0.41380	0.41140

TABLE I (Continued)

β_1 \ m	37	36	35	34	33	32	31	30	29	28
2.90	0.52370	0.52480								
3.10	0.48050	0.48070								
3.30	0.44260	0.44190	-	0.44237						
3.50		0.40800	0.40712	0.40681	0.40712	0.40806				
4.00			0.33846	-	0.33497	-	0.33373	-	0.33504	
4.50							0.27932	0.27807	0.27739	0.27733
5.00									0.23569	0.23432

β_1 \ m	27	26	25	24	23	22	21	20	19	18
4.50	0.27795	0.27919								
5.00	0.23351	0.23329	0.23376	0.23491						
5.50		0.19948	0.19877	0.19861	0.19921	0.20048				
6.00			0.17269	0.17154	0.17095	0.17104	0.17188			
6.50					0.14959	0.14871	0.14854	0.14896	0.15028	
7.00						0.13162	0.13061	0.13024	0.13048	0.13149
7.50							0.11660	0.11552	0.11511	0.11527
8.00								0.10392	0.10291	0.10242
8.50									0.09313	0.09207

TABLE I (Continued)

β_1 \ m	17	16	15	14	13	12	11	10	9	8
7.50	0.11623	0.11810	0.12102							
8.00	0.10260	0.10353	0.10540							
8.50	0.09170	0.09195	0.09301							
9.00	0.08292	0.08261	0.08299	0.08421						
9.50	0.07577	0.07496	0.07483	0.07535						
10.00	0.06979	0.06867	0.06811	0.06812	0.06908	0.07091				
11.00		0.05910	0.05788	0.05714	0.05716	0.05784	0.05955			
12.00				0.04928	0.04871	0.04863	0.04937	0.05105		
13.00				0.04354	0.04255	0.04190	0.04198	0.04284		
14.00					0.03793	0.03692	0.03651	0.03674	0.03786	
15.00						0.03312	0.03233	0.03207	0.03262	0.03412
17.00							0.02655	0.02572	0.02545	0.02584
18.00							0.02452	0.02348	0.02294	0.02298
20.00								0.02018	0.01927	0.01881
30.00										0.01065

TABLE I (Continued)

β_1 \ m	7	6	5	4	3	2	1
17.00	0.02739						
18.00	0.02401	0.02634					
20.00	0.01911	0.02036	0.02335				
30.00	0.00973	0.00910	0.00915	0.01009	0.01322		
40.00		0.00630	0.00571	0.00561	0.00646	0.01005	0.02893
50.00		0.00524	0.00446	0.00399	0.00414	0.00582	0.01592
70.00			0.00359	-	0.00266	0.00320	0.00793
90.00			0.00342	-	0.00237	0.00271	0.00645

TABLE II λ_{CR} for a Single Flat Spot Shell (R/L = 0.50, R/h = 1000, ν = 0.3)

β_1 \ m	28	27	26	25	24	23	22	21	20	19
0.90	0.98990	0.99000	0.99020							
1.10	0.97250	0.97240	0.97280	0.97330						
1.30	0.94250	0.94200	0.94220	0.94286						
1.50	0.90190	0.90010	0.89940	0.89970	0.90095					
1.70		0.85100	0.84880	0.84780	0.84818	0.84968				
1.90			0.79490	0.79229	0.79104	0.79142	0.79341			
2.10				0.73703	0.73416	0.73279	0.73316	0.73540		
2.30					0.68002	0.67690	0.67553	0.67602	0.67864	
2.50						0.62538	0.62226	0.62088	0.62163	0.62463
2.70							0.57423	0.57111	0.56999	0.57111
2.90								0.52682	0.52395	0.52321
3.10									0.48329	0.48092
3.30									0.44773	0.44374
3.50									0.41667	0.41130

TABLE II (Continued)

β_1 \ m	18	17	16	15	14	13	12	11	10	9
2.90	0.52470	0.52894								
3.10	0.48067	0.48291	0.48778							
3.30	0.44187	0.44237	0.44536							
3.50	0.40794	0.40681	0.40806	0.41218						
3.70	0.37837	0.37575	0.37538	0.37775	0.38311					
3.90	0.35255	0.34868	0.34693	0.34768	0.35117					
4.10		0.32498	0.32198	0.32124	0.32323	0.32835				
4.30		0.30427	0.30028	0.29828	0.29878	0.30215				
4.50			0.28107	0.27807	0.27732	0.27919	0.28443			
4.70				0.26036	0.25849	0.25911	0.26273			
4.90					0.24189	0.24139	0.24364	0.24938		
5.00					0.23428	0.23329	0.23491	0.23990		
5.50					0.20272	0.19948	0.19861	0.20048	0.20584	
6.00						0.17428	0.17154	0.17104	0.17341	
6.50						0.15519	0.15095	0.14871	0.14896	
7.00							0.13511	0.13162	0.13024	0.13149

TABLE II (Continued)

β_1 \ m	10	9	8	7	6	5	4	3	2	1
7.50	0.11552	0.11527	0.11802							
8.00	0.10392	0.10242	0.10355	0.10841						
9.00	0.08708	0.08384	0.08259	0.08421						
10.00		0.07136	0.06862	0.06812	0.07091	0.07863				
11.00		0.06275	0.05901	0.05714	0.05784	0.06244				
12.00			0.05215	0.04928	0.04863	0.05105	0.05908			
13.00			0.04703	0.04354	0.04190	0.04284	0.04819			
14.00					0.03692	0.03674	0.04016	0.05130		
15.00					0.03312	0.03207	0.03412	0.04246		
17.00					0.02777	0.02572	0.02584	0.03045		
18.00					0.02590	0.02348	0.02298	0.02634	0.03997	
20.00					0.02310	0.02018	0.01881	0.02036	0.02945	
30.00							0.01065	0.00910	0.01009	0.02260
40.00							0.00847	0.00630	0.00561	0.01003
50.00								0.00524	0.00399	0.00580
70.00										0.00318

TABLE III - λ_{CR} for a Single Flat Spot Shell (R/L = 0.50, R/h = 1000, ν = 0.3)

β_1 \ m	15	14	13	12	11	10	9	8	7
0.90	0.99027	0.98989	0.99014	0.99077					
1.10	0.97355	0.97243	0.97280	0.97418					
1.30	0.94573	0.94249	0.94212	0.94424	0.94823				
1.50	0.90843	0.90182	0.89945	0.90095	0.90594				
1.70		0.85442	0.84868	0.84818	0.85255	0.86190			
1.90		0.80452	0.79491	0.79104	0.79341	0.80202			
2.00			-	-	0.76322	0.77083	0.78543		
2.20			0.71607	0.70659	0.70384	0.70871	-		
2.50				0.63049	0.62226	0.62163	0.62999	0.64833	
3.00					0.51223	0.50300	0.50200	0.51110	0.53269
3.50					0.43251	0.41667	0.40794	0.40806	0.41941
4.00						0.35529	0.34095	0.33408	0.33670
5.00							0.25824	0.24277	0.23428
6.00								0.19349	0.17914
7.00									0.14721

TABLE III (Continued)

β_1 \ m	6	5	4	3	2	1
4.00	0.35242					
5.00	0.23491	0.24913				
6.00	0.17154	0.17341	0.19100			
7.00	0.13511	0.13024	0.13648	0.16417		
8.00	0.11290	0.10392	0.10355	0.11877	0.17366	
9.00	0.09843	0.08708	0.08259	0.08995	0.12675	
10.00	0.08870	0.07585	0.06862	0.07086	0.09556	
11.00		0.06787	0.05901	0.05776	0.07411	0.16916
12.00		0.06225	0.05215	0.04866	0.05901	0.13199
13.00		0.05789	0.04703	0.04192	0.04816	0.10454
14.00		0.05464	0.04329	0.03693	0.04017	0.08396
15.00		0.05215	0.04030	0.03306	0.03406	0.06849
17.00			0.03618	0.02782	0.02583	0.04728
18.00			0.03456	0.02583	0.02296	0.03992
20.00			0.03231	0.02308	0.01884	0.02944
30.00			0.02745	0.01734	0.01061	0.01011

TABLE IV - λ_{CR} for a Single Flat Spot Shell (R/L = 0.25, R/h = 500, ν = 0.3)

β_1 \ m	43	42	41	40	39	38	37	36	35	34
0.90	0.99862	0.99856	0.99856	0.99856	0.99856					
1.10		0.99556	0.99550	0.99538	0.99544	0.99551				
1.30		0.98906	0.98887	0.98877	0.98881	0.98890				
1.50			0.97719	0.97692	0.97687	0.97692	0.97719			
1.70				0.95896	0.95869	0.95858	0.95881	0.95921		
1.90				0.93488	0.93419	0.93376	0.93381	0.93413	0.93487	
2.10					0.90456	0.90357	0.90312	0.90319	0.90362	0.90457
2.30						0.86951	0.86837	0.86776	0.86781	0.86839
2.50								0.82984	0.82919	0.82909
2.70								0.79092	0.78944	0.78867
2.90										0.74825
3.10										0.70908

TABLE IV (Continued)

β_1 \ m	33	32	31	30	29	28	27	26	25	24
2.50	0.82987	0.83121								
2.70	0.78869	0.78942	0.79100							
2.90	0.74744	0.74738	0.74831	0.75006						
3.10	0.70737	0.70646	0.70650	0.70744						
3.50		0.63061	0.62875	0.62794	0.62806	0.62924				
4.00				0.54310	0.54100	0.53992	0.53995	0.54109	0.54354	
4.50						0.46769	0.46566	0.46461	0.46470	0.46607
5.00								0.40397	0.40214	0.40132

β_1 \ m	23	22	21	20	19	18	17	16
5.00	0.40187	0.40369						
5.50	0.34902	0.34880	0.34999	0.35255				
6.00	0.30746	0.30564	0.30501	0.30564	0.30772			
6.50		0.27146	0.26940	0.26847	0.26887	0.27059		
7.00			0.24096	0.23878	0.23781	0.23803	0.23974	
7.50				0.21507	0.21287	0.21183	0.21217	0.21395

TABLE IV (Continued)

β_1 \ m	19	18	17	16	15	14	13	12	11	10
8.00	0.19275	0.19075	0.18986	0.19025	0.19222					
8.50		0.17341	0.17157	0.17091	0.17166	0.17402				
9.00			0.15661	0.15507	0.15477	0.15591	0.15871			
9.50			0.14419	0.14197	0.14077	0.14095	0.14261			
10.00				0.13099	0.12914	0.12844	0.12914	0.13149		
11.00						0.10916	-	0.10891		
12.00						0.09516	0.09335	0.09257	0.09335	0.09569
13.00						0.08475	0.08219	0.08059	0.08015	0.08109
14.00							0.07375	0.07149	0.07022	0.07011
15.00								0.06437	0.06259	0.06176
17.00									0.05187	0.04990
18.00										0.04579
20.00										0.03955

TABLE IV (Continued)

β_1 \ m	9	8	7	6	5	4	3	2	1
13.00	0.08410								
14.00	0.07174	0.07546							
15.00	0.06229	0.06465							
17.00	0.04915	0.04964	0.05203						
18.00	0.04451	0.04437	0.04587	0.04978					
20.00	0.03765	0.03661	0.03684	0.03893					
30.00			0.01917	0.01784	0.01779	0.01946	0.02504	0.04192	
40.00			0.01448	-	0.01126	-	0.01247	0.01904	0.05290
50.00			0.01265	0.01036	0.00884	0.00786	0.00808	0.01111	0.02965
70.00			0.01132	-	0.00716	-	0.00523	0.00612	0.01502
90.00			0.01103	-	0.00681	-	0.00467	0.00524	0.01228

TABLE V - λ_{CR} for a Single Flat Spot Shell (R/L = 0.50, R/h = 500, ν = 0.3)

β_1 \ m	21	20	19	18	17	16	15	14	13	12
1.10	0.99551	0.99538	0.99551	0.99563						
1.30	0.98902	0.98877	0.98890	0.98915						
1.50	0.97754	0.97692	0.97692	0.97742	0.97842					
1.70	0.96033	0.95896	0.95858	0.95921	0.96070					
2.10		0.90594	0.90357	0.90319	0.90457	0.90768				
2.30		0.87363	0.86951	0.86776	0.86839	0.87126				
2.50			0.83321	0.82984	0.82909	0.83121	0.83608			
2.70			0.79616	0.79092	0.78867	0.78942	0.79341			
3.10				0.71520	0.70908	0.70646	0.70746	0.71233		
3.50					0.63698	0.63061	0.62787	0.62924	0.63511	
4.00						0.55015	0.54304	0.53992	0.54104	0.54728
4.50							0.47493	0.46769	0.46457	0.46607
5.00								0.41068	0.40394	0.40132
5.50									0.35629	0.35043
6.00									0.31874	0.31026
6.50										0.27848

TABLE V (Continued)

β_1 \ m	11	10	9	8	7	6	5	4	3	2
4.50	0.47293									
5.00	0.40369	0.41193								
5.50	0.34880	0.35255	0.36290							
6.00	0.30564	0.30564	0.31150	0.32485						
6.50	0.27146	0.26847	0.27059	0.27944						
7.00	0.24414	0.23878	0.23803	0.24314	0.25612					
7.50	0.22218	0.21507	0.21183	0.21395	0.22293					
8.00		0.19574	0.19075	0.19025	0.19599	0.21058				
8.50		0.18002	0.17341	0.17091	0.17391	0.18488				
9.00		0.16692	0.15918	0.15507	0.15594	0.16368				
9.50			0.14733	0.14197	0.14097	0.14609	0.16093			
10.00			0.13748	0.13099	0.12850	0.13149	0.14309			
11.00				0.11390	0.10916	0.10891	0.11565	0.13411		
12.00				0.10147	0.09506	0.09257	0.09569	0.10854		
13.00				0.09214	0.08471	0.08059	0.08109	0.08957		
14.00					0.07673	0.07149	0.07011	0.07535	0.09394	

TABLE V (Continued)

β_1 \ m	7	6	5	4	3	2	1
15.00	0.07061	0.06437	0.06176	0.06462	0.07847		
17.00		0.05452	0.04990	0.04953	0.05726	0.08596	
18.00		0.05103	0.04579	0.04429	0.04978	0.07323	
20.00		0.04566	0.03955	0.03656	0.03893	0.05464	
30.00			0.02683	0.02109	0.01784	0.01946	0.04192
50.00			0.02171	0.01522	0.01036	0.00786	0.01111

TABLE VI - λ_{CR} for a Single Flat Spot Shell (R/L = 1.0, R/h = 500, ν = 0.3)

β_1 \ m	12	11	10	9	8	7	6	5	4	3
0.90	0.99900	0.99863	0.99850	0.99850	0.99875					
1.10	0.99688	0.99575	0.99538	0.99563	0.99613					
1.30	0.99227	0.98965	0.98877	0.98915	0.99039					
1.50	0.98416	0.97892	0.97692	0.97742	0.97979					
1.70	0.97206	0.96282	0.95896	0.95921	0.96282					
2.10		0.91679	0.90594	0.90319	0.90768	0.91854				
2.30		0.88885	0.87363	0.86776	0.87126	0.88348				
2.50		0.85916	0.83920	0.82984	0.83121	0.84344				
2.70			0.80439	0.79092	0.78942	0.80552	0.82410			
3.10			0.73653	0.71520	0.70646	0.71233	0.73441			
3.50				0.64671	0.63061	0.62924	0.64583	0.68388		
4.00				0.57423	0.55015	0.53992	0.54728	0.57747		
4.50					0.48553	0.46769	0.46607	0.48628	0.53755	
5.00					0.43451	0.41068	0.40132	0.41193	0.45185	
6.00						0.33059	0.31026	0.30564	0.32485	0.38548

TABLE VI (Continued)

β_1 \ m	7	6	5	4	3	2	1
7.00	0.28007	0.25312	0.23878	0.24314	0.28044		
8.00		0.21607	0.19574	0.19025	0.21058	0.29030	
9.00		0.19112	0.16692	0.15507	0.16368	0.21944	
10.00		0.17366	0.14708	0.13099	0.13149	0.16954	
11.00			0.13286	0.11390	0.10891	0.13411	0.28044
12.00			0.12238	0.10147	0.09257	0.10854	0.22430
13.00			0.11440	0.09219	0.08059	0.08957	0.18114
14.00			0.10829	0.08508	0.07149	0.07535	0.14796
15.00			0.10355	0.07947	0.06437	0.06462	0.12213
17.00				0.07161	0.05452	0.04953	0.08596
18.00				0.06874	0.05103	0.04429	0.07323
20.00				0.06437	0.04566	0.03656	0.05464
30.00				0.05489	0.03456	0.02109	0.01946
50.00				0.05053	0.02982	0.01522	0.00786

TABLE VII - λ_{CR} for a Single Flat Spot Shell (R/L = 0.25, R/h = 100, ν = 0.3)

β_1 \ m	20	19	18	17	16	15	14	13	12	11
2.10	0.99838	0.99800	0.99850	0.99775						
2.50		0.99513	0.99513	0.99488		0.99576				
3.10		0.98515	0.98466	0.98453		0.98590				
3.50		0.97330	0.97218	0.97193	0.97255	0.97393				
4.00		0.95210	0.94973	0.94885	0.94948	0.95122				
5.00			0.88585	0.88174	0.88036	0.88174	0.88560			
6.00				0.80077	0.79528	0.79329	0.79520	0.80102		
7.00					0.71058	0.70409	0.70195	0.70447	0.71183	
8.00						0.66425	0.61754	0.61552	0.61889	0.62800
9.00							0.54607	0.53980	0.53842	0.54304
10.00							0.48743	0.47730	0.47193	0.47206
11.00									0.41792	0.41405
12.00									0.37438	0.36707
13.00									0.33920	0.32934
14.00										0.29866
15.00										0.27371

TABLE VII (Continued)

β_1 \ m	10	9	8	7	6	5	4	3	2	1
9.00	0.55441									
10.00	0.47859									
11.00	0.41622	0.42553								
12.00	0.36542	0.37026	0.38349							
13.00	0.32446	0.32548	0.33408							
14.00	0.29122	0.28905	0.29367	0.30739						
15.00	0.26408	0.25936	0.26073	0.27021						
17.00	0.22362	0.21507	0.21146	0.21432	0.22655					
20.00		0.17266	0.16442	0.16118	0.16460	0.17852				
30.00				0.09145	0.08393	0.08109	0.08555	0.10442		
40.00					0.06065	0.05365	0.05081	0.05552	0.07970	
50.00						0.04279	0.03749	0.03718	0.04882	0.11627
70.00						0.03518	0.02828	0.02483	0.02828	0.06288
90.00						0.03356	0.02641	0.02233	0.02429	0.05252

TABLE VIII - λ_{CR} for a Single Flat Spot Shell (R/L = 0.50, R/h = 100, ν = 0.3)

β_1 \ m	10	9	8	7	6	5	4
1.00	0.99987	1.00000	1.00000				
2.00	0.99875	0.99900	0.99938				
3.00	0.98840	0.98703	0.98740	0.98890			
3.50	0.97555	0.97218	0.97255	0.97567			
4.00	0.95634	0.94973	0.94948	0.95422	0.96245		
5.00	0.90269	0.88585	0.88036	0.88560	0.90032		
6.00		0.81001	0.79528	0.79520	0.81075	0.84114	
7.00		0.73519	0.71058	0.70195	0.71183	0.74291	
8.00		0.66858	0.63523	0.61754	0.61889	0.64380	
9.00			0.57173	0.54607	0.53842	0.55441	0.60217
10.00			0.51946	0.48743	0.47193	0.47859	0.51672

TABLE VIII (Continued)

β_1 \ m	7	6	5	4	3	2	1
11.00	0.43987	0.41792	0.41622	0.44386	0.51871		
12.00	0.40153	0.37438	0.36542	0.38349	0.44636		
13.00	0.37028	0.33920	0.32446	0.33408	0.38498		
14.00	0.34500	0.31063	0.29122	0.29367	0.33371		
15.00		0.28718	0.26408	0.26073	0.29117	0.39421	
17.00		0.25212	0.22362	0.21146	0.22655	0.30240	
20.00		0.21807	0.18465	0.16442	0.16460	0.20983	
30.00			0.13199	0.10223	0.08393	0.08555	0.16112
40.00				0.08343	0.06065	0.05081	0.07970
50.00				0.07571	0.05143	0.03749	0.04882
70.00				0.06986	0.04459	0.02828	0.02828
90.00				0.06861	0.04322	0.02641	0.02429

TABLE IX - λ_{CR} for a Single Flat Spot Shell

($R/L = 1.0$, $R/h = 100$, $\nu = 0.3$)

β_1 \ m	5	4	3	2	1
1.00	0.99987	1.00000			
2.00	0.99875	0.99938	0.99938	1.00000	
3.00	0.98840	0.98740	0.99077	0.99913	
3.50	0.97555	0.97255	0.98041		
4.00	0.95684	0.94948	0.96245	0.98341	
5.00	0.90269	0.88036	0.90032	0.94723	
6.00	0.83820	0.79528	0.81075	0.88336	
7.00	0.77358	0.71058	0.71183	0.79578	
8.00	0.71495	0.63523	0.61889	0.69786	0.88947
9.00	0.66417	0.57173	0.53482	0.60217	0.82498
10.00	0.62151	0.51946	0.47193	0.51672	0.74925
11.00	0.58620	0.47692	0.41792	0.44386	0.66916
12.00	0.55689	0.44237	0.37438	0.38349	0.59045
13.00		0.41417	0.33920	0.33408	0.51734
14.00		0.39106	0.31063	0.29367	0.45172
15.00		0.37201	0.28718	0.26073	0.39421
17.00		0.34294	0.25212	0.21146	0.30240
20.00		0.31425	0.21807	0.16442	0.20983
30.00		0.27283	0.17079	0.10223	0.08555
40.00		0.25898	0.15544	0.08343	0.05081
50.00		0.25275	0.14883	0.07571	0.03749
70.00		0.24801	0.14372	0.06986	0.02828
90.00		0.24688	0.14259	0.06861	0.02641

TABLE X - λ_{CR} of a Multi-spot Shell (N = 2, r/L = 1.0, r/h = 1000, ν = 0.3)

R/r	β_1	m / 2b/r	18	17	16	15	14	13	12	11
1.00	0.25	0.00872	0.93569	0.92544	0.92137	0.92263	0.92781	0.93531		
1.00	0.50	0.01746			0.83302	0.82508	0.82298	0.82637	0.83458	
1.00	0.75	0.02618			0.75869	0.74240	0.73203	0.72779	0.72953	
		m / 2b/r	13	12	11	10	9	8	7	6
1.00	1.00	0.03492	0.64681	0.64150	0.64269	0.65062	0.66544			
1.00	1.50	0.05238	0.53131	0.51450	0.50375	0.49962	0.50300	0.51475		
1.00	2.00	0.06984		0.43394	0.41500	0.40187	0.39544	0.39666	0.40718	
1.00	3.00	0.10482			0.31812	-	0.27742	0.26525	0.26021	0.26401
		m / 2b/r	8	7	6	5	4	3	2	1
1.00	4.00	0.13986	0.20232	0.18931	0.18291	0.18545	0.20132			
1.00	5.00	0.17498	0.16846	0.15146	0.13971	0.13472	0.13976			
1.00	6.00	0.21020	0.14835	0.12931	0.11464	0.10540	0.10390	0.11528	0.15431	
1.00	8.00	0.28108	0.12679	0.10589	0.08859	0.07527	0.06736	0.06740	0.08452	0.16094

TABLE X (Continued)

R/r	β_1	2b/r \ m	4	3	2	1
1.00	10.00	0.35266	0.05071	0.04809	0.05402	0.09737
1.00	12.00	0.42512	0.04318	0.03498	0.03387	0.06360
1.00	15.00	0.53590	0.03535	0.02580	0.02086	0.02995
1.00	17.00	0.61146	0.03248	0.02258	0.01662	0.02012
1.00	20.00	0.73794	0.02980	0.01963	0.01291	0.01243

TABLE XI - λ_{CR} of a Multi-spot Shell (N = 3, r/L = 1.0, r/h = 1000, ν = 0.3)

R/r	β_1	m / 2b/r	15	14	13	12	11	10	9	8
0.995	0.50	0.01734	0.82944	0.82818	0.83182	0.84023	0.85240			
0.990	0.99	0.03466		0.66472	0.65356	0.64865	0.65028	0.65875	0.67402	
0.985	1.49	0.05198				0.52118	0.51089	0.50734	0.51128	0.52372
0.980	1.98	0.06930					0.42112	0.40845	0.40248	0.40447
0.975	2.48	0.08662						0.34365	0.33075	0.32469
0.970	2.97	0.10394							0.28228	0.27062
0.960	3.96	0.13858								0.20609

		m / 2b/r	7	6	5	4	3	2	1
0.980	1.98	0.06930	0.41576						
0.975	2.48	0.08662	0.32695	0.33968					
0.970	2.97	0.10394	0.26614	0.27078	0.28775				
0.960	3.96	0.13858	0.19345	0.18761	0.19100	0.20812			
0.950	4.95	0.17322	0.15452	0.14314	0.13876	0.14469	0.16827		
0.940	5.93	0.20786		0.11726	0.10847	0.10765	0.12028	0.16203	

TABLE XI (Continued)

R/r	β_1	m / 2b/r	6	5	4	3	2	1
0.930	6.91	0.24250	0.10105	0.08969	0.08474	0.09027	0.11853	
0.920	7.89	0.27715	0.09032	0.07736	0.06979	0.07066	0.08950	
0.910	8.86	0.31179		0.06884	0.05954	0.05732	0.06957	0.13369
0.900	9.83	0.34643		0.06273	0.05242	0.04814	0.05552	0.10549
0.880	11.74	0.41570			0.04330	0.03626	0.03573	0.06852
0.850	14.56	0.51963			0.03604	0.02678	0.02214	0.03299
0.800	19.11	0.69283			0.03049	0.02037	0.01380	0.01417
0.700	27.46	1.03924			0.02661	0.01650	0.00900	0.00729
0.500	40.89	1.73205			0.02490	0.01438	0.00714	0.00254
0.300	50.48	2.42486				0.01390	0.00647	0.00217
0.000	60.00	3.46410				0.01367	0.00622	0.00175

TABLE XII - λ_{CR} of a Multi-spot Shell (N = 4, r/L = 1.0, r/h = 1000, ν = 0.3)

R/r	β_1	m / 2b/r	18	17	16	15	14	13	12
0.995	0.29	0.0100	0.92904	0.91735	0.91195	0.91209	0.91672		
0.990	0.57	0.0200			0.81593	0.80570	0.80142	0.80292	0.80987
0.985	0.86	0.0300					0.70527	0.69803	0.69698
0.980	1.15	0.0400						0.61519	0.60642
0.975	1.43	0.0500							0.53619

		m / 2b/r	11	10	9	8	7	6	5
0.985	0.86	0.0300	0.70248	0.71406					
0.980	1.15	0.0400	0.60424	0.60909	0.62131				
0.975	1.43	0.0500	0.52729	0.52517	0.53068	0.54665			
0.970	1.72	0.0600	0.46745	0.45946	0.45875	0.46636	0.48369		
0.965	2.00	0.0700	0.42098	0.40820	0.40216	0.40397	0.41524		
0.960	2.29	0.0800			0.35761	0.35453	0.36030	0.37709	
0.950	2.86	0.1000			0.29398	0.28361	0.28073	0.28737	0.30687

TABLE XII (Continued)

R/r	β_1	2b/r \ m	8	7	6	5	4	3	2	1
0.940	3.43	0.1200	0.23726	0.22846	0.22771	0.23791	0.26426			
0.930	4.00	0.1400	0.20576	0.19304	0.18713	0.19044	0.20753			
0.920	4.57	0.1600		0.16821	0.15871	0.15705	0.16709	0.19704		
0.900	5.71	0.2000		0.13687	0.12311	0.11530	0.11603	0.13133		
0.880	6.84	0.2400				0.09167	0.08695	0.09352	0.12360	
0.850	8.53	0.3000				0.07193	0.06333	0.06234	0.07704	0.14936
0.800	11.31	0.4000				0.05659	0.04532	0.03852	0.03916	0.07756
0.700	16.70	0.6000					0.03283	0.02297	0.01713	0.02127
0.500	26.57	1.0000					0.02696	0.01656	0.00932	0.00574
0.00	45.00	2.0000						0.01419	0.00674	0.00233

TABLE XIII - λ_{CR} of a Multi-spot Shell (N = 8, r/L = 1.0, r/h = 1000, ν = 0.3)

R/r	β_1	m / 2b/r	18	17	16	15	14	13	12	11
0.990	0.24	0.00828	0.94722	0.93801	0.93487	0.93688	0.94242			
0.980	0.47	0.01656			0.85528	0.84894	0.84846	0.85309	0.86215	
0.970	0.71	0.02486				0.77100	0.76262	0.76038	0.76414	0.77361
0.960	0.95	0.03314					0.69061	0.68140	0.67849	0.68214
0.950	1.19	0.04142						0.61652	0.60739	0.60486
0.940	1.42	0.04970							0.54942	0.54132
0.930	1.66	0.05798							0.50234	0.48953

R/r	β_1	m / 2b/r	11	10	9	8	7	6	5	4
0.960	0.95	0.03314	0.68214	0.69244						
0.950	1.19	0.04142	0.60486	0.60943	0.62154					
0.940	1.42	0.04970	0.54132	0.54019	0.54681	0.56201				
0.930	1.66	0.05798	0.48953	0.48333	0.48466	0.49459				
0.920	1.90	0.06628	0.44733	0.43683	0.43344	0.43834	0.45311			
0.910	2.13	0.07456	0.41276	0.39871	0.39130	0.39171	0.40158	0.42316		

TABLE XIII (Continued)

R/r	β_1	m / 2b/r	10	9	8	7	6	5	4	3
0.90	2.37	0.08284	0.36730	0.35652	0.35306	0.35851	0.37522			
0.88	2.85	0.09942		0.30359	0.29406	0.29231	0.30049	0.32210		
0.85	3.56	0.12426			0.23618	0.22707	0.22602	0.23602	0.26252	
0.80	4.74	0.16568				0.16732	0.15761	0.15578	0.16559	0.19584
0.75	5.91	0.20710				0.13628	0.12240	0.11439	0.11503	0.13057
0.70	7.08	0.24852					0.10221	0.09108	0.08653	0.09324

R/r	β_1	m / 2b/r	4	3	2	1
0.60	9.41	0.33138	0.05815	0.05437	0.06405	0.13098
0.50	11.70	0.41422	0.04444	0.03648	0.03604	0.06958
0.40	13.96	0.49706	0.03742	0.02817	0.02415	0.03797
0.30	16.17	0.57990	0.03353	0.02373	0.01813	0.02357
0.10	20.45	0.74558	0.02820	0.01880	0.01230	0.01150
0.05	21.48	0.78700			0.01140	0.00920
0.00	22.50	0.82842		0.01813	0.01110	0.00900

TABLE XIV - λ_{CR} of a Multi-spot Shell (N = 8, r/L = 1.0, r/h = 100, ν = 0.3)

R/r	β_1	m / 2b/r	6	5	4	3	2	1
0.99	0.24	0.00828	1.00012	0.99855	0.98800	1.01010		
0.98	0.47	0.01656	0.99162	0.97774	0.97072	0.99374		
0.97	0.71	0.02486	0.97947	0.95567	0.95045	0.97397		
0.96	0.95	0.03314	0.96670	0.93333	0.92786	0.95202		
0.95	1.19	0.04142	0.95355	0.91112	0.90362	0.92828		
0.92	1.90	0.06628		0.84701	0.82723	0.84957		
0.90	2.37	0.08284		0.80781	0.77726	0.79448	0.82128	
0.85	3.56	0.12426		0.72459	0.66706	0.66371	0.69868	
0.82	4.26	0.14912		0.68421	0.61293	0.59563	0.62848	
0.80	4.74	0.16568		0.66069	0.58143	0.55522	0.58460	0.84207
0.75	5.91	0.20710		-	-	0.47149	0.48837	0.75081
0.70	7.08	0.24852		0.57437	0.46849	0.40814	0.41117	0.66526
0.65	8.25	0.28994			-	0.36028	0.35123	0.58871

TABLE XIV (Continued)

R/r	β_1	m 2b/r	6	5	4	3	2	1
0.60	9.41	0.33138			0.40262	0.32388	0.30493	0.51725
0.55	10.56	0.37280				0.29598	0.26947	0.41498
0.50	11.70	0.41422			0.36192	0.27422	0.24218	0.33260
0.45	12.83	0.45564				0.25764	0.22111	0.26631
0.40	13.96	0.49706			0.33710	0.24457	0.19867	0.21327
0.35	15.07	0.53848				0.23049	0.17531	0.17151
0.30	16.17	0.57990				0.21703	0.15513	0.14007
0.25	17.26	0.62132				0.20536	0.13856	0.11788
0.20	18.33	0.66274				0.19550	0.12575	0.10355
0.15	19.40	0.70416				0.18780	0.11727	0.09560
0.10	20.45	0.74558				0.18330	0.11300	0.09190
0.00	22.50	0.82842				0.18142	0.11117	0.09015

TABLE XV - λ_{CR} of an N-sided Regular Polygonal Shell (r/L = 1.0, r/h = 1000, ν = 0.3)

N	β_1	m / 2b/r	1	2	3	4	5	6	λ^*_{CR}	m*
3	60.00	3.46410	0.00175	0.00622	0.01367				0.00175	1
4	45.00	2.00000	0.00233	0.00674	0.01419				0.00233	1
8	22.50	1.20711	0.00900	0.01110	0.01813				0.00902	1
10	18.00	0.64984	0.01690	0.01511	0.02141				0.01514	2
15	12.00	0.42512	0.06481	0.03426	0.03518	0.04333			0.03393	2
20	9.00	0.31676	0.17955	0.07271	0.05960	0.06277	0.07294		0.05968	3
25	7.20	0.25266		0.14522	0.10135	0.09384	0.09895	0.11085	0.09358	4
30	6.00	0.21020			0.16600	0.13928	0.13551	0.14258	0.13552	5
		m / 2b/r	5	6	7	8	9	10	λ^*_{CR}	m*
40	4.50	0.15740	0.25519	0.24188	0.24334	0.25412			0.24189	6
50	3.60	0.12582		0.40785	0.38338	0.37725	0.38312	0.39751	0.37729	8
60	3.00	0.10482			0.59747	0.56070	0.54554	0.54490	0.54491	10
70	2.57	0.08982				0.79038	0.75892	0.74152	0.74052	11
75	2.40	0.08382					0.84278	0.82470	0.85013	12

*These terms are obtained by considering each side of the polygonal shell as a simply-supported panel.

TABLE XV (Continued)

N	β_1	m / 2b/r	11	12	13	14	15	16	λ^*_{CR}	m*
60	3.00	0.10482	0.55476						0.54491	10
70	2.57	0.08982	0.73633	0.74160					0.74052	11
75	2.40	0.08382	0.81618	0.81628	0.82373	0.83703			0.85013	12
80	2.25	0.07858	0.87572	0.87258	0.87522	0.88269			0.96781	13
85	2.12	0.07396	0.91769	0.91313	0.91300	0.91633				
90	2.00	0.06984		0.94145	0.93976	0.94073	0.94396			
100	1.80	0.06286			0.97130	0.97038	0.97075	0.97223		

*These terms are obtained by considering each side of the polygonal shell as a simply-supported panel.

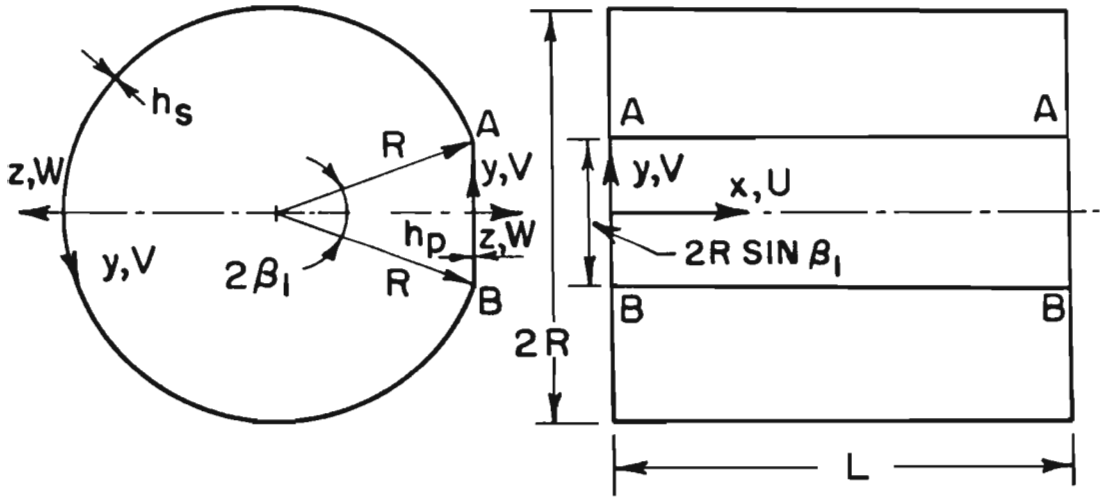

FIG. 1 A SINGLE FLAT SPOT SHELL

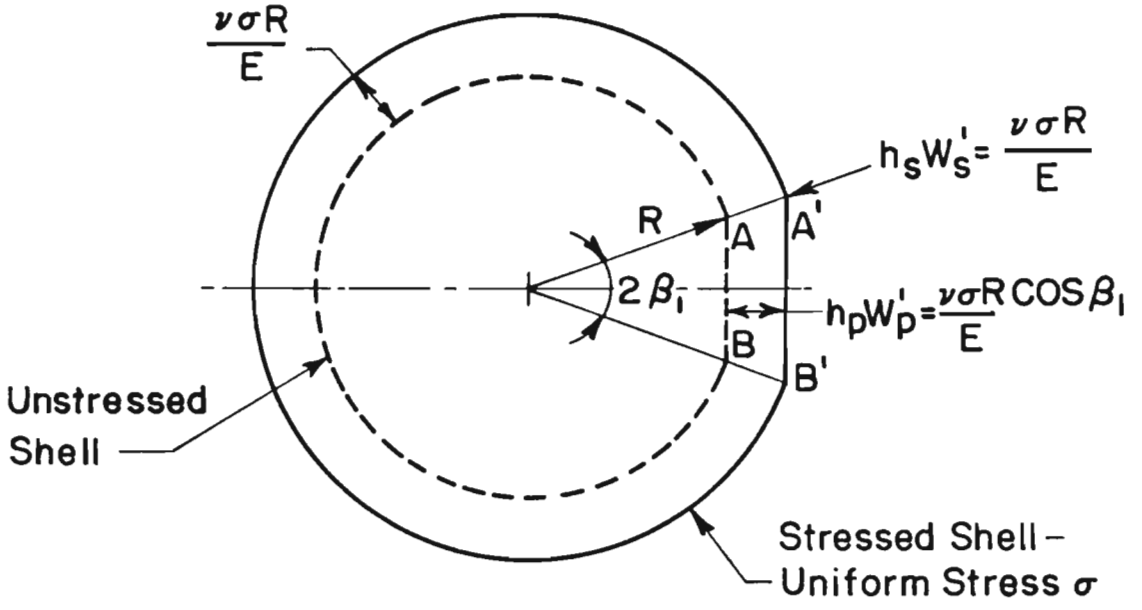

FIG. 1a PREBUCKLING DEFORMATION

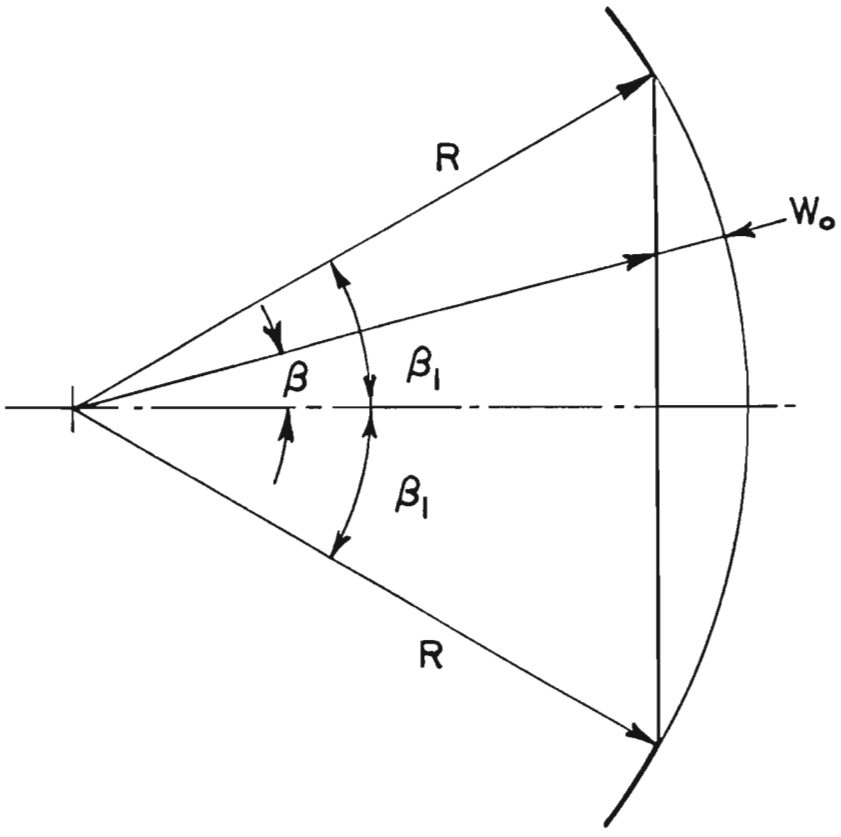

$$W_o = R\left(1 - \frac{\cos\beta_1}{\cos\beta}\right) \qquad -\beta_1 \leq \beta \leq \beta$$

$$= 0 \qquad |\beta| \geq \beta_1$$

FIG. 2 FLAT SPOT AS AN IMPERFECTION ON A PERFECT CIRCULAR CYLINDRICAL SHELL

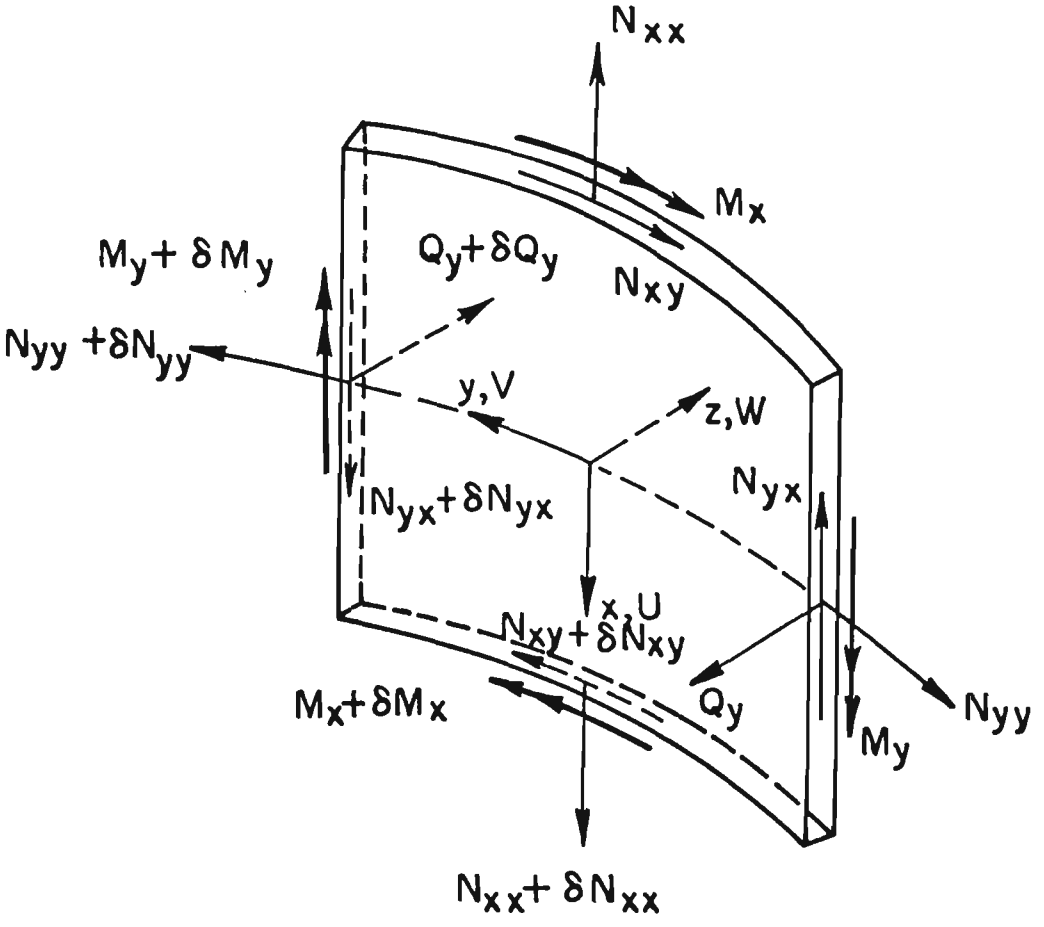

FIG. 3 AN ELEMENT OF CYLINDRICAL SHELL

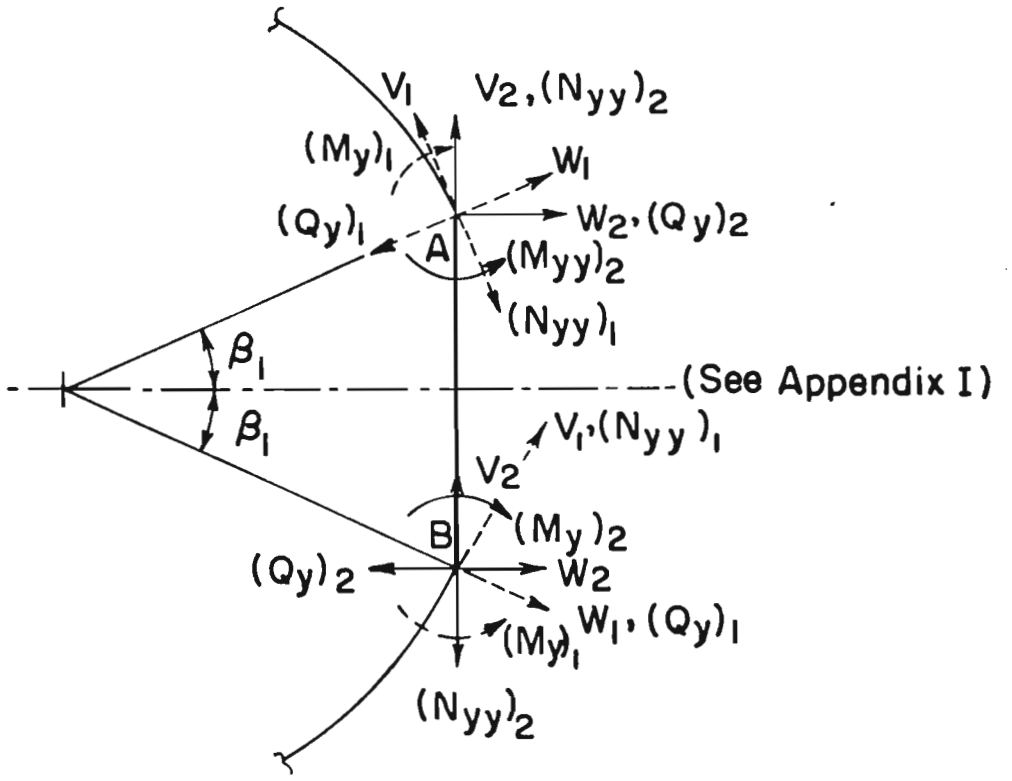

FIG. 4a MATCHING CONDITIONS IN SINGLE FLAT SPOT SHELLS

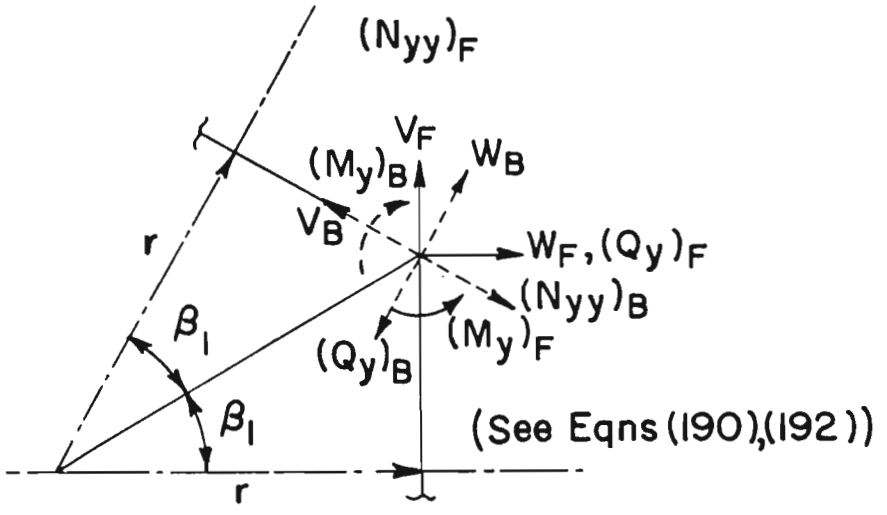

FIG. 4b MATCHING CONDITIONS IN POLYGONAL SHELLS

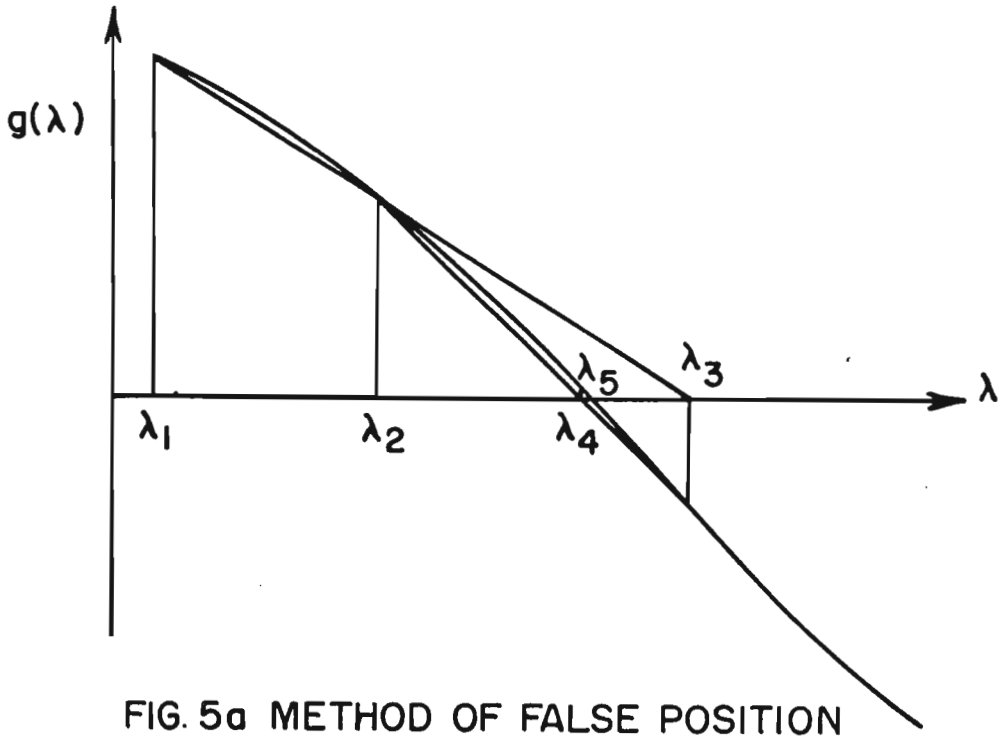

FIG. 5a METHOD OF FALSE POSITION

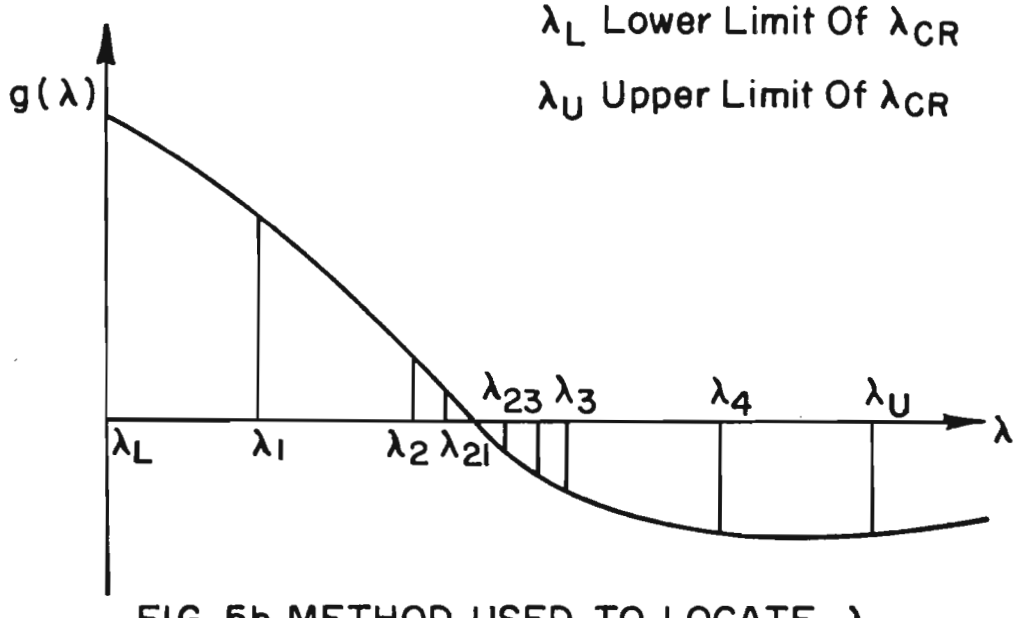

FIG. 5b METHOD USED TO LOCATE λ_{CR}

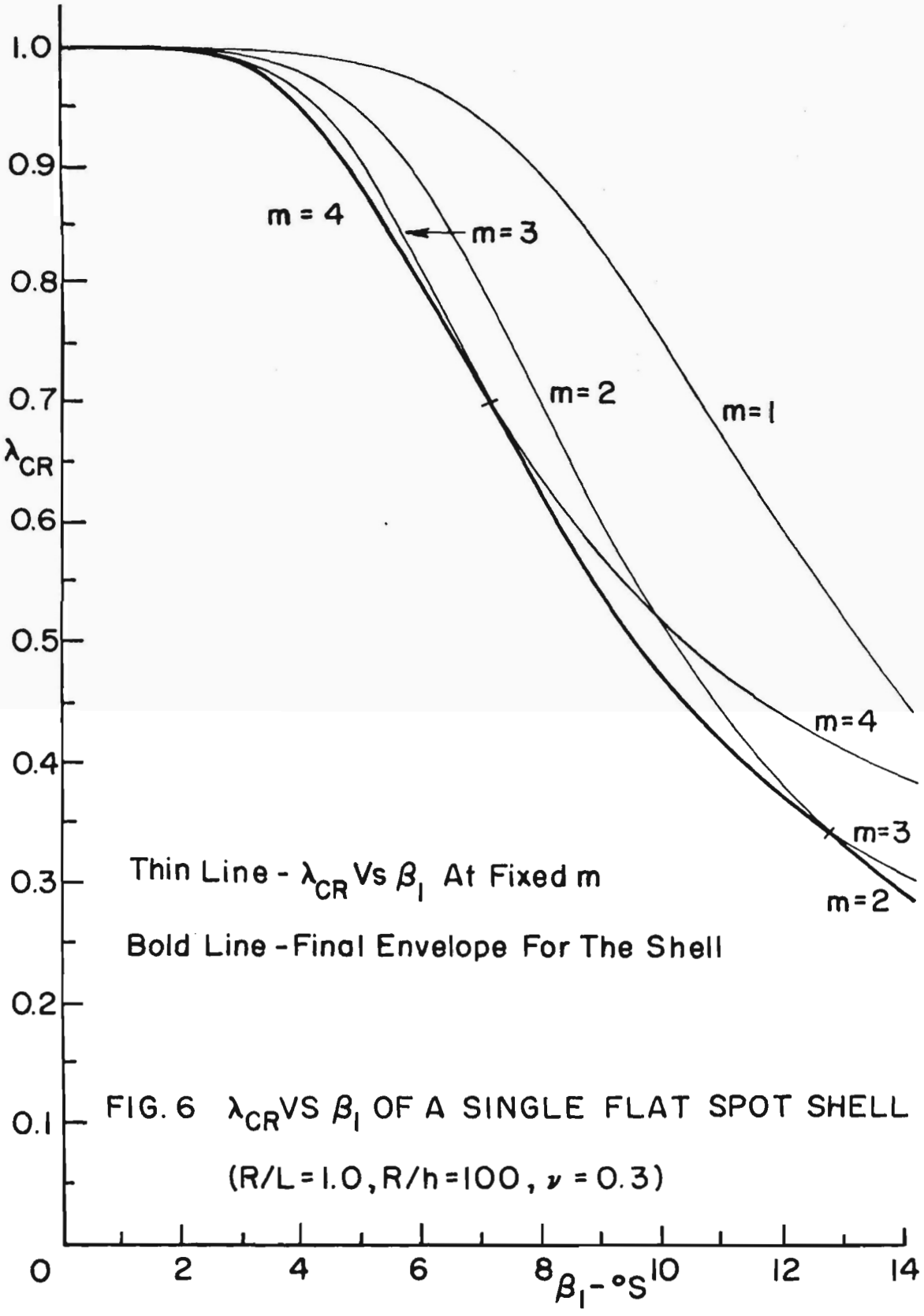

FIG. 6 λ_{CR} VS β_1 OF A SINGLE FLAT SPOT SHELL

(R/L = 1.0, R/h = 100, ν = 0.3)

FIG. 7 λ_{CR} VS HALF OF THE ANGLE OF FLAT SPOT

R/h = 1000, R/L = 0.25

$\upsilon = 0.3$

$\lambda_{CR} = \sigma_{CR}/\sigma_{CL}$ (R, h)

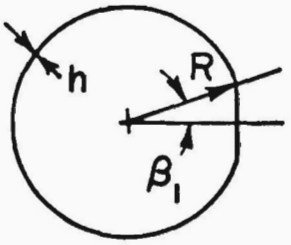

FIG. 8 λ_{CR} VS HALF OF THE ANGLE OF FLAT SPOT

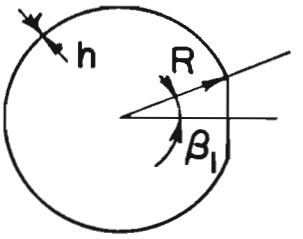

$R/h = 1000$, $R/L = 1.0$

$\nu = 0.3$

$\lambda_{CR} = \sigma_{CR} / \sigma_{CL}(R,h)$

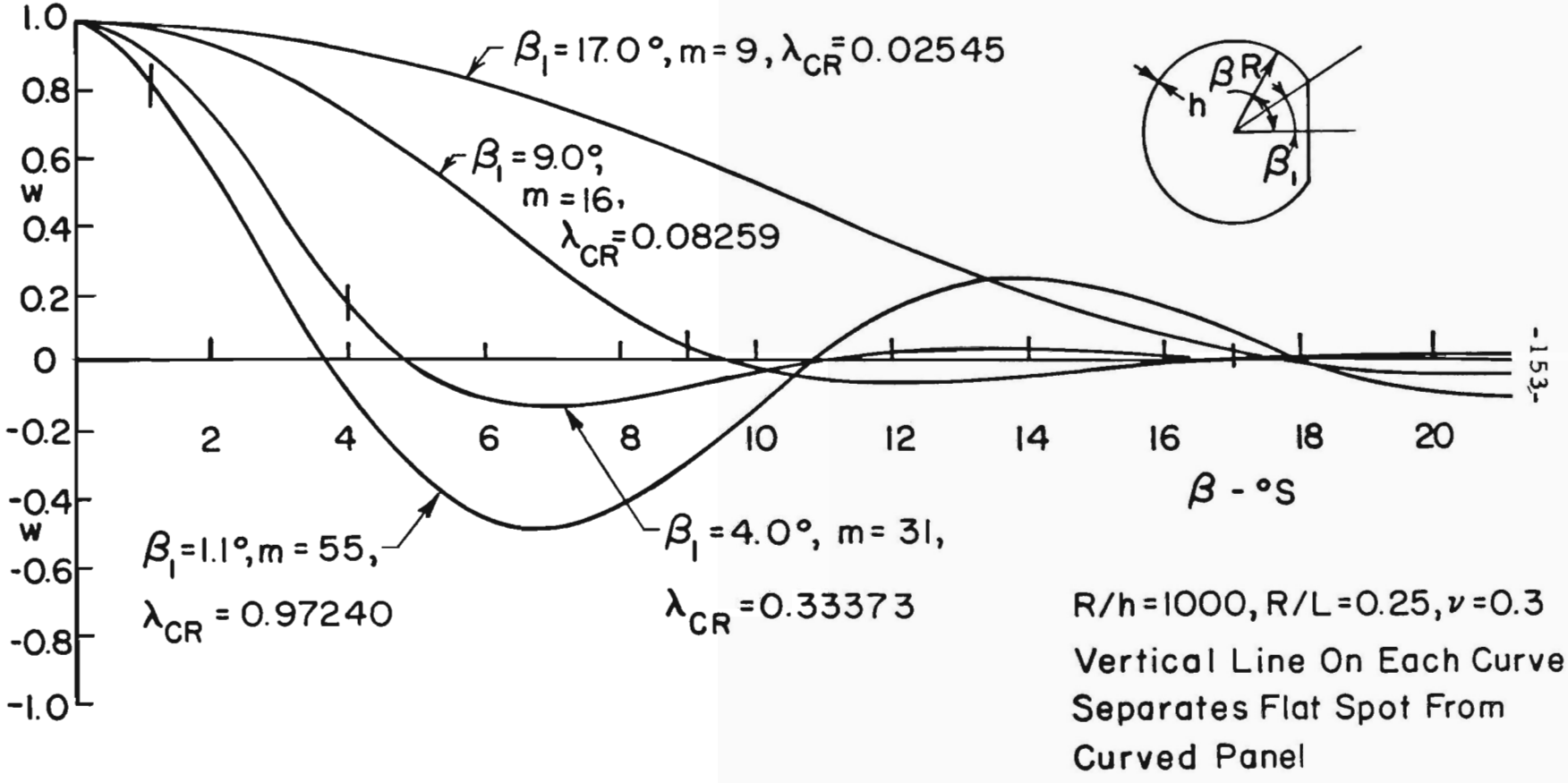

FIG.9 W-DISPLACEMENT FOR A SINGLE SPOT SHELL
(EFFECT OF VARYING FLAT SPOT WIDTH)

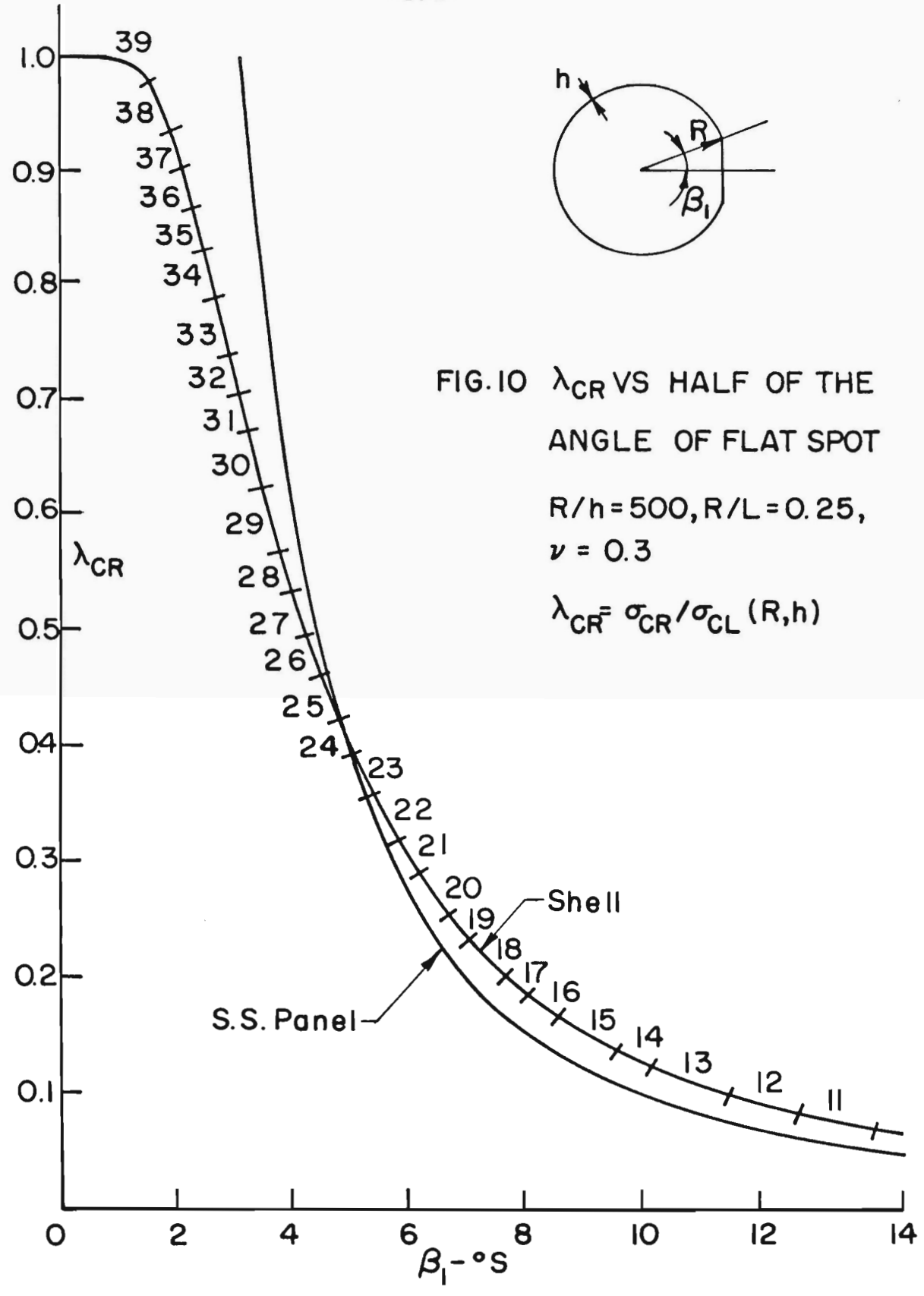

FIG. 10 λ_{CR} VS HALF OF THE ANGLE OF FLAT SPOT

$R/h = 500, R/L = 0.25,$
$\nu = 0.3$

$\lambda_{CR} = \sigma_{CR}/\sigma_{CL}(R,h)$

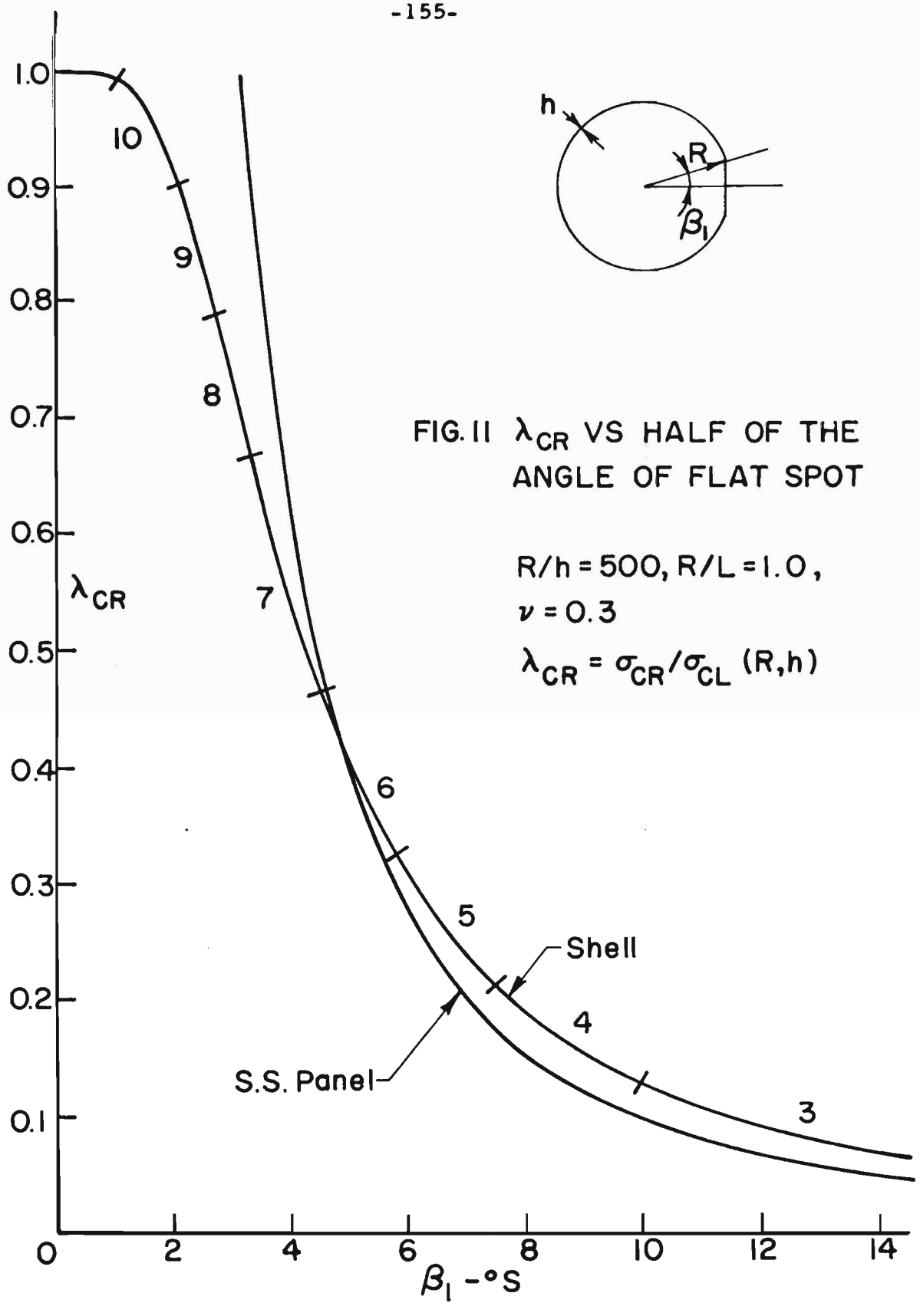

FIG. 11 λ_{CR} VS HALF OF THE ANGLE OF FLAT SPOT

$R/h = 500, R/L = 1.0,$
$\nu = 0.3$
$\lambda_{CR} = \sigma_{CR}/\sigma_{CL}\ (R,h)$

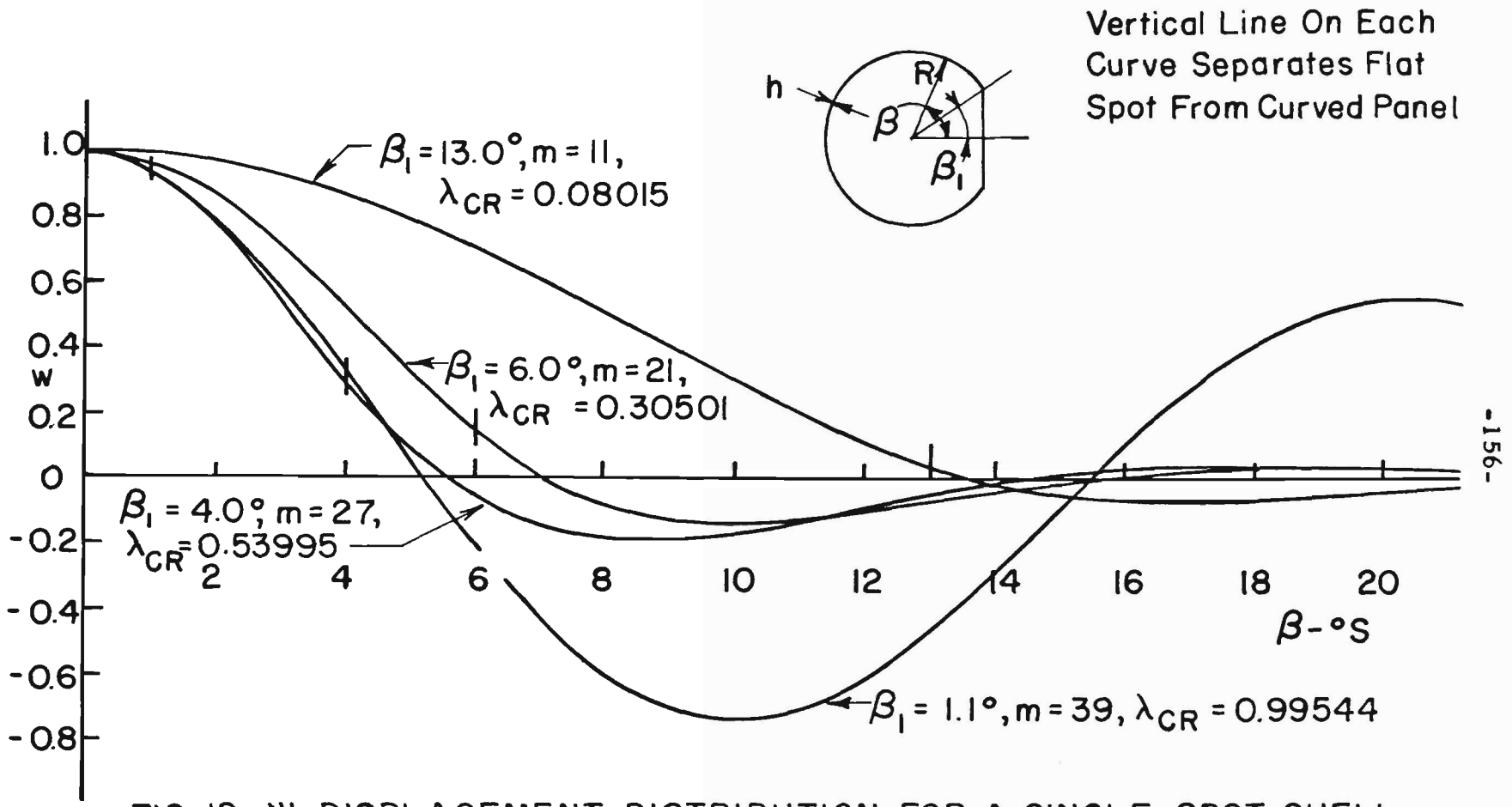

FIG. 12 W-DISPLACEMENT DISTRIBUTION FOR A SINGLE SPOT SHELL
(EFFECT OF VARYING FLAT SPOT WIDTH)
$R/h = 500$, $R/L = 0.25$, $\nu = 0.3$ $\quad \lambda_{CR} = \sigma_{CR} / \sigma_{CL}(R,h)$

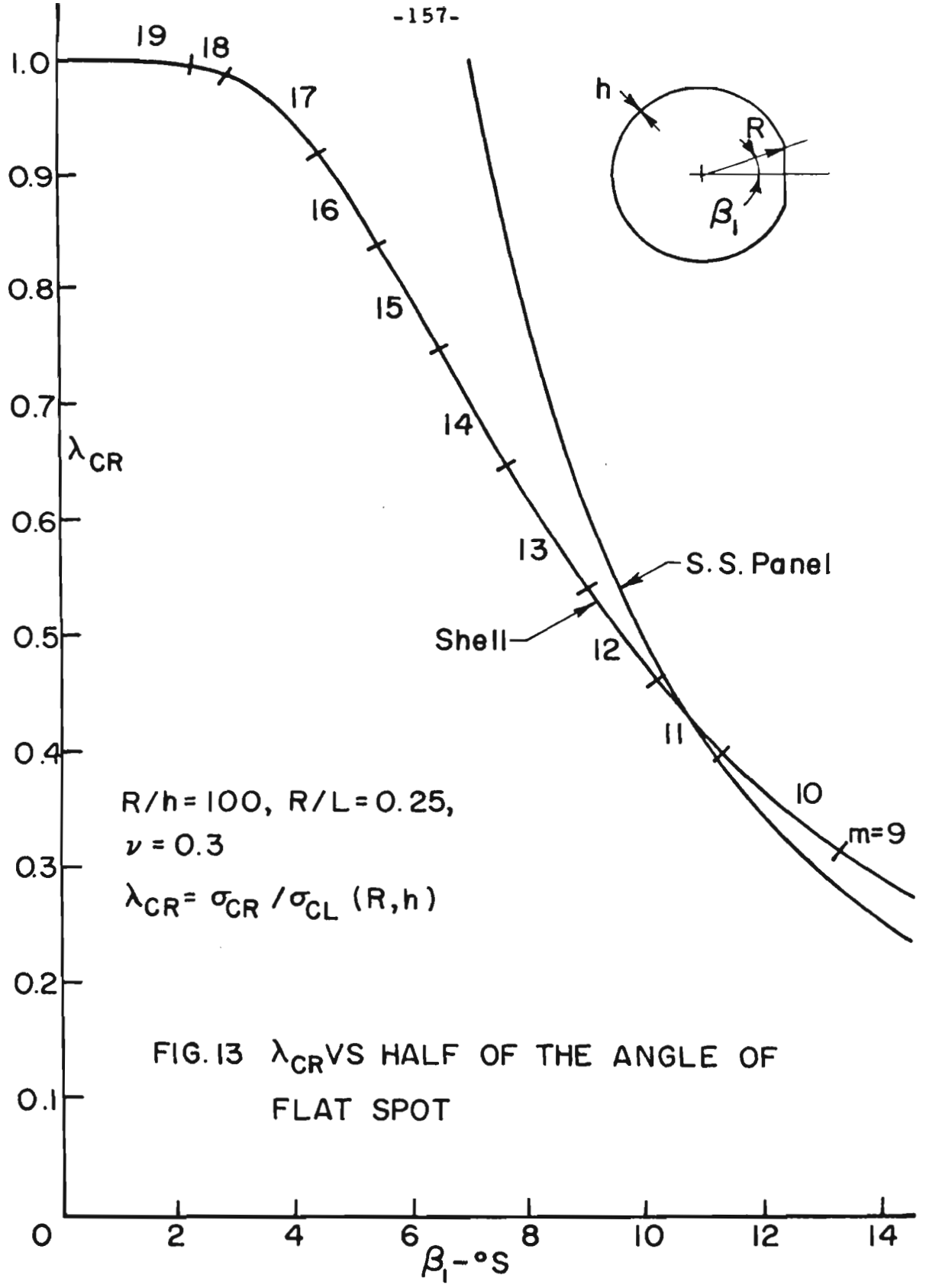

FIG. 13 λ_{CR} VS HALF OF THE ANGLE OF FLAT SPOT

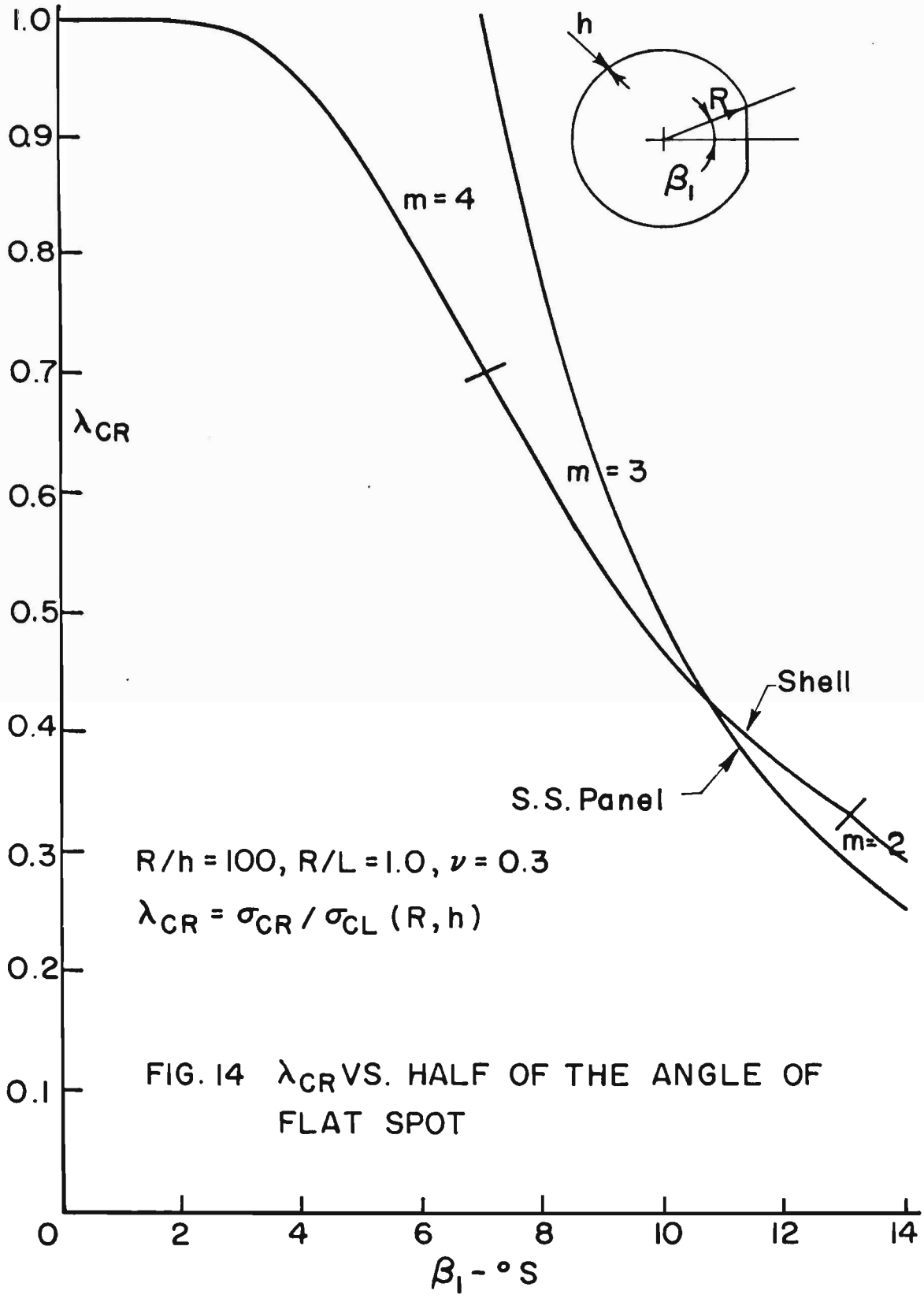

FIG. 14 λ_{CR} VS. HALF OF THE ANGLE OF FLAT SPOT

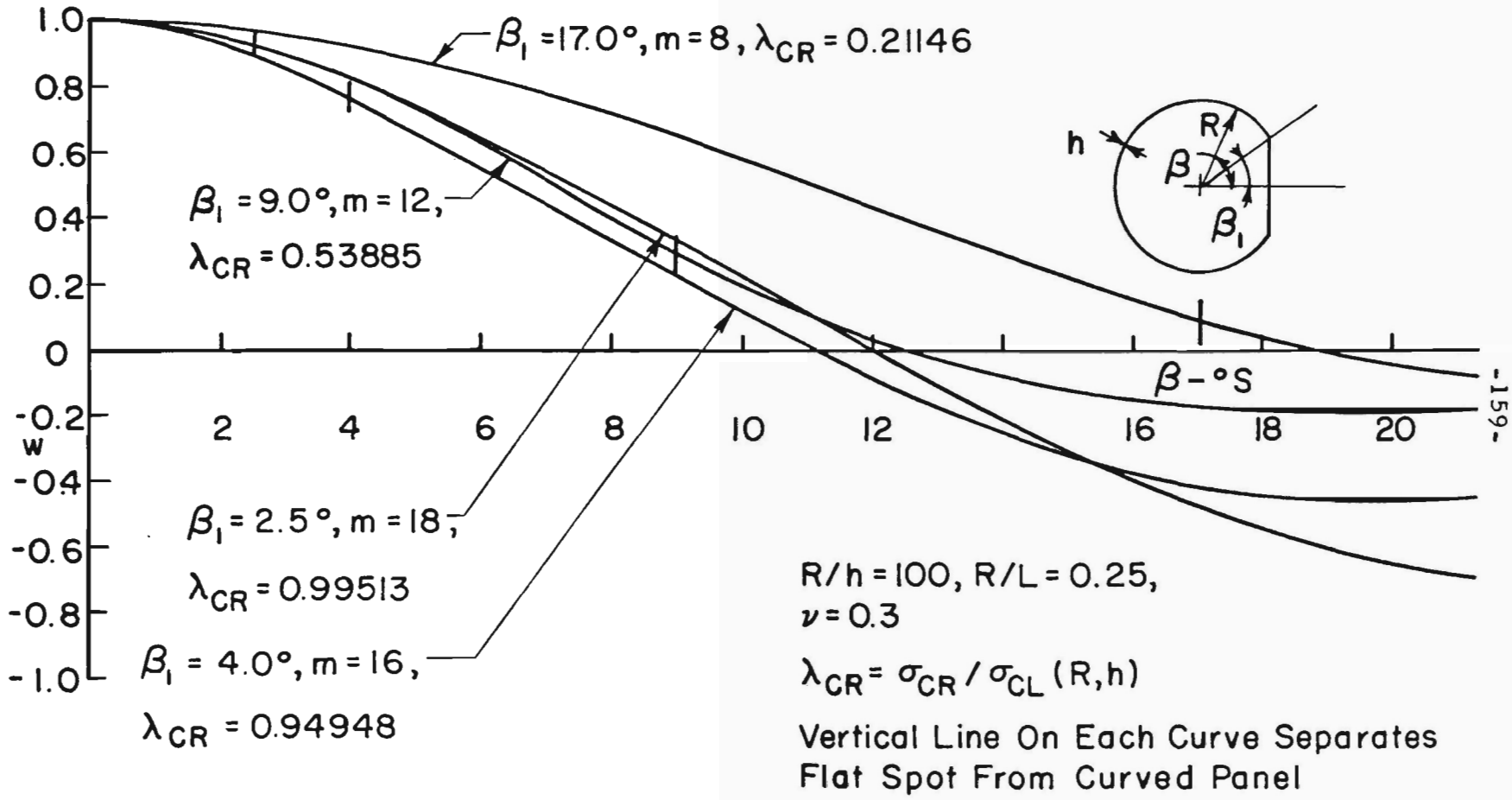

FIG. 15 W-DISPLACEMENT DISTRIBUTION FOR A SINGLE FLAT SPOT SHELL (EFFECT OF VARYING FLAT SPOT WIDTH)

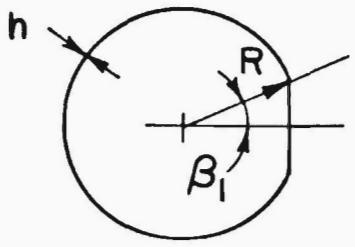

FIG. 16 λ_{CR} VS HALF OF THE ANGLE OF FLAT SPOT

$R/h = 100$, $R/L = 1.0$, $\nu = 0.3$

$\lambda_{CR} = \sigma_{CR} / \sigma_{CL}(R,h)$

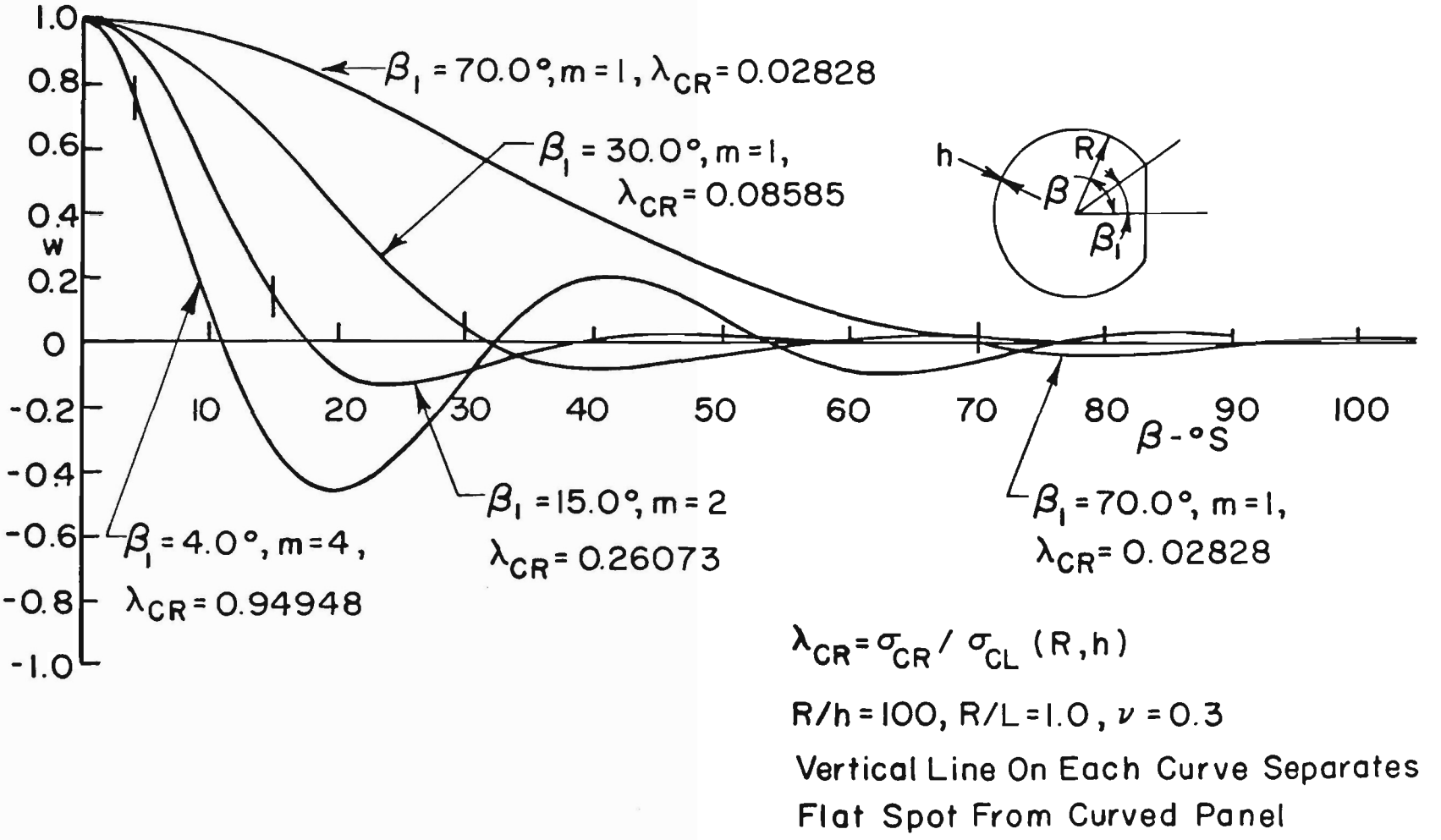

$\lambda_{CR} = \sigma_{CR} / \sigma_{CL}\ (R, h)$

$R/h = 100,\ R/L = 1.0,\ \nu = 0.3$

Vertical Line On Each Curve Separates Flat Spot From Curved Panel

FIG.17 W-DISPLACEMENT DISTRIBUTION FOR A SINGLE FLAT SPOT SHELL (EFFECT OF VARYING FLAT SPOT WIDTH - LARGE FLAT SPOTS)

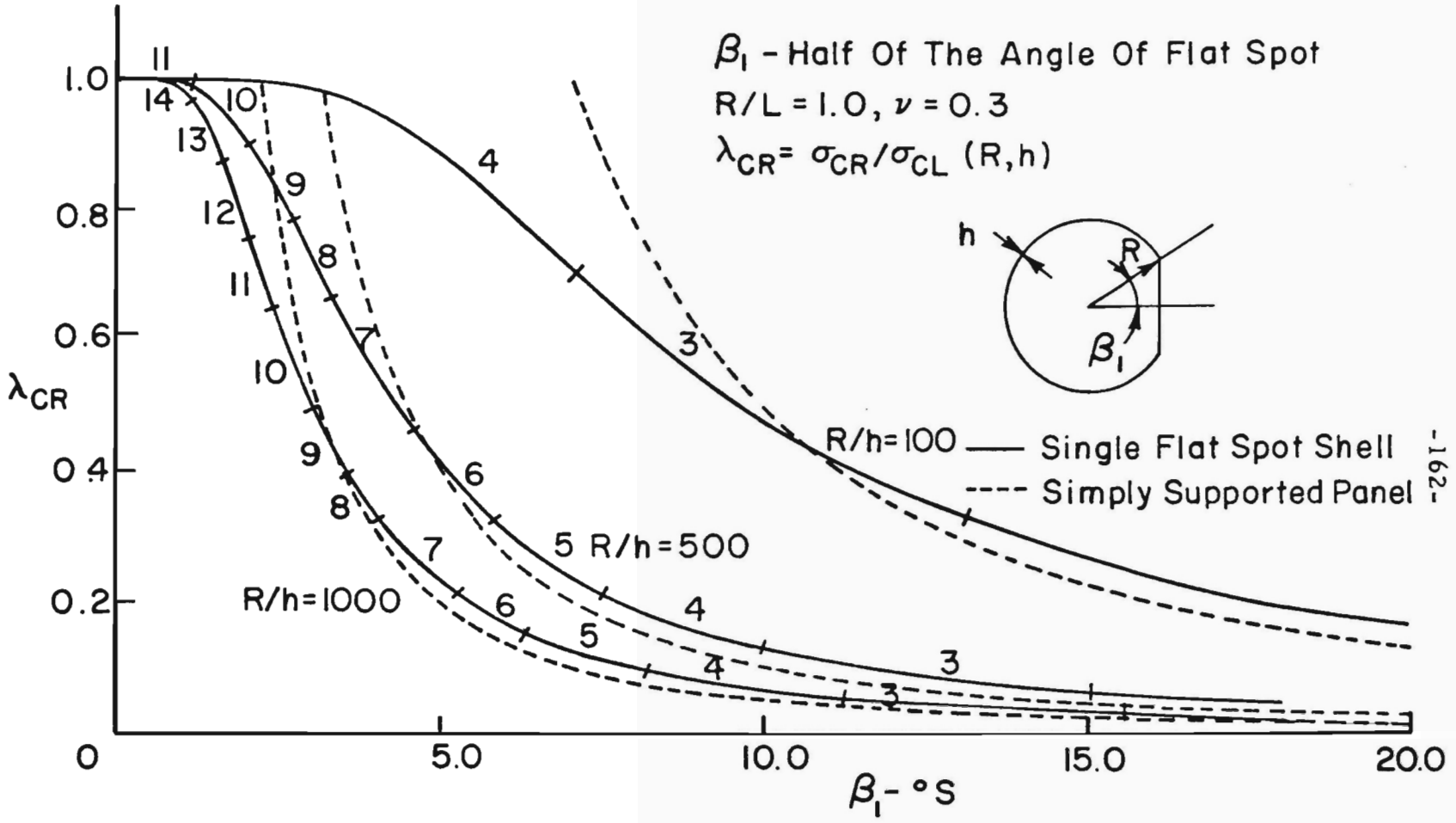

FIG. 18 EFFECT OF THICKNESS RATIO ON THE BUCKLING LOAD OF A SINGLE FLAT SPOT SHELL

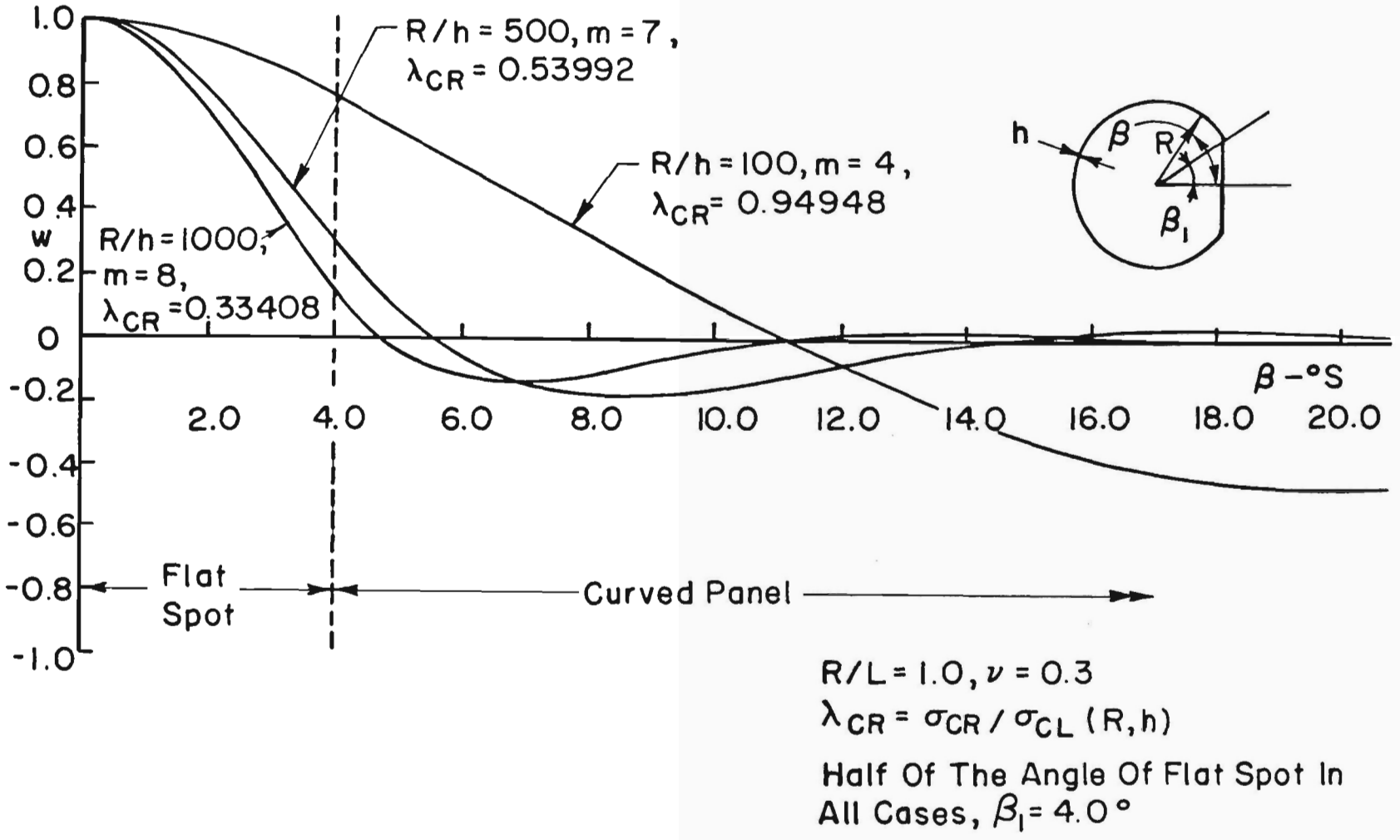

FIG.19 EFFECT OF THICKNESS ON λ_{CR} AND CORRESPONDING W-DISPLACEMENT DISTRIBUTION

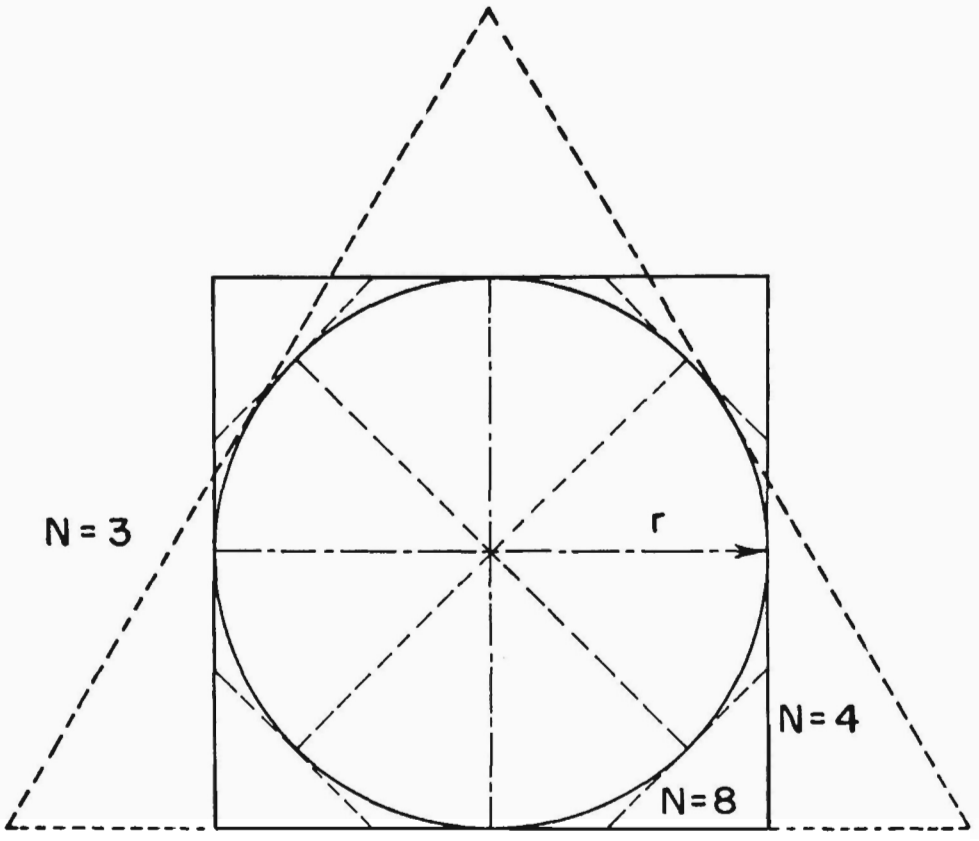

Fixed Radius R Of The Curved Panels (Here R=0), But Varying N

Fixed Number Of Panels Of Each Kind (Here N=4), But Varying Radius Of Curved Panels

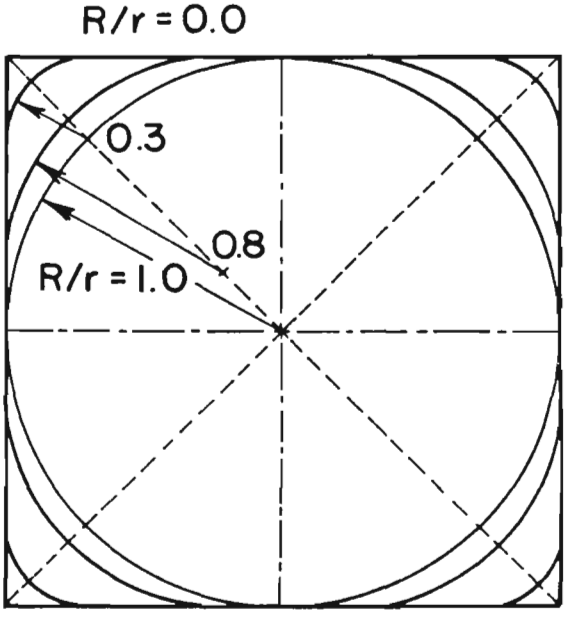

FIG. 20 SOME OF THE APPROXIMATIONS TO A CIRCULAR SHELL

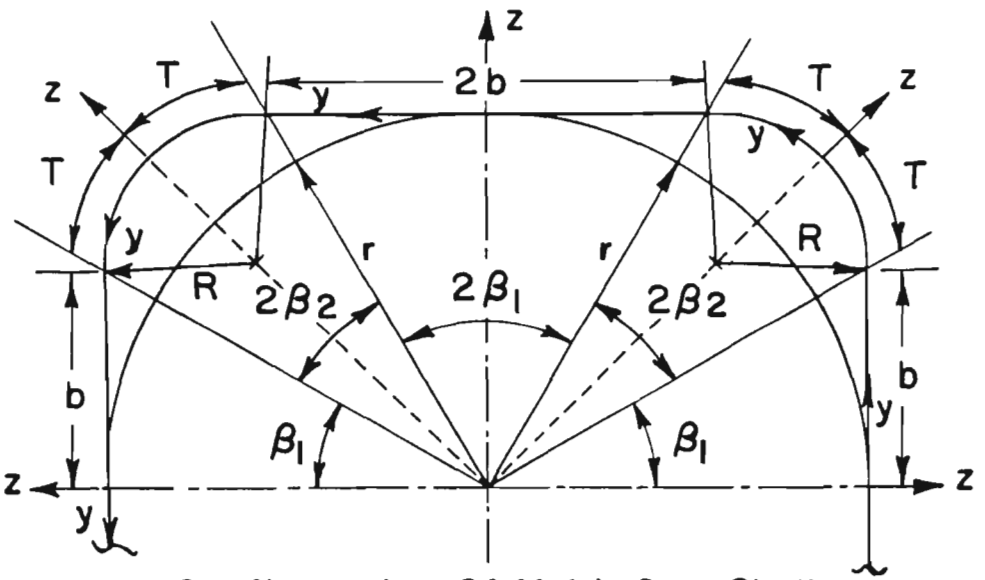

Configuration Of Multi-Spot Shell

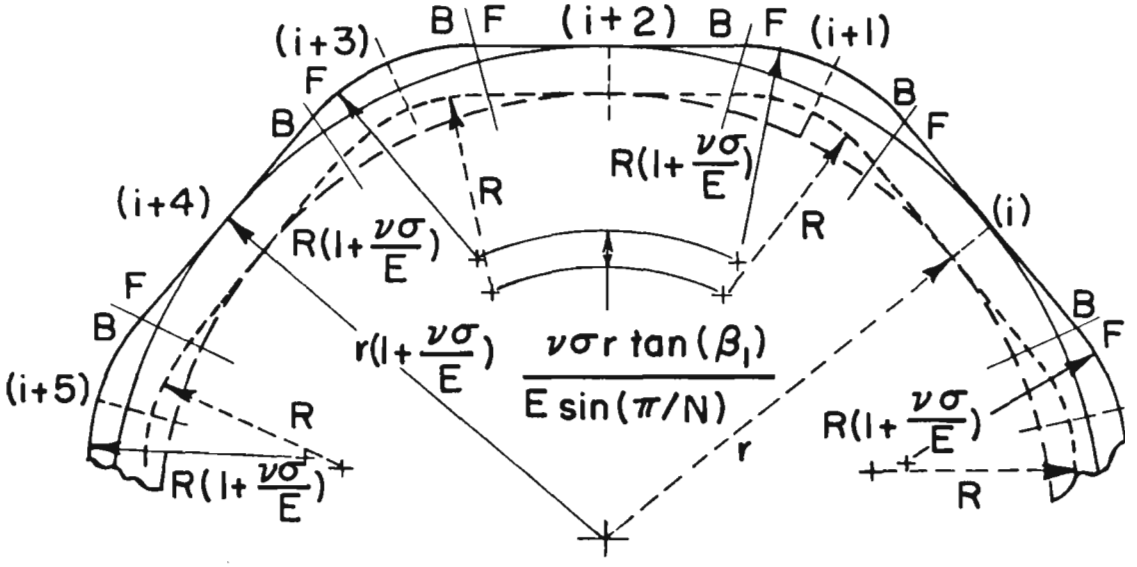

------ Unstressed State

——— Stressed State(Uniform Axial Comp. Stress = σ)

Prebuckling Solution

FIG. 21a

-·——·——Line Of Symmetry

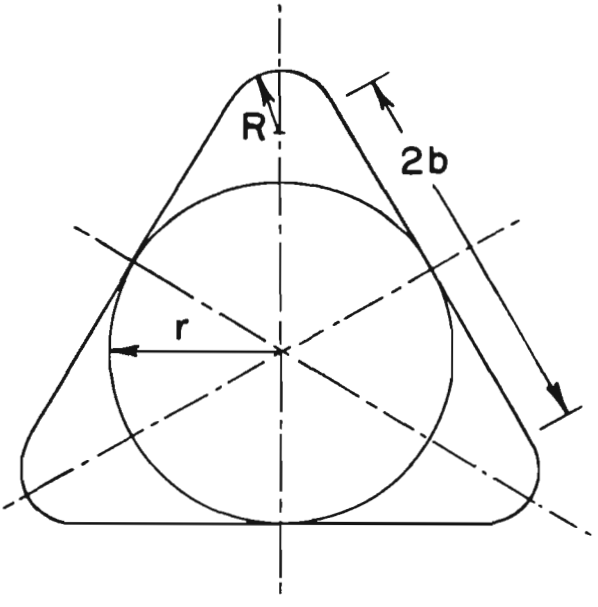

No. Of Panels Of Each Kind = 3
No. Of Lines Of Symmetry = 3

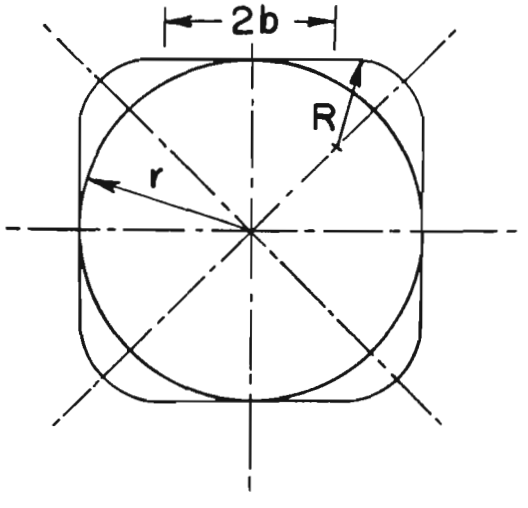

No. Of Panels Of Each Kind = 4
No. Of Lines Of Symmetry = 4

FIG. 21b LINES OF SYMMETRY OF MULTI-SPOT SHELLS

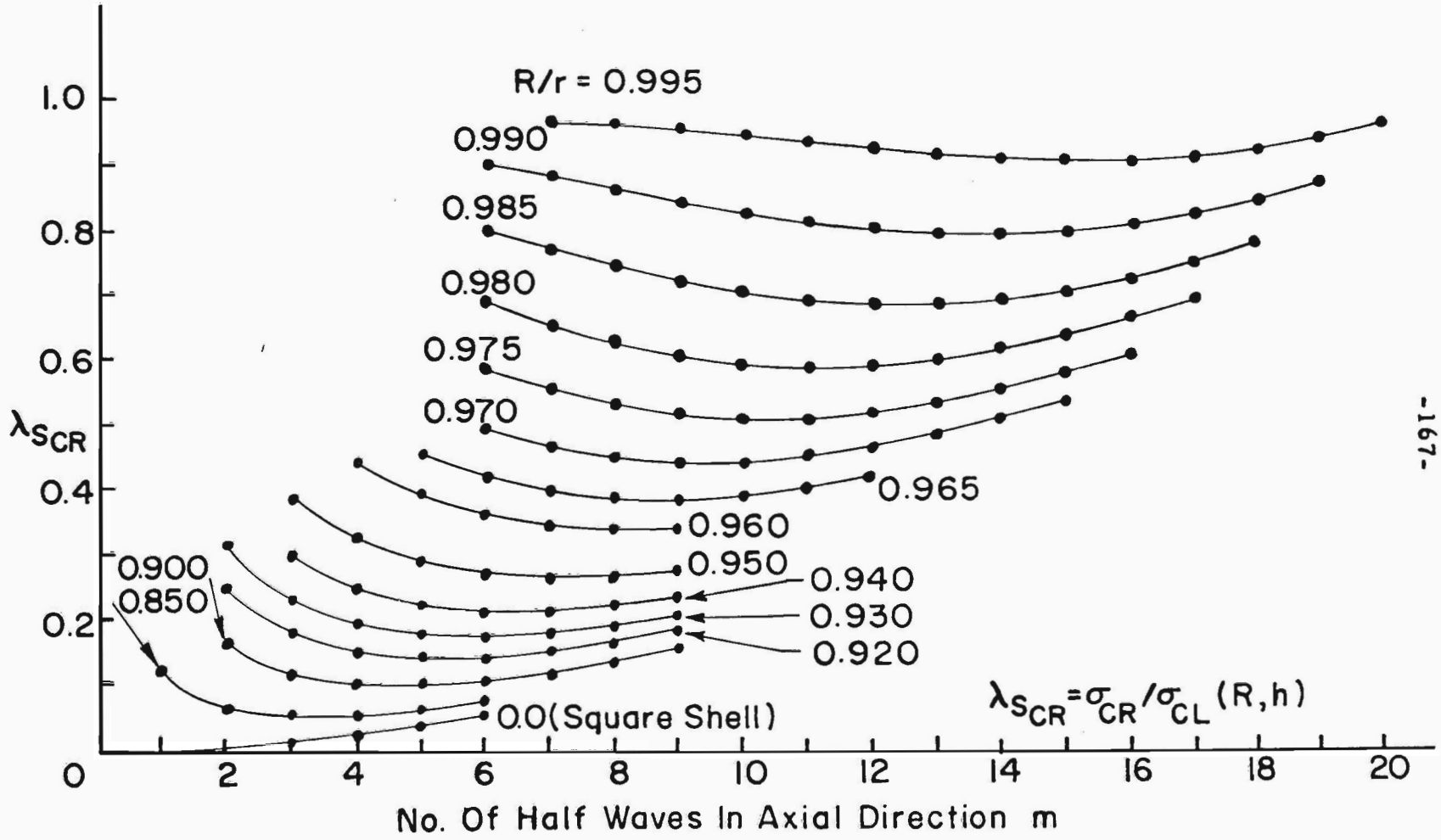

FIG. 22 A TYPICAL DATA SET FOR MULTI-SPOT SHELLS
(FOR N = 4, R/L = 1.0, R/h = 1000, ν = 0.3)

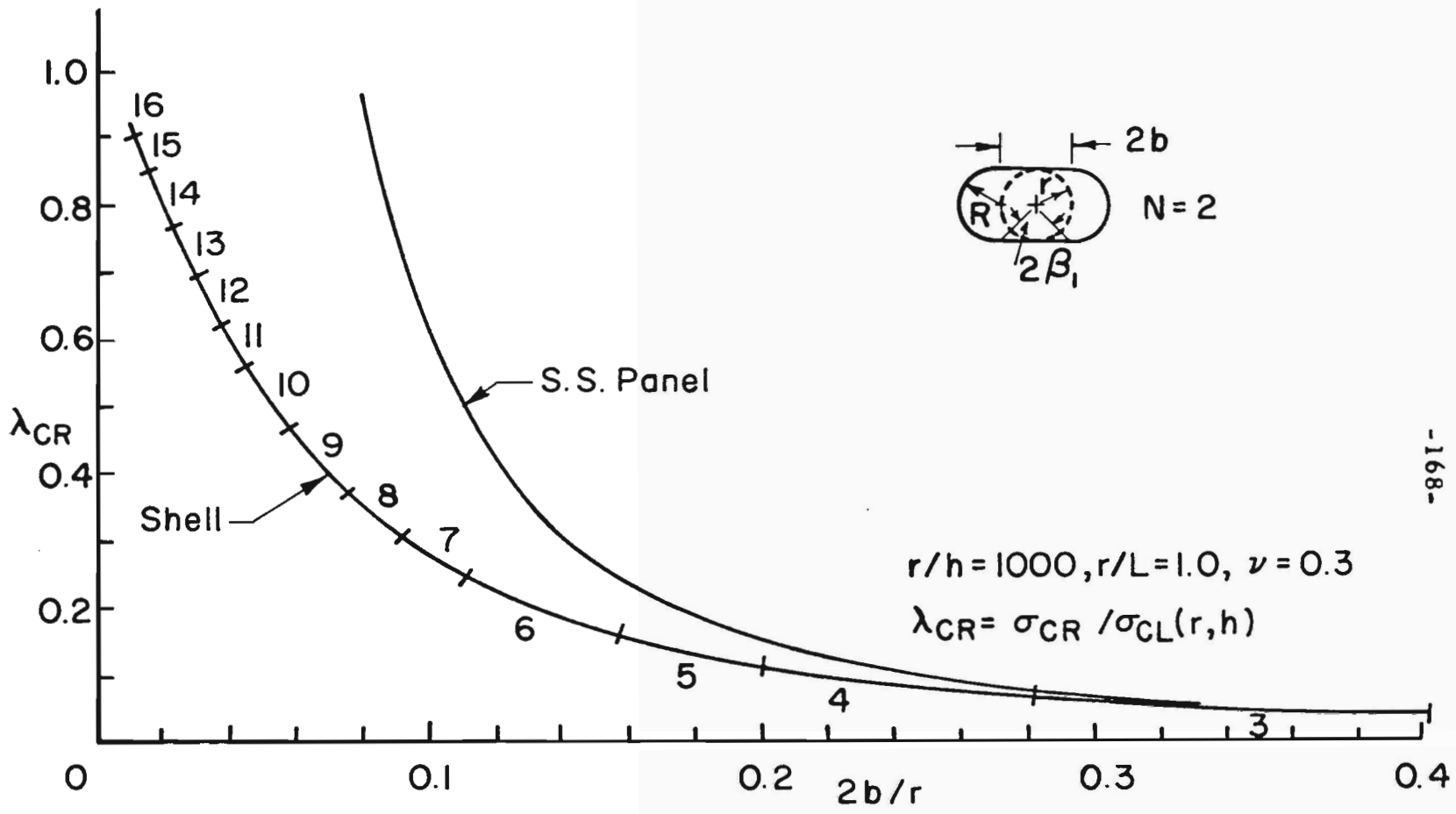

FIG. 23 λ_{CR} VS WIDTH OF FLAT PANELS - NO. OF PANELS OF EACH KIND = 2

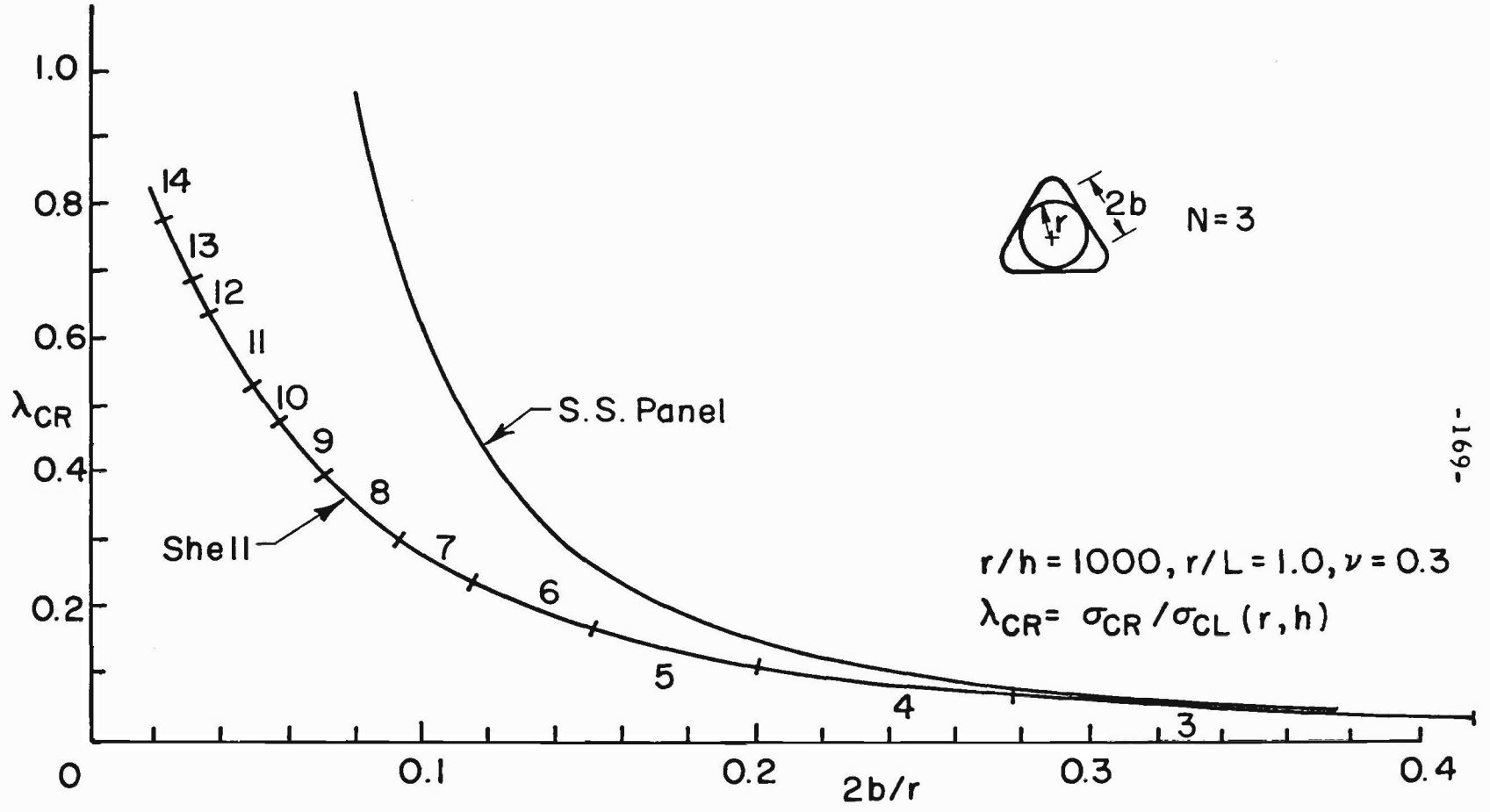

FIG. 24 λ_{CR} VS WIDTH OF FLAT PANELS–NO. OF PANELS OF EACH KIND = 3

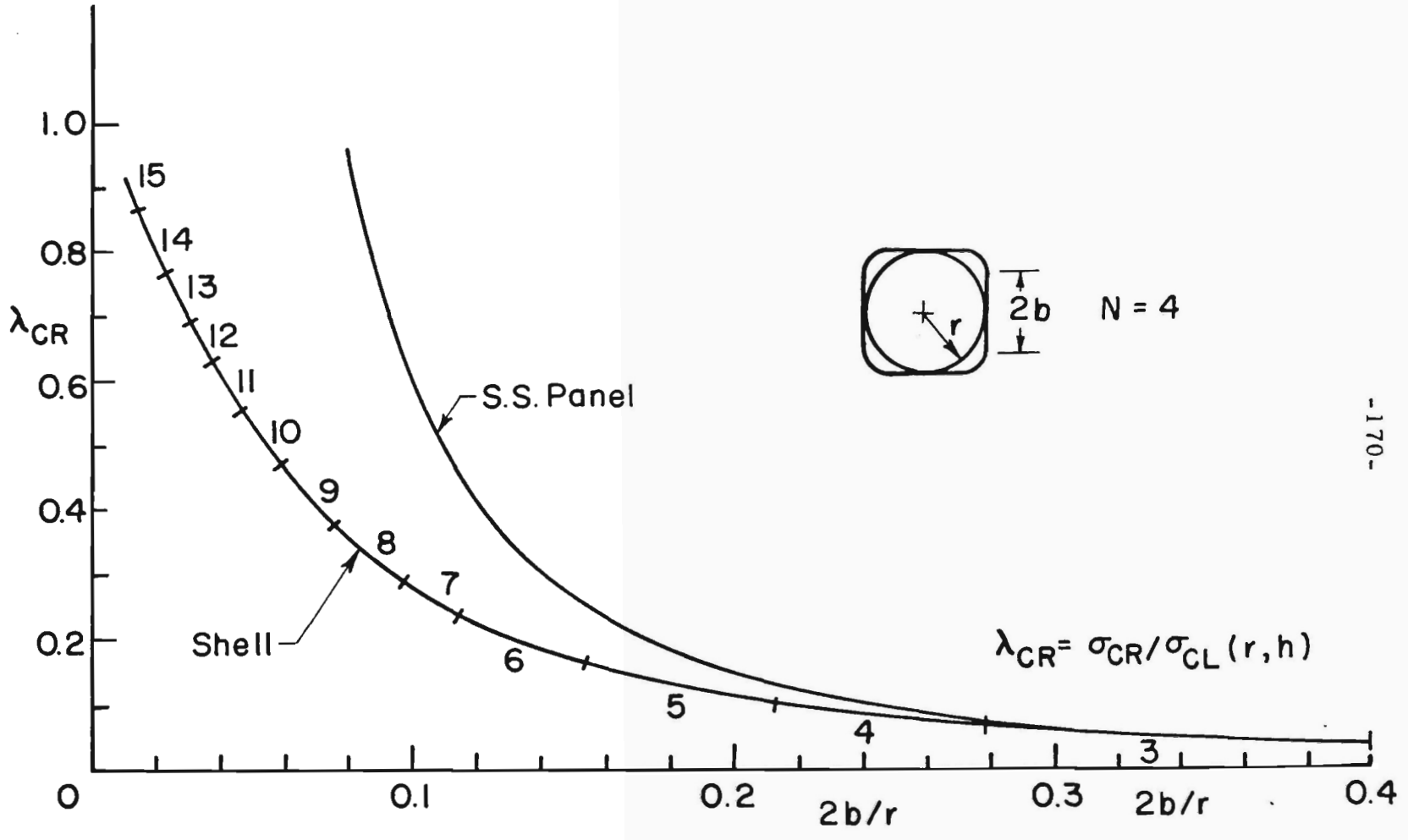

FIG. 25 λ_{CR} VS WIDTH OF FLAT PANELS - NO. OF PANELS OF EACH KIND = 4 - $r/h = 1000$, $r/L = 1.0$, $\nu = 0.3$

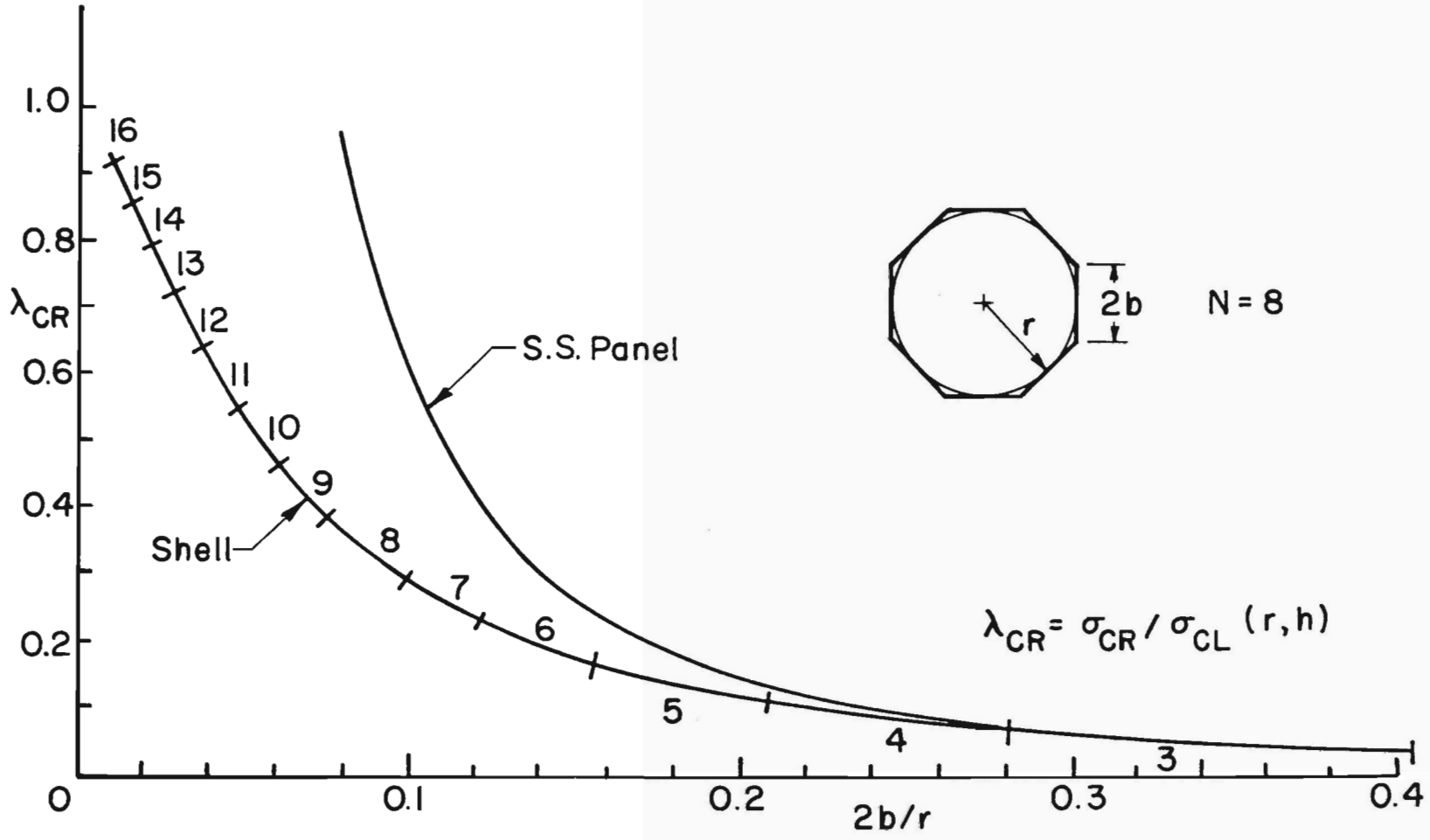

FIG. 26 λ_{CR} VS WIDTH OF FLAT PANELS - NO. OF PANELS OF EACH KIND = 8 — r/h = 1000, r/L = 1.0, ν = 0.3

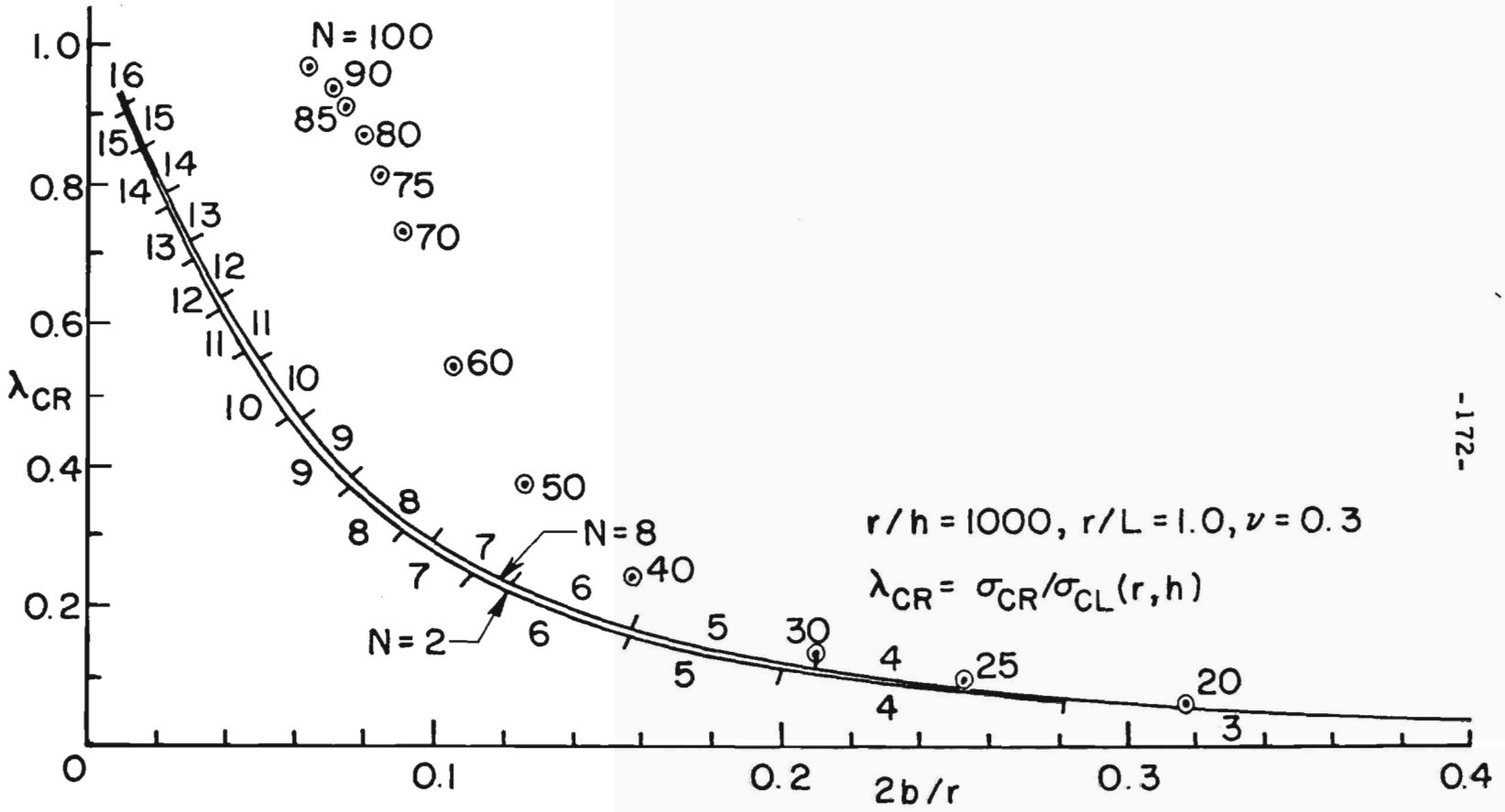

FIG. 27 λ_{CR} VS WIDTH OF FLAT SPOT FOR N-SPOT SHELLS
(CIRCLED POINTS FOR SHELL MADE UP OF FLAT PANELS ONLY)

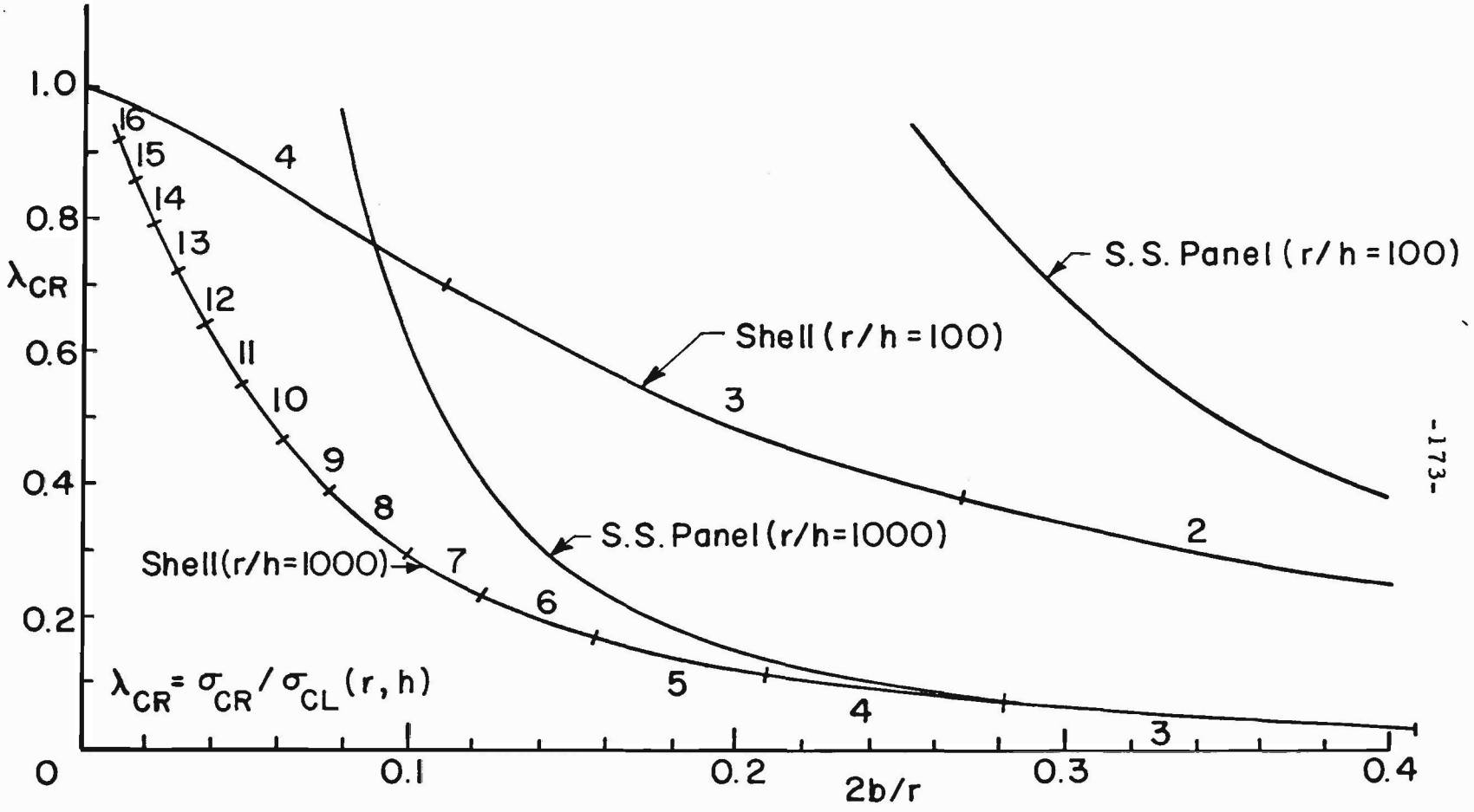

FIG. 28 EFFECT OF THICKNESS VARIATION ON BUCKLING LOAD OF A MULTIPLE FLAT SPOT SHELL - NO. OF PANELS OF EACH KIND = 8 - r/L = 1.0, ν = 0.3

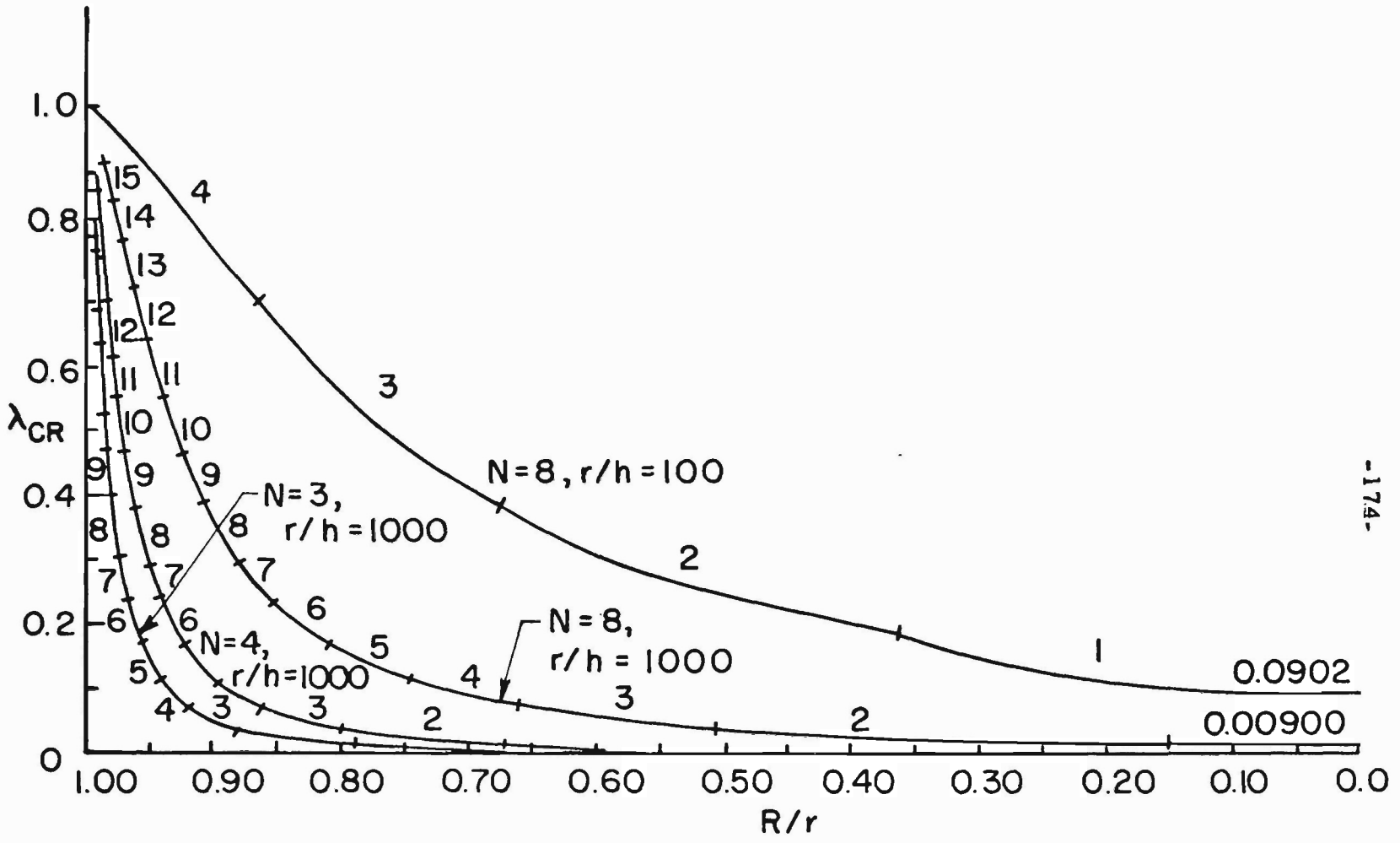

FIG. 29 λ_{CR} VS RADIUS OF CURVED PANELS OF MULTI-SPOT SHELLS
R = Radius Of Curved Panel, r = Radius Of Inscribed Circle
$r/L = 1.0$, $\nu = 0.3$ $\lambda_{CR} = \sigma_{CR} / \sigma_{CL}(r, h)$

FIG. 30 λ_{CR} VS RADIUS OF CURVED PANELS OF MULTI-SPOT SHELLS

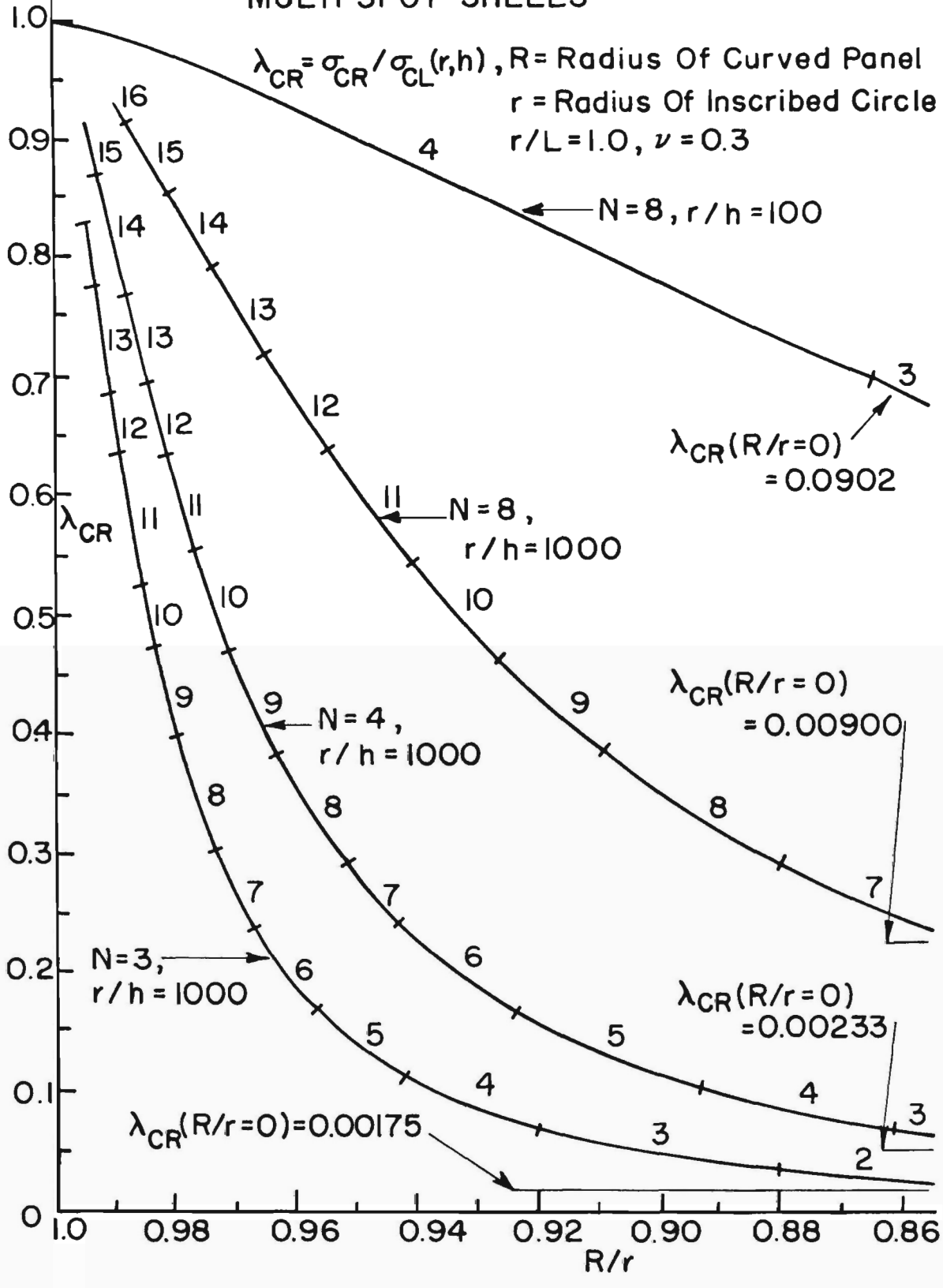

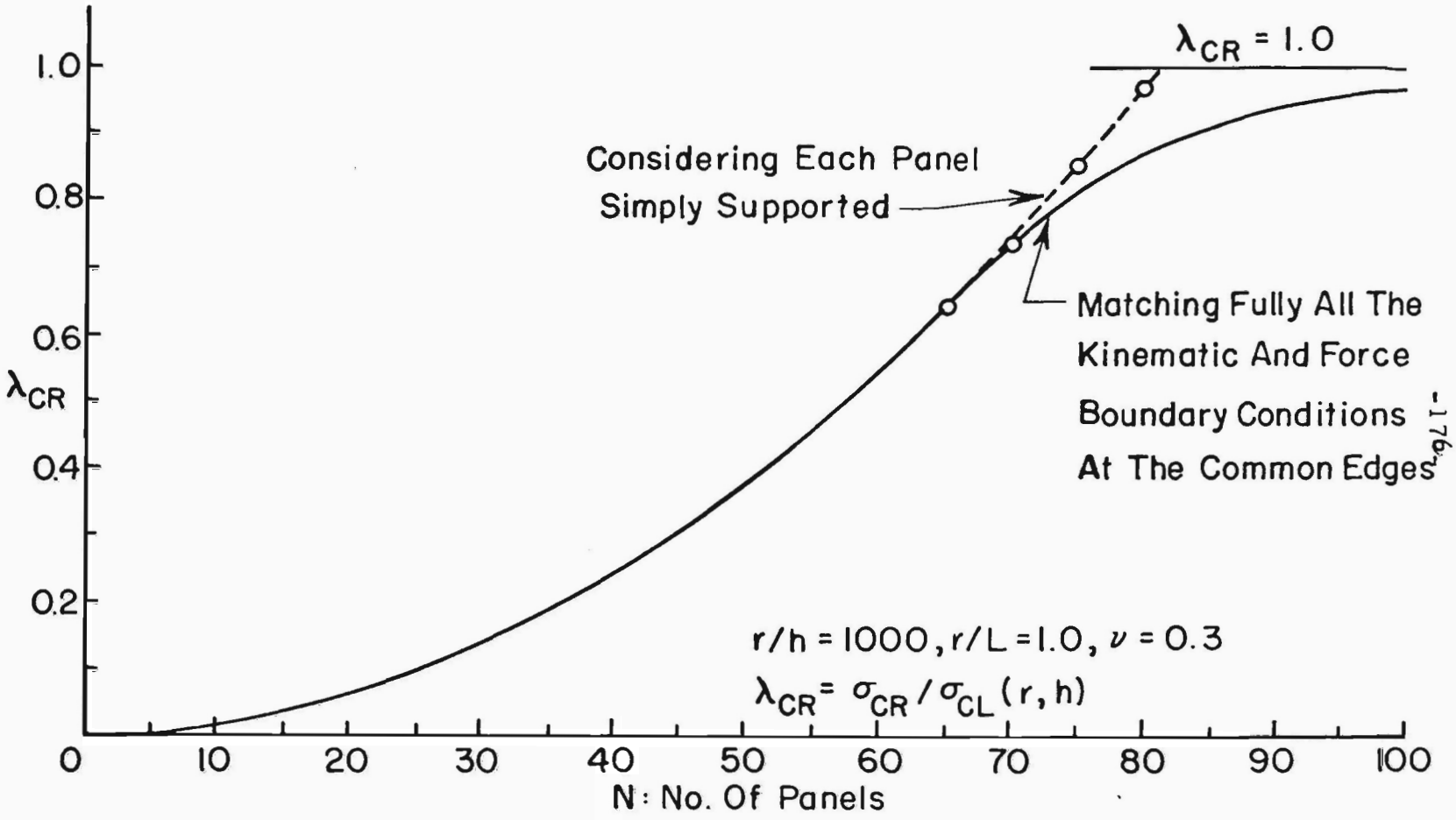

FIG. 31 BUCKLING OF A CLOSED CYLINDRICAL SHELL MADE UP OF FLAT PANELS UNDER AXIAL COMPRESSION

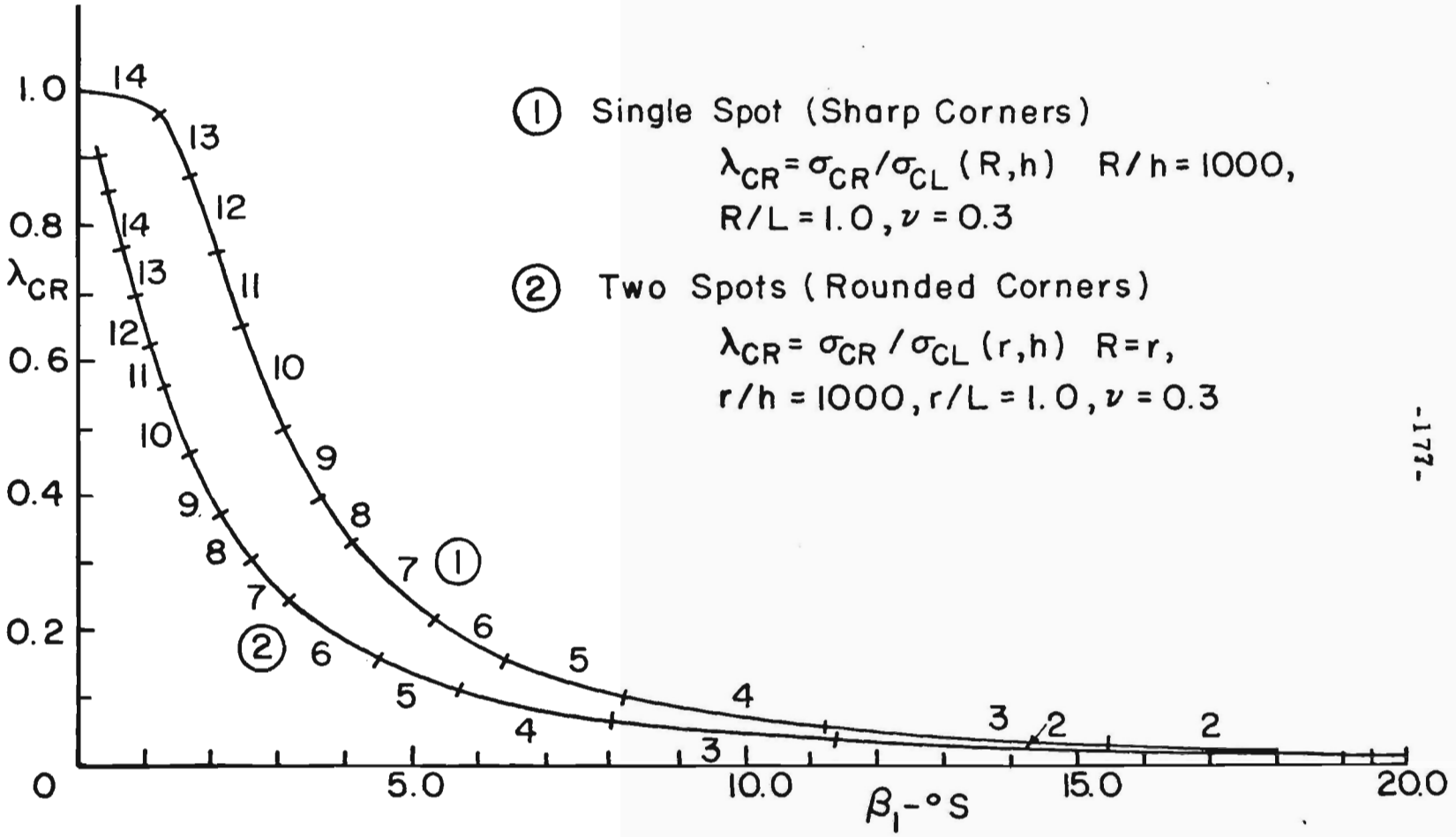

FIG. 32 COMPARISON OF BUCKLING LOADS OF SINGLE SPOT AND MULTIPLE FLAT SPOT SHELLS